Accepted Manuscript

Potent dual inhibitors of *Plasmodium falciparum* M1 and M17 aminopeptidases through optimization of S1 pocket interactions

Nyssa Drinkwater, Natalie B. Vinh, Shailesh N. Mistry, Rebecca S. Bamert, Chiara Ruggeri, John P. Holleran, Sasdekumar Loganathan, Alessandro Paiardini, Susan A. Charman, Andrew K. Powell, Vicky M. Avery, Sheena McGowan, Peter J. Scammells

PII: S0223-5234(16)30015-0

DOI: 10.1016/j.ejmech.2016.01.015

Reference: EJMECH 8305

To appear in: *European Journal of Medicinal Chemistry*

Received Date: 19 November 2015

Revised Date: 11 January 2016

Accepted Date: 11 January 2016

Please cite this article as: N. Drinkwater, N.B. Vinh, S.N. Mistry, R.S. Bamert, C. Ruggeri, J.P. Holleran, S. Loganathan, A. Paiardini, S.A. Charman, A.K. Powell, V.M. Avery, S. McGowan, P.J. Scammells, Potent dual inhibitors of *Plasmodium falciparum* M1 and M17 aminopeptidases through optimization of S1 pocket interactions, *European Journal of Medicinal Chemistry* (2016), doi: 10.1016/j.ejmech.2016.01.015.

Potent dual inhibitors of *Plasmodium falciparum* M1 and M17 aminopeptidases through optimization of S1 pocket interactions

Nyssa Drinkwater [a,b,1], Natalie B. Vinh [c,1], Shailesh N. Mistry [c,1,3], Rebecca S. Bamert [a,b], Chiara Ruggeri [g], John P. Holleran [f] , Sasdekumar Loganathan [f], Alessandro Paiardini [e], Susan A. Charman [d], Andrew K. Powell [d], Vicky M. Avery [f], Sheena McGowan [a,b,*,2], Peter J. Scammells [c,*,2]

[a] Biomedicine Discovery Institute and Department of Microbiology and [b] Department of Biochemistry and Molecular Biology Monash University (Clayton Campus), Melbourne, VIC 3800, Australia.

[c] Medicinal Chemistry and [d] Centre for Drug Candidate Optimisation, Monash Institute of Pharmaceutical Sciences, Monash University (Parkville Campus), Parkville, VIC 3052, Australia.

[e] Dipartimento di Scienze Biochimiche “A. Rossi Fanelli”, Sapienza Università di Roma, 00185 Roma, Italy.

[f] Discovery Biology, Eskitis Institute for Drug Discovery, Griffith University, Nathan, Queensland 4111, Australia.

[g] Dipartmento di Biologia e Biotecnologie “Charles Darwin”, Sapienza Universita di Roma, 00185 Roma, Italy.

Keywords:

P. falciparum
Malaria
Aminopeptidase inhibitors
hydroxamic acid
zinc-binding group

Abbreviations: MAP, metalloaminopeptidase; ZBG, zinc binding group; *Pf*, *Plasmodium falciparum*; Dd2 SpiroR, NITD609-RDd2 clone#2; CDI, carbonyldiimidazole; FCC, flash column chromatography.

* Corresponding authors; For P.J.S.: phone: +61 (0)3 9903 9542; E-mail: Peter.Scammells@monash.edu. For S.M.: phone: +61 (0)3 9902 9309; fax, +61 (0)3 9902 9500; E-mail: Sheena.McGowan@monash.edu.

[1] Contributed equally to this work.

[2] Co-corresponding and joint senior authors

[3] Present address: School of Pharmacy, Centre for Biomolecular Sciences, University of Nottingham, University Park, Nottingham, NG7 2RD, United Kingdom.

ABSTRACT

Malaria remains a global health problem, and though international efforts for treatment and eradication have made some headway, the emergence of drug-resistant parasites threatens this progress. Antimalarial therapeutics acting via novel mechanisms are urgently required. *P. falciparum* M1 and M17 are neutral aminopeptidases which are essential for parasite growth and development. Previous work in our group has identified inhibitors capable of dual inhibition of *Pf*A-M1 and *Pf*A-M17, and revealed further regions within the protease S1 pockets that could be exploited in the development of ligands with improved inhibitory activity. Herein, we report the structure-based design and synthesis of novel hydroxamic acid analogues that are capable of potent inhibition of both *Pf*A-M1 and *Pf*A-M17. Furthermore, the developed compounds potently inhibit *Pf* growth in culture, including the multi-drug resistant strain Dd2. The ongoing development of dual *Pf*A-M1/*Pf*A-M17 inhibitors continues to be an attractive strategy for the design of novel antimalarial therapeutics.

1. Introduction

Malaria is a parasitic disease that kills over half a million people each year, posing a huge burden to public health [1]. Almost half of the global population, particularly those living in sub-Saharan Africa and South-east Asia, remain vulnerable to malaria [1]. The disease is caused by five parasites of the genus *Plasmodium*, with *Plasmodium falciparum (Pf)* the most virulent. Alarmingly, *Pf* has developed widespread resistance to commonly used antimalarials such as chloroquine, mefloquine, pyrimethamine, and sulfadoxine, and further resistance to the artemisinins, our last line of defense, has emerged in five countries of the Greater Mekong subregion (Cambodia, Thailand, Myanmar, Vietnam and Laos) [2]. If we are to prevent a resurgence of malaria, new therapeutics of diverse chemistry and different mechanisms of action are urgently required.

Many of the clinical symptoms of malaria develop during the erythrocytic stage of infection. During this stage, multiple metabolic pathways are initiated within the parasites, which present a wide range of potential drug targets. Among the essential metabolic pathways that occur within erythrocytes, is hemoglobin digestion; host hemoglobin is degraded into free amino acids that are absolutely required for parasite survival [3, 4]. Interference with this pathway is therefore an attractive strategy for the development of novel antimalarial compounds. The final stage of this process is mediated by *Pf*A-M1 [5] as well as several other metalloaminopeptidases (MAPs) that are proposed to work in concert to remove of the N-terminal amino acid residue from peptide fragments [6-8].

Two of the neutral, zinc-dependent metalloaminopeptidases from *Pf*, *Pf*A-M1 and *Pf*A-M17, are essential for parasite survival, and selective inhibition of either enzyme is lethal for parasites *in vitro* [5]. Further, *in vivo* studies have shown that inhibition of *Pf*A-M1 and *Pf*A-M17 controls *Plasmodium chabaudi chabaudi* murine models of malaria [9-11]. Both enzymes are therefore validated antimalarial therapeutic targets. *Pf*A-M1 and *Pf*A-M17 are from different enzyme families, and have very different structural arrangements. *Pf*A-M1 is a monomeric protein of 1085 amino acids in length

(Supp. Fig. 1A). Cleavage of an N-terminal extension (residues 1-194) forms the proteolytically active species that consists of four domains (residues 195-1085). *Pf*A-M17 is a hexamer composed of six identical two-domain subunits (Supp. Fig. 1B) [9, 12]. The active site of both enzymes is located within domain II, the catalytic domain. The active site of *Pf*A-M1 is enclosed deep within the catalytic domain and is accessed by putative substrate entry and exit channels [9]. In contrast, the six active sites of *Pf*A-M17 are located on the edge of the catalytic domain, and exposed to solvent in the interior cavity of the hexameric assembly [12]. Despite these major differences between *Pf*A-M1 and *Pf*A-M17, the enzymes share similar architecture within the active sites (Fig. 1A and 1B). Both enzymes possess S1 and S1' pockets (to accommodate P1 and P1' residues of the peptide substrates), and contain catalytic zinc ion/s at the junction of the two sites (Fig. 1A and 1B). These similarities prompted suggestions that a single compound capable of inhibiting both enzymes could be developed [12]. A drug that can effectively inhibit more than one target could potentially slow the emergence of drug resistance parasites. *Pf*A-M1 possesses one catalytic zinc ion (Zn^{2+}), whereas *Pf*A-M17 has two Zn^{2+} and a catalytic carbonate atom. Previous inhibition studies show that cross inhibition of *Pf*A-M1/*Pf*A-M17 is achievable by targeting these catalytic zinc ion/s [9, 10, 12-15], and led us to develop ((4-(*1H*-pyrazol-1-yl)phenyl)(amino)methyl)phosphonic acid (**1**) (Fig. 1C) (*Pf*A-M1 K_i = 104 μM and *Pf*A-M17 K_i = 0.011 μM), which binds within the S1 pocket of both enzymes [16]. However, differences in the compound binding profiles of the enzymes meant that compound elaboration tended toward improved inhibition of one enzyme target at the expense of the other.

We have recently developed the first inhibitor series capable of potent dual inhibition of both *Pf*A-M1 and *Pf*A-M17, by introducing a hydroxamic acid moiety as a tighter zinc-binding group (ZBG) and exploring the S1' pockets [17]. Two compounds were characterized as potent dual inhibitors of *Pf*A-M1 and *Pf*A-M17: *tert*-butyl (1-(4-(1*H*-pyrazol-1-yl)phenyl)-2-(hydroxyamino)-2-oxoethyl)carbamate (**2**) and *N*-(1-(4-(1*H*-pyrazol-1-yl)phenyl)-2-(hydroxyamino)-2-oxoethyl)pivalamide (**3**) (Fig. 1C).

Both compounds bind the catalytic zinc ion/s through the hydroxamic acid moiety, and prevent growth of *Pf*-3D7 parasites (IC_{50} of **2** = 783 nM; IC_{50} of **3** = 227 nM) with no observable human cell cytotoxicity [17].

Hydroxamic acid and hydroxamate-containing compounds have previously been investigated as potential antimalarials. The search for *Pf*A-M1 inhibitors identified a malono-hydroxamic druggable hit [14, 18]. Chemical modification of the compound led to the discovery of BDM14471, a selective inhibitor of *Pf*A-M1 [14]. The compound showed only moderate anti-parasitic activity, but *in vivo* distribution studies revealed the compound was able to reach the digestive vacuole in blood-stage parasites [13]. The hydroxamate-containing compound CHR-2863 is a potent *Pf*A-M17 and moderate *Pf*A-M1 inhibitor. Excitingly, this compound was shown to be orally bioavailable and efficacious in a murine model of malaria [11].

In the present study, we aimed to improve our hydroxamic acid series as dual inhibitors of *Pf*A-M1 and *Pf*A-M17 and improve their *Pf* parasiticidal activity. To achieve this, we selected the two optimized S1' binding moieties identified in our previous work; the *N*-Boc group of **2** and *N*-pivaloyl group of **3**, and using them as 'anchors' explored the S1 pocket with a range of substituted-phenyl and heteroaromatic rings. One of these series, the *N*-(2-(hydroxyamino)-2-oxoethyl)pivalamides, showed superior dual enzyme inhibitory activity compared to other *Pf*A-M1 and *Pf*A-M17 inhibitors, and resulted in greater inhibition of *Pf* growth in culture, including the multi-drug resistant strain Dd2. As such, the inhibitors described herein represent promising lead compounds for further development.

2. Results and discussion

The 4-(1*H*-pyrazol-1-yl)phenyl framework of **2** and **3** was originally selected by optimization of *Pf*A-M1 and *Pf*A-M17 inhibitor series which coordinated the catalytic Zn^{2+} ion/s through a phosphonic acid moiety [16]. By exchanging the phosphonate zinc binding group for a hydroxamic acid, the

binding position of the 4-(1*H*-pyrazol-1-yl)phenyl scaffold within the S1 pocket shifted considerably [17]. This provided us with an avenue to build into the S1' pocket with short aliphatic groups and substituted-phenyl moieties, which identified the *tert*-butyl group as the ideal substituent to satisfy both the larger *Pf*A-M17 S1' pocket while remaining bound within the smaller *Pf*A-M1 S1' pocket. However, the observed shift of the inhibitor scaffold indicated that further optimization of this region into the S1 pockets of both enzymes was necessary. Therefore, in order to probe the S1 pocket, we chose to make two compound series based on *tert*-butyl-containing *N*-Boc and *N*-pivaloyl 'anchors' in the S1' pocket, with which we determined detailed SAR based on enzyme inhibitory activities and X-ray crystal structures.

2.1 Chemistry

Analogues of phenylglycine derivatives **2** and **3** were synthesized in which the pyrazole moiety was replaced with a variety of aromatic rings. The hydroxamic acid analogues were prepared by a facile four-step synthesis shown in Scheme 1. In this way, 2-amino-2-(4-bromophenyl)acetic acid (**4b**) or 2-amino-3-(4-bromophenyl)propanoic acid (**4d**) were efficiently elaborated to provide a number of derivatives in good overall yields.

Access to the target derivatives of **2**, bearing pyrazole ring-replacements was achieved from commercially available **4b** (Scheme 1). This reagent proved to be a highly useful starting point, allowing installation of a number of aromatic moieties through parallel Suzuki chemistry. In addition, we considered the *N*-Boc-protected hydroxamic acid derivative **9b** to be a valid analogue in its own right. The hydrophobic nature of the bromo group makes it a potential surrogate for an aromatic ring. Indeed, Weik and co-workers noted that non-classical bioisosteric replacement of a biphenyl moiety with a bromophenyl group in their series of peptidomimetic protease inhibitors gave comparable activity in the inhibition assay [19]. *N*-Boc protection of **4b** was achieved in high yield following a procedure based on the protection of the homologous phenylalanine [20]. Subsequent conversion to the

desired hydroxamic acid derivative **9b** proceeded smoothly in good yield using the previously described CDI-mediated activation method [17].

The remaining aryl derivatives were synthesized by conversion of **4b** to the corresponding α-amino ester using previously described esterification conditions [17]. The crude product then underwent *N*-Boc protection to give **5b** in quantitative yield over two steps. Parallel Suzuki coupling of **5b** with a number of aromatic boronic acid or boronate ester partners, in the presence of $PdCl_2(PPh_3)_2$ at 100 °C in degassed 1M $Na_2CO_{3\ (aq)}$/THF readily afforded the desired 4-arylphenyl compounds **7a-p** in generally good to excellent yield. Only coupling with 2-cyanophenylboronic acid proved difficult, affording the desired product in low yield (18%). Final conversion to the target hydroxamic acids **9f-u** was successful with the exception of the nitrile containing derivatives. In the case of the 2-cyanophenyl derivative, no desired product was recoverable from the reaction mixture. In contrast, LC-MS analysis of the reactions containing 3- and 4-cyanophenyl derivatives **7m-n** indicated conversion to the corresponding hydroxamic acid after 1 hour. After overnight stirring, aminolysis of the ester to the hydroxamic acid was complete, however additional attack on the nitrile groups had also occurred. The isolated compounds **9r-s** bore amidoxime groups in place of the nitrile groups, and proved difficult to purify, though inhibitory activity at *Pf*A-M1/*Pf*A-M17 of these unexpected analogues was still evaluated (Table 1). The transformation of arylnitriles to arylamidoximes under similar conditions has been previously investigated [21].

The *N*-pivaloyl analogues were important target compounds that possess the *tert*-butyl 'anchor' optimal for binding to the S1' pocket. Additionally, the *N*-pivaloyl moiety is expected to impart better metabolic stability as replacement of the more labile carbamate with an amide group reduces the potential for hydrolysis to the free amine, which is significantly less potent [17]. Most reactions used for the synthesis of the *N*-Boc derivatives were similarly applied for the preparation of the *N*-pivaloyl analogues. Compound **4b** was esterified and subsequently reacted with Et_3N and pivaloyl chloride in DCM at room temperature to afford compound **6b** in excellent yield (94%) over 2 steps. The Suzuki

reaction was again used to incorporate an additional aromatic ring, to give compounds **8a-q**. Conversion of the methyl esters to the corresponding hydroxamic acids proceeded smoothly, affording the final compounds **10f-v** in excellent yields. The transformation of the nitrile moieties to amidoxime groups, which was previously observed for the *N*-Boc series, was again observed for the corresponding members of the *N*-pivaloyl series (analogues **10s** and **10t**).

This synthetic strategy was also easily adapted to investigate the effect of inserting an extra methylene unit between the α-carbon (to the hydroxamic acid moiety) and phenyl ring. This homologous scaffold was anticipated to improve compound stability, by reducing the acidity of the α-proton, whilst enabling us to probe space in the S1 pockets of *Pf*A-M1 and *Pf*A-M17. Using **4d** as the starting material, the established procedures for esterification, attachment of the *N*-Boc/pivaloyl group, Suzuki coupling and aminolysis were applied. In this study, the 4-fluoro (**9c**, **10c**), 4-bromo (**9d**, **10d**), 4-iodo (**9e**, **10e**), 4-phenyl (**9t**, **10u**) and 1-methylpyrazol-4-yl (**9u**, **10v**) derivatives were synthesized for direct comparison to their more truncated counterpart. Representative NMR spectra for the synthesized compounds are shown in Supp. Fig. 2–6.

2.2 PfA-M1 and PfA-M17 inhibitor-bound crystal structures guide compound development

Here, we determined nine *Pf*A-M1 co-crystal structures (with compounds **9b**, **9f**, **9m**, **9q**, **9r**, **10b**, **10o**, **10q**, **10s**; Supp. Table 1 and 2, Supp. Fig. 1C), and six *Pf*A-M17 co-crystal structures (with compounds **9b**, **10b**, **10o**, **10q**, **10r**, **10s**) (Supp. Table 3, Supp. Fig. 1D). In all structures clear electron density for the bound compounds was observed in the active sites (Supp. Fig. 7). For *Pf*A-M17, which has two copies of the hexamer in the asymmetric unit, the compound binding modes are largely conserved in all twelve active sites. Therefore, when describing *Pf*A-M17 structures, we are referring to Chain I, which has the clearest electron density.

We first investigated the effect of replacing the pyrazole ring of **2** and **3** with either a fluoro- or bromo-substituent (**9a**, **9b** and **10a, 10b**). Irrespective of the S1' anchor used, the bromo-substituted

compounds **9b** and **10b** demonstrated the highest *Pf*A-M1 and *Pf*A-M17 inhibitory activity (for *Pf*A-M1, the K_i of **9b** = 27 nM and **10b** = 65 nM; for *Pf*A-M17 the K_i of **9b** = 80 nM and **10b** = 41 nM, Table 1). Placement of a phenyl ring in the same position resulted in **9f** and **10f**. While both **9f** and **10f** demonstrated good *Pf*A-M17 inhibitory activity (K_i values of 55 nM and 7 nM respectively), only moderate *Pf*A-M1 inhibition was observed (K_i values of 37 μM and 1.6 μM respectively, Table 1).

To inform elaboration of the series, we determined the crystal structures of both *Pf*A-M1 and *Pf*A-M17 with **9b** (**9b**:*Pf*A-M1 at 2.0Å and **9b**:*Pf*A-M17 at 2.7Å) and **10b** (**10b**:*Pf*A-M1 at 2.0Å and **10b**:*Pf*A-M17 at 2.6Å). Although a racemic mixture of both compounds was used for the crystallization experiments, the crystal structures showed that both *Pf*A-M1 and *Pf*A-M17 demonstrate enantiomeric selectivity. Electron density in the active site of *Pf*A-M1 demonstrated that only ***S*-9b** is bound in the crystal, whereas ***R*-10b** is preferentially bound (Fig. 2A). In contrast, only the *R*-enantiomer of both **9b** and **10b** could be fit to electron density in the *Pf*A-M17 binding pocket (Fig. 2B). It should be noted however, that the observed electron density is an average of many molecules, and it is therefore possible that small fractions of the different enantiomers are bound, but unobserved, within the crystal. Compounds **9b** and **10b** bear different linkers to the *tert*-butyl moieties, a carbamate on **9b** and an amide on **10b**, that alters the disposition of substituents in the *Pf*A-M1 S1' cavity. The carbamate of **9b** forms three hydrogen bonds to the main chain of Gly460 and Ala461, which places the *tert*-butyl group in a position to form hydrophobic interactions with Val493 at the end of the pocket. Selection of the *R*-enantiomer of **10b** allows the equivalent *tert*-butyl group to occupy a similar position in the *Pf*A-M1 pocket despite the shorter linker (Fig. 2A). A comparison of these *Pf*A-M1 structures to the **9b**:*Pf*A-M17 and **10b**:*Pf*A-M17 structures suggest that the different enantiomeric selectivity of the enzymes is due to spatial differences in the S1' cavities. *Pf*A-M1 has an enclosed S1' pocket, while the S1' cavity of *Pf*A-M17 is exposed to solvent and is both larger and shallower than the *Pf*A-M1 pocket. While the interaction between the *tert*-butyl substituents and Val493 in the *Pf*A-M1

cavity is vital, the *tert*-butyl groups of neither **9b** nor **10b** form direct interactions with *Pf*A-M17. Instead the linkers themselves dominate the protein-inhibitor interactions and bind similarly in both **9b**:*Pf*A-M17 and **10b**:*Pf*A-M17; the carbamate of **9b** forms water mediated hydrogen bonds with the main chain of Gly489 and Ala490, while the carbonyl of **10b** forms a direct hydrogen bond with the main chain amine of Gly489 (Fig. 2B). Unfortunately, the different enantiomeric preference exhibited by *Pf*A-M1 and *Pf*A-M17 make it difficult to directly compare inhibitory activities between the *N*-Boc and *N*-pivaloyl series. As a result, we have largely restricted our comparisons to compounds within the same series.

Despite the different poses adopted by **9b** and **10b** within the S1' pockets, the position of the hydroxamic acid and bromophenyl moieties are conserved (Fig. 2A and 2B). Compounds **9b** and **10b** form identical zinc binding interactions with *Pf*A-M1, and the bromophenyl positions overlay closely. Similarly, in *Pf*A-M17, the hydroxamic acid and bromophenyl moieties of both **9b** and **10b** make identical active site interactions. The interactions formed by the hydroxamic acid and bromophenyl group of **10b** with the enzymes are shown in Fig. 2C (*Pf*A-M1) and 2D (*Pf*A-M17). In both *Pf*A-M1 and *Pf*A-M17, the hydroxamic acid of **10b** forms a dense network of metallo- and hydrogen bonding interactions with the zinc ion/s and surrounding residues (Fig. 2C and 2D), and additionally to the catalytic carbonate ion in *Pf*A-M17 (Fig. 2D). The bromophenyl moiety sits within the hydrophobic S1 pocket of both enzymes. In **10b**:*Pf*A-M1, the bromine atom is ideally placed to interact with the aromatic ring of Tyr575, while the phenyl ring is aligned with the side chain of Val459 (Fig. 2C). Similarly, in **10b**:*Pf*A-M17, the bromophenyl interacts through hydrophobic interactions with Met396, Phe398 and Met392 (Fig. 2D).

While the bromo-substituted compounds **9b** and **10b** represent some of the most potent dual *Pf*A-M1 and *Pf*A-M17 inhibitors to date, they provide little opportunity to build further into the S1 pocket. In an effort to probe further into the S1 pocket, we incorporated an extra methylene between the phenyl

ring and the α-proton (Table 2). However, regardless of the substituent incorporated (halogen, phenyl or 1-methylpyrazol-4-yl), homologues containing an extra methylene linker generally demonstrated poor inhibition. Compounds bearing the *N*-Boc moiety were poor inhibitors of both *Pf*A-M1 (K_i values of 4.3 – >500 μM, Table 2) and *Pf*A-M17 (K_i values of 2.8 – 21 μM, Table 2), while the *N*-acyl series were reasonable *Pf*A-M17 inhibitors (K_i values of 16 – 740 nM, Table 2) but poor *Pf*A-M1 inhibitors (K_i values of 15 – 87 μM, Table 2). As a result, the compounds of this type were not pursued further.

Since the incorporation of an extra methylene linker did not improve potency, we sought to determine whether the bromo-substituent could be replaced with a phenyl ring that, through further elaboration, would allow deeper access within the S1 pocket. While the biphenyl compounds **9f** and **10f**, were excellent inhibitors of *Pf*A-M17 (*Pf*A-M17 K_i of **9f** = 55 nM and **10f** = 7 nM, Table 1), they demonstrated substantially less activity against *Pf*A-M1 than their corresponding bromophenyl analogues **9b** and **10b** (*Pf*A-M1 K_i of **9b** = 0.027 μM, while **9f** = 37 μM and **10b** = 0.065 μM and **10f** = 1.6 μM, Table 1). To elucidate any structural reason for this loss of activity, we also determined the structure of **9f** in complex with *Pf*A-M1 (2.1Å). The **9f**:*Pf*A-M1 structure showed that the biphenyl dihedral angle is approximately 60° in **9f** (Fig. 2E). In an energetically ideal state, biphenyl systems rapidly convert between two chiral conformations with dihedral angles of approximately 45°. Therefore, restricting the biphenyl system of **9f** to a non-ideal 60° dihedral angle likely contributes to the reduced inhibitory activity of **9f**. Regardless, the observed conformation of the biphenyl places the second aromatic ring in a position to interact via edge-face π-stacking with Tyr575, carbonyl-π interactions with the main chain oxygen of Glu319, and hydrophobic contacts with Met1034 (Fig. 2E). Further, insight into the reduced activity of the biphenyl-substituted **9f** and **10f** is gained by comparison of the S1 pocket structure of **9f**:*Pf*A-M1, **9b**:*Pf*A-M1, and unliganded *Pf*A-M1. In **9b**:*Pf*A-M1 and unliganded *Pf*A-M1, Glu572 sits on an active site helix, and the side chain has no set position. However, in **9f**:*Pf*A-M1, the added phenyl ring of **9f** presses against Glu572, which occupies a position

away from the S1 pocket (Fig. 2E). To adopt this position, the main chain of Glu572 has undergone a substantial movement, which has shifted a single turn of the active site helix it lies on by > 1Å (Fig. 2E). Although aminopeptidases, including *Pf*A-M1, are known to be capable of substantial active site flexibility [9, 22], such main chain movements are likely to come at an energetic cost, which may account for the loss in *Pf*A-M1 inhibitory activity of **9f** compared to **9b**. Despite the kinetic liability of the biphenyl group to both the **9f** and **10f**, its incorporation allows us access to the hydrophilic end of the pocket, which is occupied by ordered water molecules in **9f**:*Pf*A-M1 (Fig. 2E), and which has not previously been accessible to the hydroxamic acid-based compound series.

2.2 Different S1' anchors result in different SAR

Substituting the α-carbon with a biphenyl system has allowed us access deeper into the S1 pocket of *Pf*A-M1 and *Pf*A-M17. Therefore, a variety of substituted-phenyl and heteroaromatic rings were used to probe the region. Compounds **2** and **3**, which are both substituted with a pyrazole but differ in the S1' anchor (*N*-Boc *vs N*-pivaloyl respectively), demonstrated very similar inhibitory activities for each of *Pf*A-M1 (K_i of **2** = 0.85 μM, K_i of **3** = 0.72 μM) and *Pf*A-M17 (K_i of **2** = 0.028 μM, K_i of **3** = 0.028 μM). Further, the bromo-substituted phenyl compounds (**9b** and **10b**) behaved similarly (for *Pf*A-M1, K_i of **9b** = 0.027 μM and K_i of **10b** = 0.065 μM; for *Pf*A-M17, K_i of **9b** = 0.080 μM and K_i of **10b** = 0.041 μM). Therefore for each of the compound pairs **2**/**3** and **9b**/**10b**, the *N*-Boc analogues inhibited *Pf*A-M1 and *Pf*A-M17 with similar activities to their corresponding *N*-pivaloyl compounds. This trend is not conserved for the remainder of the compounds investigated, with a general trend toward greater potency (against both enzymes) for the *N*-pivaloyl compounds (Table 1). Although the *N*-Boc series **9f-s** demonstrates reduced inhibitory activities, the series has allowed us to extract some notable SAR.

In the *N*-Boc **9f-s** series, fluoro- and trifluoromethyl-substituents were tolerated in both the 2- and 3-positions of the phenyl ring (**9g, 9h**, **9j** and **9k**). When placed at the 4-position (**9i, 9l**), a substantial

loss in binding to *Pf*A-M1 was observed. In contrast, substitution at all of the positions was well tolerated by *Pf*A-M17. Isosteric replacement of the phenyl ring with pyridyl (**9n** and **9o**) and thiophenyl rings (**9p**) was also investigated. Both 3- and 4-pyridyl analogues **9n** and **9o** demonstrated reasonable inhibitory activity for *Pf*A-M1, but lost activity against *Pf*A-M17. The thiophenyl analogue **9p** and the phenyl analogue **9f** have similar inhibition activities. The more polar substituted compounds **9q**-**9s** were able to maintain inhibitory activity against both enzymes. Although the most potent of these, **9s**, which bears an amidoxime moiety in the 4-position of the phenyl ring, has regained the *Pf*A-M17 inhibitory activity of the bromophenyl substituted compound **9b** (K_i of **9b** for *Pf*A-M17 = 80 nM; K_i of **9s** for *Pf*A-M17 = 18 nM), it still demonstrates substantially reduced *Pf*A-M1 inhibitory activity (K_i of **9b** for *Pf*A-M1 = 27 nM; K_i of **9s** for *Pf*A-M1 = 400 nM). Generally, replacement of the pyrazole ring of compound **2** did not improve binding to *Pf*A-M17, and only the bromo analogue **9b** demonstrated notable improvement for *Pf*A-M1 binding. With the aim of finding a binding feature of the *N*-Boc series that we could exploit to improve the activity of the series, we determined the crystal structures of *Pf*A-M1 in complex with **9m**, **9q** and **9r** (Supp. Table 1 & Supp. Fig 1C). However, the structures gave us no added insight into the reason for the reduced activity of this series, and the series was therefore discontinued.

2.3 Phenyl substituted N-pivaloyl series probes new region of PfA-M1 and PfA-M17 S1 pocket

Similarly to the *N*-Boc series **9f-s**, a variety of substituted-phenyl and heteroaromatic rings were used to probe the S1 pocket of *Pf*A-M1 and *Pf*A-M17 with the *N*-pivaloyl series **10f-t**. Fluoro-substitution of the phenyl ring at the 2-, 3- or 4-positions (**10g**, **10h** and **10i**, respectively) alone had little effect on inhibition of either *Pf*A-M1 or *Pf*A-M17. This trend is translated to the di-fluorinated compounds (**10j**-**10m**) that exhibited only minor differences in *Pf*A-M1 and *Pf*A-M17 inhibitory activity. However, while the 2,4,6-trifluorophenyl substituted **10n** was a moderate *Pf*A-M1 inhibitor (K_i = 5.9 μM) and an excellent *Pf*A-M17 inhibitor (K_i = 2.5 nM), the 3,4,5-trifluorophenyl substituted

10o is a potent, nanomolar inhibitor of both *Pf*A-M1 (K_i = 78 nM) and *Pf*A-M17 (K_i = 60 nM). Finally, compounds **10r**-**10t**, which are substituted with more polar groups, potently inhibited *Pf*A-M17, but were less active against *Pf*A-M1. Overall, compound **10o** represents the most exciting lead, having regained the potent, dual inhibition activity of the bromo-substituted compound **10b**. Therefore, we determined the crystal structures of **10o** in complex with *Pf*A-M1 (1.9Å) and *Pf*A-M17 (2.1Å). Since **10q** also demonstrates reasonable dual inhibition, and represents a substantially different chemotype to **10o**, we also determined the crystal structures of **10q**:*Pf*A-M1 (1.95Å) and **10q**:*Pf*A-M17 (2.2Å).

When bound to *Pf*A-M1, the position of the biaryl of **10o** compares with that of **9f**, despite the different S1' anchors. The moiety therefore makes the same interactions with Tyr575 (edge-face π-stacking), Met1034 (hydrophobic) and Glu319 (carbonyl-π) (Fig. 3A). The fluoro-substituents sit deeper into the S1 pocket than any other hydroxamic-acid based inhibitor. In fact, the only other *Pf*A-M1 inhibitor that has probed this region is the organophosphorus aminopeptidase inhibitor, Co4 [9, 10, 23]. Although the fluoro groups of **10o** did not displace any of the ordered water molecules as anticipated from the **9f**:*Pf*A-M1 structure, they have entered into an intricate network of water-mediated hydrogen-bonds, in which the fluorine atoms act as acceptors. These additional interactions are likely to account for the improved *Pf*A-M1 inhibitory activity of **10o** over **10f**.

The structure of **10q**:*Pf*A-M1 showed that **10q** adopts a different binding pose compared to other inhibitors of the series, aligned to the opposite face of the S1 pocket (Fig. 3B). Whereas the biaryl dihedral angle of **9p** and **10f** is approximately 60°, the thiophene ring of **10q** sits co-planar to adjacent phenyl ring (Fig. 3C). This allows the thiophene ring to maintain the π-stacking interactions with Tyr575, albeit in a face-face configuration, rather than edge-face. Interactions are also observed between the thiophene ring and Met1034 and the main chain carbonyl of Glu572 (Fig. 3C).

The presence of two different *Pf*A-M1 binding poses for **10f**/**10o** and **10q** demonstrate that there remains additional room for elaboration in the S1 pocket. Compounds **10s** and **10t** possess larger amidoxime moieties at the 3- and 4-positions of the phenyl ring, and while neither compound displayed potent *Pf*A-M1 inhibition, the crystal structure of **10s**:*Pf*A-M1 was determined to establish how the protein accommodates the larger amidoxime group. While the data showed clear electron density in the binding pocket, modelling of the compound in a single conformation could not satisfy the density. Therefore, the compound was modelled in two different conformations (Fig. 3d), that are comparable to the two different conformations adopted by **10f/10o** and **10q**. Conformation A of **10s** resembles the pose adopted by **10q**, with the phenyl ring undergoing face-face π-stacking with Tyr575. In this position, the added amidoxime substituent pushes against Glu572, pushing it further out of the pocket, and causing disorder of the loop 570-574 (shown in red in Fig. 3D). The amidoxime itself makes hydrogen bonds with the main chain oxygen of Glu572, and a water-mediated hydrogen bond with the Tyr575 carbonyl oxygen (Fig. 3D). In conformation B, the distal ring of **10s** has rotated approximately 90°, which changes the geometry of the π-interaction with Tyr575 to an edge-face configuration, similar to that undergone by **10f** and **10o**. Conformation B also places the amidoxime substituent on the opposite side of the pocket compared to conformation A, where it now forms hydrogen bonds with Gln317 and Asn458 (both direct and water-mediated, Fig. 3D). Despite the favorable hydrogen bonding interactions observed in both conformations, it is clear that the induced conformational changes within the binding pocket come at an energetic cost, thereby accounting for the relatively weak inhibition of *Pf*A-M1 by **10s** (K_i = 5.4 μM).

The crystal structures of the same three compounds, **10o**, **10q**, and **10s** bound to *Pf*A-M17 were also determined (2.1Å, 2.2Å and 2.6Å respectively). In contrast to the varying poses adopted when bound to *Pf*A-M1, all three compounds bind similarly to *Pf*A-M17, in poses comparable to **10b**:*Pf*A-M17 (Fig. 3E). In all of the *Pf*A-M17 structures, the *R*-enantiomer is preferentially bound, with the first

phenyl ring of **10b**, **10o**, **10q**, and **10s** placed in the same position. This allows the second rings (3,4,5-trifluorophenyl in **10o**, 3-(amidoximo)phenyl in **10s**, and thiophene in **10q**) to extend deep into the pocket. The different sizes of the substituents is accommodated for in *Pf*A-M17 by adjustments in the position of the Met392 side-chain, which flexes in and out of the pocket depending on the potential for interactions (with **10b**, **10o** and **10q**) or repulsion (**10s**) (Fig. 3E). The phenyl rings themselves sit against the hydrophobic side of the S1 pocket lined by Met396, Phe398 and Leu395 but cause no perturbation to the position or architecture of the pocket. In order to determine how the more polar compound **10r** is capable of potent *Pf*A-M17 inhibition, we also determined the crystal structure of **10r**:*Pf*A-M17 (2.5Å). The structure showed that **10r** binds similarly to **10o**, **10q**, and **10s,** and provided no additional information with which to elaborate.

Compound **10o** is one of the most potent, dual inhibitors of *Pf*A-M1 and *Pf*A-M17 described. Its ability to potently inhibit both enzymes is due to the dual nature of the 3,4,5-trifluorophenyl substituent. While the fluorine atoms of **10o** interact with *Pf*A-M1 through a dense hydrogen-bonding network (Fig. 3A), they interact with *Pf*A-M17 strictly through hydrophobic interactions with Leu492, Phe583, and Met392 (Fig. 3F).

2.4 Dual PfA-M1 and PfA-M17 inhibitors are active against multi-drug resistant Pf

To determine the effect of our dual *Pf*A-M1/*Pf*A-M17 inhibitors on *Pf* in culture, we used an image-based assay to measure the growth inhibition on *Pf* strain 3D7 for selected compounds in the series (Table 3). Lead compounds **2** and **3** were previously reported to inhibit *Pf*-3D7 with IC_{50} values of 783 nM and 227 nM, respectively [17]. The *N*-pivaloyl series demonstrates superior activity against *Pf*-3D7 growth compared to the *N*-Boc series, which we predict to be the result of better cellular penetration and stability. Within the *N*-pivaloyl series, we were excited to observe that incorporating a biaryl system generally led to improved inhibition of *Pf* growth compared to the parent compound **3** (IC_{50} of **10f** = 96 nM). The exceptions to this trend were compounds **10s** and **10t**, in which the

amidoxime moieties likely interfere with cellular penetration. All of the fluorophenyl-substituted compounds performed well, inhibiting *Pf*-3D7 growth in the range of 109–162 nM. The potent dual inhibitor, **10o**, demonstrated an IC_{50} of 126 nM. The best cellular inhibitors of the series included: **10f**, bearing the unsubstituted biphenyl system (IC_{50} = 96 nM), the 2,4-difluorophenyl substituted **10j** (IC_{50} = 109 nM), and **10q**, which is substituted with the thiophen-3-yl moiety (IC_{50} = 103 nM).

Given the potent inhibition of *Pf*-3D7 growth, we were also interested to determine how the compounds performed in other strains, including drug-resistant strains. Therefore, we tested the effect of compound treatment on malarial strains Dd2 [24, 25] (chloroquine-, quinine-, pyrimethamine- and sulfadoxine-resistant) and NITD609-RDd2 clone#2 (abbreviated here on as Dd2 SpiroR), which is resistant to the same parent drugs as Dd2, but additionally resistant to spiroindolones, aminopyrazoles, dihydroisoquinolones and pyrazolamindes) (Table 3) [26-29]. Again, the compounds demonstrated potent inhibition of parasite growth. The most potent inhibitors of *Pf*-3D7 growth also demonstrated potent activity against Dd2 Parent and Dd2 SpiroR, particularly **10o** (IC_{50} Dd2 Parent = 189 nM, IC_{50} Dd2 SpiroR = 107 nM), and **10q** (IC_{50} Dd2 Parent = 110 nM, IC_{50} Dd2 SpiroR = 100 nM). Finally, we also tested the compounds against human mammalian cell line HEK293, to predict whether we may encounter human toxicity with our compound series. No toxicity to HEK293 cells was observed when treated with each of the compounds listed in Table 3 up to a 40 μM concentration over a period of 72 hours.

2.5 Preliminary pharmacokinetic studies

The physicochemical and metabolic stability characteristics of the potent dual inhibitor **10o** are presented in Table 4. Compound **10o** demonstrated moderate to good solubility, with no pH dependence noted between pH 2 and 6.5. The estimated partition coefficient was moderate, with $LogD_{7.4}$ value of 3.0. The stability of **10o** in mouse and human plasma was investigated and there was no evidence of degradation over the course of a 4-6 h incubation at 37°C. The metabolic stability of **10o** was assessed by incubating the compound at 1 μM in mouse and human liver microsomes at 37°C and 0.4 mg/mL protein concentration. Compound **10o** possessed half-life of 69 minutes in mouse and 221 minutes in human microsomes, with low-to-intermediate *in vitro* intrinsic clearance (CL_{int}) values calculated in each species, which is an indicator of good metabolic stability.

3. Conclusions

Antimalarial drug resistance represents a major threat to global health. While progress towards a malaria vaccine continues [30, 31], the continued development of antimalarial agents that work via novel mechanisms is absolutely required. We have described the design, synthesis and characterisation of novel compounds that inhibit the essential *Pf* MAPs, *Pf*A-M1 and *Pf*A-M17. Using a comprehensive structure-guided medicinal chemistry approach, we elaborated the hydroxamic acid-based compounds deep into the S1 pocket of both enzymes, which resulted in a series of potent, dual *Pf*A-M1 and *Pf*A-M17 inhibitors. Furthermore, we determined that the compounds possess nanomolar anti-malarial activity against *Pf*-3D7 parasites, and excitingly, drug resistant strains Dd2 and Dd2 SpiroR. One of the most promising analogues, compound **10o**, was shown to possess good physicochemical properties and excellent plasma stability. The observed half-life and *in vitro* CL_{int} in mouse and human liver microsomes were indicators of good metabolic stability.

In summary, this study has identified a series of potent dual acting *Pf*A-M1 and *Pf*A-M17 inhibitors that show good anti-malarial activity against *Pf*-3D7 parasites and have the potential to be developed into pre-clinical candidates.

4. Experimental section

4.1. General remarks

Chemicals and solvents were purchased from standard suppliers and used without further purification. Davisil® silica gel (40-63µm), for flash column chromatography (FCC) was supplied by Grace Davison Discovery Sciences (Victoria, Australia) and deuterated solvents were purchased from Cambridge Isotope Laboratories, Inc. (USA, distributed by Novachem PTY. Ltd, Victoria, Australia).

Unless otherwise stated, reactions were carried out at ambient temperature. Reactions were monitored by thin layer chromatography on commercially available pre-coated aluminium-backed plates (Merck Kieselgel 60 F_{254}). Visualization was by examination under UV light (254 and 366 nm). General staining carried out with $KMnO_4$ or phosphomolybdic acid. A solution of Ninhydrin (in ethanol) was used to visualize primary and secondary amines. A solution of $FeCl_3$ (5% in 0.5M $HCl_{(aq)}$) was used to visualize hydroxamic acids. All organic extracts collected after aqueous work-up procedures were dried over anhydrous Na_2SO_4 before gravity filtering and evaporation to dryness. Organic solvents were evaporated *in vacuo* at ≤ 40°C (water bath temperature). Purification using preparative layer chromatography (PLC) was carried out on Analtech preparative TLC plates (200 mm x 200 mm x 2 mm).

^{1}H NMR, ^{13}C NMR and ^{19}F NMR spectra were recorded on a Bruker Avance Nanobay III 400MHz Ultrashield Plus spectrometer at 400.13 MHz, 100.62 MHz, and 376.46 MHz, respectively. Chemical shifts (δ) are recorded in parts per million (ppm) with reference to the chemical shift of the deuterated

solvent. Unless otherwise stated, samples were dissolved in $CDCl_3$. Coupling constants (*J*) and carbon-fluorine coupling constants (J_{CF}) are recorded in Hz and the significant multiplicities described by singlet (s), doublet (d), triplet (t), quadruplet (q), broad (br), multiplet (m), doublet of doublets (dd), doublet of triplets (dt). Spectra were assigned using appropriate COSY, DEPT, HSQC and HMBC sequences.

LC-MS were run to verify reaction outcome and purity using either system A or B. System A: an Agilent 6100 Series Single Quad coupled to an Agilent 1200 Series HPLC. The following buffers were used; buffer A: 0.1% formic acid in H_2O; buffer B: 0.1% formic acid in MeCN. The following gradient was used with a Phenomenex Luna 3µM C8(2) 15 x 4.6 mm column, and a flow rate of 0.5 mL/min and total run time of 12 min; 0–4 min 95% buffer A and 5% buffer B, 4–7 min 0% buffer A and 100% buffer B, 7–12 min 95% buffer A and 5% buffer B. Mass spectra were acquired in positive and negative ion mode with a scan range of 0–1000 *m/z* at 5V. UV detection was carried out at 254 nm. System B: an Agilent 6120 Series Single Quad coupled to an Agilent 1260 Series HPLC. The following buffers were used; buffer A: 0.1% formic acid in H_2O; buffer B: 0.1% formic acid in MeCN. The following gradient was used with a Poroshell 120 EC-C18 50 x 3.0 mm 2.7 micron column, and a flow rate of 0.5 mL/min and total run time of 5 min; 0–1 min 95% buffer A and 5% buffer B, from 1-2.5 min up to 0% buffer A and 100% buffer B, held at this composition until 3.8 min, 3.8–4 min 95% buffer A and 5% buffer B, held until 5 min at this composition. Mass spectra were acquired in positive and negative ion mode with a scan range of 100–1000 *m/z*. UV detection was carried out at 214 and 254 nm. All retention times (t_R) are quoted in minutes.

HRMS analyses were carried out on an Agilent 6224 TOF LC/MS Mass Spectrometer coupled to an Agilent 1290 Infinity (Agilent, Palo Alto, CA). All data were acquired and reference mass corrected via a dual-spray electrospray ionisation (ESI) source. Acquisition was performed using the Agilent

Mass Hunter Data Acquisition software version B.05.00 Build 5.0.5042.2 and analysis was performed using Mass Hunter Qualitative Analysis version B.05.00 Build 5.0.519.13.

Analytical HPLC was acquired on an Agilent 1260 Infinity Analytical HPLC fitted with a Zorbax Eclipse Plus C18 Rapid Resolution 4.6 × 100 mm 3.5-Micron column with UV detection at 254 nm. The following buffers were used; buffer A: 0.1% TFA in H_2O; buffer B: 0.1% TFA in MeCN. Samples were run in a gradient of 5 – 100% buffer B in buffer A over 9 min, followed by isocratic 100% buffer B for 1 min at a flow rate of 1.0 mL/min.

Preparative HPLC was performed using an Agilent 1260 infinity coupled with a binary preparative pump and Agilent 1260 FC-PS fraction collector, using Agilent OpenLAB CDS software (Rev C.01.04), and an Altima 5µM C8 22 x 250 mm column. The following buffers were used; buffer A: H_2O; buffer B: MeCN, with sample being run at a gradient of 5% buffer B to 100% buffer B over 20 min, at a flow rate of 20 mL/min. All screening compounds were of > 95% purity unless specified in the individual monologue.

Instant JChem was used for structure database management and SMILES string generation (Supp. Table 4); Instant JChem 6.3.3, 2014, ChemAxon (http://www.chemaxon.com).

4.2 Chemistry

4.2.1. General Procedure A: Methyl ester and N-Boc protection of amino acids

The amino acid (1.0 mmol, 1.0 eq) was dispersed in MeOH (1.0 mL per 0.21 mmol of amino acid) with concd H_2SO_4 (1.8 eq). The mixture was refluxed overnight, at which point LC-MS analysis indicated complete conversion had taken place. The mixture was cooled then concentrated under reduced pressure. The resulting residue was basified with sat. $NaHCO_{3\ (aq)}$, then extracted with DCM. The combined organic layers were concentrated under reduced pressure. This was taken up into water

and THF (5:1), before adding in Boc_2O (1.05 eq), and stirring at room temperature overnight. The mixture was diluted with water, before extraction with DCM. Concentration of the combined organic layers gave the desired product.

4.2.2. General Procedure B: Methyl ester and N-pivamide protection of amino acids

The amino acid (1.0 mmol, 1.0 eq) was dispersed in MeOH (1.0 mL per 0.21 mmol of amino acid) with concd H_2SO_4 (1.8 eq). The mixture was refluxed overnight, at which point LC-MS analysis indicated complete conversion had taken place. The mixture was cooled then concentrated under reduced pressure. The resulting residue was basified with sat. $NaHCO_{3\ (aq)}$, then extracted with DCM. The combined organic layers were concentrated under reduced pressure. The crude compound was taken up in DCM and triethylamine (2.2 eq) was added, followed by pivaloyl chloride (1.1 eq). The reaction mixture was stirred at room temperature for 2 h and then diluted with DCM, washed with water and further extracted with DCM. Concentration of the organic layer gave the desired product.

*4.2.3. General Procedure C: Suzuki coupling of arylbromide (**5b**, **5d**, **6b** or **6d**) with boronic acids or boronate esters*

Aryl bromide (0.20 g) and the appropriate boronic acid or boronate ester (1.5 eq) were dispersed in degassed THF (3 mL) and degassed 1M $Na_2CO_{3\ (aq)}$ (1 mL) in a 10 mL microwave vessel. A steady stream of nitrogen was bubbled through the mixture for 5 min, before adding $PdCl_2(PPh_3)_2$ (41 mg, 0.1 eq), then immediately sealing the tube. The mixture was heated at 100 °C in an aluminium heating block for 2 h, at which point LC-MS analysis indicated the reaction was complete. After cooling, the mixture was diluted with EtOAc (10 mL) and water (10 mL), and the aqueous layer discarded. The organic layer was filtered through a plug of cotton wool, before concentration and further purification by FCC (eluent DCM or MeOH/DCM 0:100 to 5:95 for more polar compounds).

4.2.4. General Procedure D: Direct aminolysis of methyl esters to corresponding hydroxamic acids

The appropriate methyl ester (0.40–0.55 mmol) was dissolved in anhydrous MeOH (0.5 mL) at room temperature in a nitrogen-flushed vessel. In a separate nitrogen flushed vial, $NH_2OH.HCl$ (139 mg, 2 mmol) and 5M KOH/anhydrous MeOH (0.5 mL, 2.5 mmol) were mixed, then sonicated for 30 sec. The resulting suspension was added to the methanolic ester solution with washings of anhydrous MeOH (1 mL). The mixtures were stirred at RT overnight and monitored by LC-MS analysis. The mixtures were directly dry-loaded on to Isolute HM-N® (Biotage), before purification by FCC (eluent MeOH/DCM 0:100 to 10:90).

4.2.5. General Procedure E: CDI-mediated coupling of carboxylic acids with hydroxylamine to give the corresponding hydroxamic acid

The appropriate carboxylic acid (1 eq) was dissolved in anhydrous THF (1-5 mL/mmol) at RT under an atmosphere of nitrogen, and CDI (1.5 eq) was added. The mixture was stirred at RT for 1 h, before adding in $NH_2OH.HCl$ (2 eq). Stirring was continued at RT for 24 to 48 h, before diluting the mixture with sat. $NH_4Cl_{(aq)}$ (20 mL), then extracting with EtOAc (3 x 20 mL). The combined organic layers were washed with sat. $NaHCO_{3\ (aq)}$ (20 mL) and brine (20 mL), before concentration under reduced pressure. The resulting crude product was further purified by FCC (eluent MeOH/DCM 0:100 to 10:90).

*4.2.6. Methyl 2-((tert-butoxycarbonyl)amino)-2-(4-fluorophenyl)acetate (**5a**)*

2-Amino-2-(4-fluorophenyl)acetic acid (**4a**) (0.28 g, 1.7 mmol) was converted to the title compound according to General Procedure A, to give 0.30 g (64%) of clear, colourless oil after purification by FCC (eluent EtOAc/PE 0:100 to 40:60). ^{1}H NMR δ 7.37–7.30 (m, 2H), 7.08–7.00 (m, 2H), 5.57 (br. d, J = 5.0 Hz, 1H), 5.30 (d, J = 7.0 Hz, 1H), 3.72 (s, 3H), 1.43 (s, 9H); ^{13}C NMR δ 171.6, 162.8 (d, J_{CF} = 247.2 Hz), 154.9, 133.0, 129.0 (d, J_{CF} = 8.3 Hz), 115.9 (d, J_{CF} = 21.7 Hz), 80.4, 57.0, 52.9, 28.4; *m/z* HRMS (TOF ES$^+$) $C_{14}H_{18}FNNaO_4$ $[M+Na]^+$ calcd 306.1112; found 306.1100; LC-MS t_R: 3.74 min.

*4.2.7. Methyl 2-(4-bromophenyl)-2-((tert-butoxycarbonyl)amino)acetate (**5b**)*

2-Amino-2-(4-bromophenyl)acetic acid (**4b**) (4.87 g, 21.2 mmol) was converted to the title compound according to General Procedure A, to give 7.56 g (quantitative yield) of pale brown oil, which slowly solidified to an off-white solid. ^{1}H NMR δ 7.48 (d, *J* = 8.4 Hz, 2H), 7.24 (d, *J* = 8.4 Hz, 2H), 5.77–5.34 (m, 1H), 5.35–5.00 (m, 1H), 3.72 (s, 3H), 1.49–1.22 (m, 9H)*; ^{13}C NMR δ 165.9, 156.6, 135.4, 132.2, 128.9, 122.6, 77.7, 57.2, 53.1, 28.4*, 27.6*; * multiple peaks present due to rotameric effects; *m/z* MS (TOF ES^{+}) $C_{14}H_{18}BrNNaO_4$ $[M+Na]^{+}$ calcd 366.0; found 366.0; LC-MS t_R: 4.00 min.

*4.2.8. Methyl 2-((tert-butoxycarbonyl)amino)-3-(4-fluorophenyl)propanoate (**5c**)*

2-Amino-3-(4-fluorophenyl)propanoic acid (**4c**) (0.28 g, 1.5 mmol) was converted to the title compound according to General Procedure A, to give 0.45 g (quantitative yield) of a pale yellow oil, which slowly solidified to a pale yellow solid. ^{1}H NMR δ 7.12–7.04 (m, 2H), 7.01–6.93 (m, 2H), 4.98 (br. d, *J* = 7.4 Hz, 1H), 4.56 (dd, *J* = 13.7/6.1 Hz, 1H), 3.71 (s, 3H), 3.10 (dd, *J* = 13.9/5.7 Hz, 1H), 3.00 (dd, *J* = 13.9/6.1 Hz, 1H), 1.41 (s, 9H); ^{13}C NMR δ 172.3, 162.1 (d, J_{CF} = 245.2 Hz), 155.1, 131.9 (d, J_{CF} = 3.3 Hz), 130.9 (d, J_{CF} = 8.0 Hz), 115.5 (d, J_{CF} = 21.3 Hz), 80.1, 54.6, 52.4, 37.8, 28.4; *m/z* HRMS (TOF ES^{+}) $C_{15}H_{20}FNNaO_4$ $[M+Na]^{+}$ calcd 320.1269; found 320.1283; LC-MS t_R: 3.76 min.

*4.2.9. Methyl 3-(4-bromophenyl)-2-((tert-butoxycarbonyl)amino)propanoate (**5d**)*

2-Amino-3-(4-bromophenyl)propanoic acid (**4d**) (2.00 g, 8.19 mmol) was converted to the title compound according to General Procedure A, to give 2.74 g (93%) of white solid. ^{1}H NMR δ 7.45–7.38 (m, 2H), 7.00 (app. d, *J* = 8.3 Hz, 2H), 4.97 (br. d, *J* = 7.6 Hz, 1H), 4.57 (dd, *J* = 13.7/6.1 Hz, 1H), 3.71 (s, 3H), 3.08 (dd, *J* = 13.1/5.0 Hz, 1H), 2.98 (dd, *J* = 13.0/5.4 Hz, 1H), 1.42 (s, 9H); ^{13}C NMR δ 172.2, 155.1, 135.2, 131.7, 131.1, 121.2, 80.2, 54.3, 52.4, 37.9, 28.4; *m/z* MS (TOF ES^{+}) $C_{15}H_{20}BrNNaO_4$ $[M+Na]^{+}$ calcd 380.1; found 380.1; LC-MS t_R: 3.89 min.

*4.2.10. Methyl 2-((tert-butoxycarbonyl)amino)-3-(4-iodophenyl)propanoate (**5e**)*

2-Amino-3-(4-iodophenyl)propanoic acid (**4e**) (1.00 g, 3.44 mmol) was converted to the title compound according to General Procedure A, to give 0.615 g (44%) of white solid after purification by FCC (eluent DCM). ^{1}H NMR δ 7.64–7.59 (m, 2H), 6.87 (app. d, *J* = 8.2 Hz, 2H), 4.97 (br. d, *J* = 7.8 Hz, 1H), 4.56 (dd, *J* = 13.3/5.7 Hz, 1H), 3.71 (s, 3H), 3.07 (dd, *J* = 13.8/5.6 Hz, 1H), 2.97 (dd, *J* = 13.7/6.0 Hz, 1H), 1.41 (s, 9H); ^{13}C NMR δ 172.2, 155.1, 137.7, 135.9, 131.5, 92.7, 80.2, 54.3, 52.5, 38.0, 28.4; *m/z* MS (TOF ES$^+$) $C_{15}H_{20}INNaO_4$ $[M+Na]^+$ calcd 428.0; found 428.1; LC-MS t_R: 3.93 min.

*4.2.11. Methyl 2-(4-fluorophenyl)-2-pivalamidoacetate (**6a**)*

2-Amino-2-(4-fluorophenyl)acetic acid (**4a**) (0.28 g, 1.7 mmol) was converted to the title compound according to General Procedure B, to give 0.39 g (88%) of white solid after purification by FCC (eluent EtOAc/PE 0:100 to 40:60). ^{1}H NMR δ 7.36–7.29 (m, 2H), 7.08–7.00 (m, 2H), 6.65 (br. d, *J* = 5.8 Hz, 1H), 5.50 (d, *J* = 6.7 Hz, 1H), 3.73 (s, 3H), 1.22 (s, 9H); ^{13}C NMR δ 177.9, 171.7, 162.8 (d, J_{CF} = 247.3 Hz), 132.9 (d, J_{CF} = 3.2 Hz), 129.0 (d, J_{CF} = 8.4 Hz), 116.1 (d, J_{CF} = 21.8 Hz), 55.8, 53.0, 38.8, 27.5; *m/z* MS (TOF ES$^+$) $C_{14}H_{19}FNO_3$ $[MH]^+$ calcd 268.1; found 268.2; LC-MS t_R: 3.61 min.

*4.2.12. Methyl 2-(4-bromophenyl)-2-pivalamidoacetate (**6b**)*

2-Amino-2-(4-bromophenyl)acetic acid (**4b**) (1.00 g, 4.35 mmol) was converted to the title compound according to General Procedure B, to give 1.34 g (94%) of white solid. ^{1}H NMR δ 7.51–7.45 (m, 2H), 7.25–7.20 (m, 2H), 6.68 (br. d, *J* = 6.1 Hz, 1H), 5.48 (d, *J* = 6.6 Hz, 1H), 3.73 (s, 3H), 1.21 (s, 9H); ^{13}C NMR δ 177.9, 171.4, 136.1, 132.2, 128.9, 122.7, 56.0, 53.1, 38.8, 27.5; *m/z* MS (TOF ES$^+$) $C_{14}H_{19}BrNO_3$ $[MH]^+$ calcd 328.1; found 328.1; LC-MS t_R: 3.76 min.

*4.2.13. Methyl 3-(4-fluorophenyl)-2-pivalamidopropanoate (**6c**)*

2-Amino-3-(4-fluorophenyl)propanoic acid (**4c**) (0.28 g, 1.5 mmol) was converted to the title compound according to General Procedure B, to give 0.12 g (28%) of white solid, after purification by

FCC (eluent DCM). ^{1}H NMR δ 7.07–6.92 (m, 4H), 6.06 (br. d, *J* = 6.7 Hz, 1H), 4.83 (ddd, *J* = 7.5/5.8/5.8 Hz, 1H), 3.73 (s, 3H), 3.15 (dd, *J* = 13.9/5.8 Hz, 1H), 3.05 (dd, *J* = 13.9/5.6 Hz, 1H), 1.15 (s, 9H); ^{13}C NMR δ 178.0, 172.3, 162.1 (d, J_{CF} = 245.3 Hz), 131.8 (d, J_{CF} = 3.3 Hz), 130.9 (d, J_{CF} = 7.9 Hz), 115.5 (d, J_{CF} = 21.3 Hz), 53.0 (d, J_{CF} = 0.9 Hz), 52.5, 38.8, 37.1, 27.5; *m/z* MS (TOF ES^{+}) $C_{15}H_{21}FNO_3$ $[MH]^{+}$ calcd 282.2; found 282.2; LC-MS t_R: 3.64 min.

*4.2.14. Methyl 3-(4-bromophenyl)-2-pivalamidopropanoate (**6d**)*

2-Amino-3-(4-bromophenyl)propanoic acid (**4d**) (2.00 g, 8.19 mmol) was converted to the title compound according to General Procedure B, to give 2.57 g (92%) of white solid. ^{1}H NMR δ 7.39 (app. d, *J* = 8.3 Hz, 2H), 6.94 (app. d, *J* = 8.3 Hz, 2H), 6.07 (br. d, *J* = 7.0 Hz, 1H), 4.83 (dd, *J* = 13.0/5.8 Hz, 1H), 3.73 (s, 3H), 3.13 (dd, *J* = 13.9/5.9 Hz, 1H), 3.04 (dd, *J* = 13.9/5.5 Hz, 1H), 1.15 (s, 9H); ^{13}C NMR δ 178.0, 172.2, 135.1, 131.7, 131.1, 121.2, 52.8, 52.5, 38.8, 37.3, 27.5; *m/z* MS (TOF ES^{+}) $C_{15}H_{21}BrNO_3$ $[MH]^{+}$ calcd 342.1; found 342.1; LC-MS t_R: 3.78 min.

*4.2.15. Methyl 3-(4-iodophenyl)-2-pivalamidopropanoate (**6e**)*

2-Amino-3-(4-iodophenyl)propanoic acid (**4e**) (1.00 g, 3.44 mmol) was converted to the title compound according to General Procedure B, to give 0.768 g (57%) of yellow solid after purification by FCC (eluent DCM). ^{1}H NMR δ 7.53–7.47 (m, 2H), 6.79–6.72 (m, 2H), 6.12 (d, *J* = 7.5 Hz, 1H), 4.73 (ddd, *J* = 7.5/5.9/5.9 Hz, 1H), 3.63 (s, 3H), 3.04 (dd, *J* = 13.8/5.7 Hz, 1H), 2.93 (dd, *J* = 13.8/6.0 Hz, 1H), 1.06 (s, 9H); ^{13}C NMR δ 177.7, 171.8, 137.3, 135.6, 131.1, 92.4, 52.6, 52.2, 38.4, 37.0, 27.2; *m/z* MS (TOF ES^{+}) $C_{15}H_{21}INO_3$ $[MH]^{+}$ calcd 390.1; found 390.1; LC-MS t_R: 3.80 min.

*4.2.16. Methyl 2-([1,1'-biphenyl]-4-yl)-2-((tert-butoxycarbonyl)amino)acetate (**7a**)*

Phenylboronic acid (106 mg) underwent Suzuki coupling according to General Procedure C, with variation to the workup procedure as follows: the cooled reaction mixture was diluted with water (20 mL) and extracted with EtOAc (3 x 20 mL). The combined organic layers were washed with brine (20

mL), before concentration and FCC purification (DCM) to give 162 mg of colourless crystalline solid (81%). ^{1}H NMR δ 7.65–7.53 (m, 4H), 7.50–7.40 (m, 4H), 7.36 (ddd, *J* = 7.3/3.8/1.2 Hz, 1H), 5.66 (d, *J* = 6.7 Hz, 1H), 5.39 (d, *J* = 7.3 Hz, 1H), 3.75 (s, 3H), 1.58–1.32 (m, 9H); ^{13}C NMR δ 171.7, 155.0, 141.5, 140.5, 136.0, 128.9, 127.7, 127.7, 127.6, 127.2, 80.3, 57.4, 52.9, 28.4; *m/z* MS (TOF ES^{+}) $C_{20}H_{23}NNaO_4$ $[M+Na]^{+}$ calcd 364.2; found 364.2; LC-MS t_R: 4.09 min.

*4.2.17. Methyl 2-((tert-butoxycarbonyl)amino)-2-(2'-fluoro-[1,1'-biphenyl]-4-yl)acetate (**7b**)*

2-Fluorophenylboronic acid (122 mg) underwent Suzuki coupling according to General Procedure C, to give 163 mg (78%) of white solid. ^{1}H NMR δ 7.54 (dd, *J* = 8.3/1.6 Hz, 2H), 7.48–7.38 (m, 3H), 7.32 (dddd, *J* = 7.0/7.0/5.0/1.8 Hz, 1H), 7.21 (ddd, *J* = 7.5/7.5/1.2 Hz, 1H), 7.15 (ddd, *J* = 10.8/8.2/1.1 Hz, 1H), 5.60 (d, *J* = 7.1 Hz, 1H), 5.38 (d, *J* = 7.2 Hz, 1H), 3.75 (s, 3H), 1.51–1.30 (m, 9H); ^{19}F NMR δ -117.99; ^{13}C NMR δ 170.5, 159.9 (d, J_{CF} = 247.9 Hz), 154.0, 136.4, 136.1, 130.8 (d, J_{CF} = 3.4 Hz), 129.7 (d, J_{CF} = 2.0 Hz), 129.4 (d, J_{CF} = 8.1 Hz), 127.4, 124.6 (d, J_{CF} = 3.7 Hz), 116.3 (d, J_{CF} = 22.7 Hz), 78.3, 57.5, 53.0, 28.5; *m/z* MS (TOF ES^{+}) $C_{20}H_{22}FNNaO_4$ $[M+Na]^{+}$ calcd 382.1; found 382.3; LC-MS t_R: 3.99 min.

*4.2.18. Methyl 2-((tert-butoxycarbonyl)amino)-2-(3'-fluoro-[1,1'-biphenyl]-4-yl)acetate (**7c**)*

3-Fluorophenylboronic acid (122 mg) underwent Suzuki coupling according to General Procedure C, to give 175 mg (84%) of white solid. ^{1}H NMR δ 7.61–7.52 (m, 2H), 7.50–7.31 (m, 4H), 7.30–7.20 (m, 1H), 7.09–7.00 (m, 1H), 5.62 (d, *J* = 6.6 Hz, 1H), 5.37 (d, *J* = 7.0 Hz, 1H), 3.75 (s, 3H), 1.52–1.30 (m, 9H); ^{19}F NMR δ -112.97; ^{13}C NMR δ 174.3, 163.3 (d, J_{CF} = 245.7 Hz), 163.3, 141.4, 140.2, 132.9, 130.4 (d, J_{CF} = 8.4 Hz), 127.8, 122.9 (d, J_{CF} = 2.8 Hz), 114.5 (d, J_{CF} = 21.4 Hz), 114.1 (d, J_{CF} = 22.0 Hz), 79.7, 57.4, 53.0, 28.5; *m/z* MS (TOF ES^{+}) $C_{20}H_{22}FNNaO_4$ $[M+Na]^{+}$ calcd 382.1; found 382.2; LC-MS t_R: 4.03 min.

*4.2.19. Methyl 2-((tert-butoxycarbonyl)amino)-2-(4'-fluoro-[1,1'-biphenyl]-4-yl)acetate (**7d**)*

4-Fluorophenylboronic acid (122 mg) underwent Suzuki coupling according to General Procedure C, to give 149 mg (72%) of clear, colourless oil. ^{1}H NMR δ 7.58–7.48 (m, 4H), 7.43 (d, *J* = 8.2 Hz, 2H), 7.18–7.06 (m, 2H), 5.64 (d, *J* = 6.7 Hz, 1H), 5.37 (d, *J* = 7.2 Hz, 1H), 3.74 (s, 3H), 1.80–1.08 (m, 9H); ^{19}F NMR δ -115.31; ^{13}C NMR δ 171.7, 162.7 (d, J_{CF} = 246.7 Hz), 155.0, 140.5, 136.7 (d, J_{CF} = 2.7 Hz), 136.1, 128.8 (d, J_{CF} = 8.1 Hz), 127.7, 127.6, 115.8 (d, J_{CF} = 21.5 Hz), 80.4, 57.4, 52.9, 28.4; *m/z* MS (TOF ES^{+}) $C_{20}H_{22}FNNaO_4$ $[M+Na]^{+}$ calcd 382.1; found 382.2; LC-MS t_R: 4.02 min.

4.2.20. Methyl 2-((tert-butoxycarbonyl)amino)-2-(2'-(trifluoromethyl)-[1,1'-biphenyl]-4-yl)acetate (7e)

2-(Trifluoromethyl)phenylboronic acid (165 mg) underwent Suzuki coupling according to General Procedure C, to give 184 mg (78%) of white solid. ^{1}H NMR δ 7.74 (d, *J* = 7.8 Hz, 1H), 7.56 (dd, *J* = 11.0/4.0 Hz, 1H), 7.46 (dd, *J* = 7.6/7.6 Hz, 1H), 7.43–7.35 (m, 2H), 7.34–7.27 (m, 3H), 5.76–4.98 (m, 2H), 3.76 (s, 3H), 1.57–0.89 (m, 9H); ^{19}F NMR δ -56.74; ^{13}C NMR δ 171.8, 155.0, 140.8 (d, J_{CF} = 1.9 Hz), 140.1, 136.2, 132.1, 131.5 (d, J_{CF} = 0.7 Hz), 129.6, 128.5 (q, J_{CF} = 30.0 Hz), 127.7, 126.7, 126.2 (q, J_{CF} = 5.3 Hz), 124.2 (q, J_{CF} = 273.6 Hz), 80.4, 57.5, 52.9, 28.4; *m/z* MS (TOF ES^{+}) $C_{21}H_{22}F_3NNaO_4$ $[M+Na]^{+}$ calcd 432.1; found 432.2; LC-MS t_R: 4.11 min.

*4.2.21. Methyl 2-((tert-butoxycarbonyl)amino)-2-(3'-(trifluoromethyl)-[1,1'-biphenyl]-4-yl)acetate (**7f**)*

3-(Trifluoromethyl)phenylboronic acid (165 mg) underwent Suzuki coupling according to General Procedure C, to give 181 mg (76%) of colourless oil. ^{1}H NMR δ 7.80 (s, 1H), 7.73 (d, *J* = 7.6 Hz, 1H), 7.65–7.51 (m, 4H), 7.47 (d, *J* = 8.2 Hz, 2H), 5.91–5.09 (m, 2H), 3.75 (s, 3H), 1.57–1.12 (m, 9H); ^{19}F NMR δ -62.63; ^{13}C NMR δ 171.6, 155.0, 141.4, 140.0, 137.0, 131.3 (q, J_{CF} = 32.2 Hz), 130.5 (q, J_{CF} = 1.0 Hz), 129.4, 127.9, 127.9, 124.3 (q, J_{CF} = 3.6 Hz), 124.2 (q, J_{CF} = 272.4 Hz), 124.0 (q, J_{CF} = 3.8 Hz), 80.5, 57.4, 53.0, 28.4; *m/z* MS (TOF ES^{+}) $C_{21}H_{22}F_3NNaO_4$ $[M+Na]^{+}$ calcd 432.1; found 432.2; LC-MS t_R: 4.15 min.

*4.2.22. Methyl 2-((tert-butoxycarbonyl)amino)-2-(4'-(trifluoromethyl)-[1,1'-biphenyl]-4-yl)acetate (**7g**)*

4-(Trifluoromethyl)phenylboronic acid (165 mg) underwent Suzuki coupling according to General Procedure C, to give 196 mg (83%) of off-white solid. ^{1}H NMR δ 7.69 (d, *J* = 8.6 Hz, 2H), 7.66 (d, *J* = 8.7 Hz, 2H), 7.58 (d, *J* = 8.2 Hz, 2H), 7.48 (d, *J* = 8.3 Hz, 2H), 5.88–5.01 (m, 2H), 3.74 (s, 3H), 1.82–1.10 (m, 9H); ^{19}F NMR δ -62.43; ^{13}C NMR δ 171.5, 154.9, 144.1, 140.0, 137.2, 129.6 (q, J_{CF} = 32.4 Hz), 127.9, 127.9, 127.5, 125.9 (q, J_{CF} = 3.7 Hz), 124.3 (q, J_{CF} = 272.0 Hz), 80.4, 57.4, 52.9, 28.4; *m/z* MS (TOF ES^{+}) $C_{21}H_{22}F_3NNaO_4$ $[M+Na]^+$ calcd 432.1; found 432.2; LC-MS t_R: 4.15 min.

*4.2.23. Methyl 2-((tert-butoxycarbonyl)amino)-2-(3',4',5'-trifluoro-[1,1'-biphenyl]-4-yl)acetate (**7h**)*

3,4,5-Trifluorophenylboronic acid (153 mg) underwent Suzuki coupling according to General Procedure C, to give 158 mg (69%) of white solid. ^{1}H NMR δ 7.48 (d, *J* = 8.6 Hz, 2H), 7.45 (d, *J* = 8.6 Hz, 2H), 7.16 (dd, *J* = 8.1/6.8 Hz, 2H), 5.69 (d, *J* = 4.2 Hz, 1H), 5.37 (d, *J* = 7.0 Hz, 1H), 3.74 (s, 3H), 1.64–1.11 (m, 9H); ^{19}F NMR δ -133.95 (d, *J* = 20.5 Hz), -162.26 (dd, *J* = 20.4/20.4 Hz); ^{13}C NMR δ 171.4, 154.9, 151.5 (ddd, J_{CF} = 249.8/10.0, 4.2 Hz), 139.5 (ddd, J_{CF} = 251.4/16.1/16.1 Hz), 137.5, 136.7, 127.9, 127.5, 111.2 (dd, J_{CF} = 15.9/6.0 Hz), 80.5, 57.3, 53.0, 28.4; *m/z* MS (TOF ES^{+}) $C_{20}H_{20}F_3NNaO_4$ $[M+Na]^+$ calcd 418.1; found 418.2; LC-MS t_R: 4.11 min.

*4.2.24. Methyl 2-((tert-butoxycarbonyl)amino)-2-(4-(pyridin-3-yl)phenyl)acetate (**7i**)*

Pyridin-3-ylboronic acid (107 mg) underwent Suzuki coupling according to General Procedure C, to give 120 mg (60%) of yellow solid. ^{1}H NMR δ 8.82 (s, 1H), 8.60 (d, *J* = 4.5 Hz, 1H), 8.02–7.82 (m, 1H), 7.56 (d, *J* = 8.3 Hz, 2H), 7.48 (d, *J* = 8.2 Hz, 2H), 7.45–7.35 (m, 1H), 5.93–5.03 (m, 2H), 3.74 (s, 3H), 1.75–0.96 (m, 9H); ^{13}C NMR δ 171.4, 154.9, 147.8, 147.4, 137.6, 137.4, 136.5, 135.3, 128.1, 127.8, 124.0, 80.4, 57.4, 53.0, 28.4; *m/z* MS (TOF ES^{+}) $C_{19}H_{23}N_2O_4$ $[MH]^+$ calcd 343.2; found 343.2; LC-MS t_R: 3.40 min.

*4.2.25. Methyl 2-((tert-butoxycarbonyl)amino)-2-(4-(pyridin-4-yl)phenyl)acetate (**7j**).*

Pyridin-4-ylboronic acid (107 mg) underwent Suzuki coupling according to General Procedure C, to give 170 mg (85%) of dark brown oil. ^{1}H NMR δ 8.66 (s, 2H), 7.89–7.30 (m, 6H), 5.75 (d, *J* = 4.8 Hz, 1H), 5.39 (d, *J* = 6.4 Hz, 1H), 3.73 (s, 3H), 1.43 (s, 9H); ^{13}C NMR δ 171.3, 154.9, 149.7, 148.5, 138.5, 138.0, 128.0, 127.7, 121.9, 80.5, 57.4, 53.0, 28.4; *m/z* MS (TOF ES^{+}) $C_{19}H_{23}N_2O_4$ $[MH]^{+}$ calcd 343.2; found 343.2; LC-MS t_R: 3.28 min.

*4.2.26. Methyl 2-((tert-butoxycarbonyl)amino)-2-(4-(thiophen-3-yl)phenyl)acetate (**7k**)*

Thiophen-3-ylboronic acid (111 mg) underwent Suzuki coupling according to General Procedure C, to give 135 mg (67%) of yellow solid. ^{1}H NMR δ 7.64–7.53 (m, 2H), 7.44 (s, 1H), 7.42–7.31 (m, 4H), 5.61 (d, *J* = 6.6 Hz, 1H), 5.34 (d, *J* = 7.2 Hz, 1H), 3.73 (s, 3H), 1.61–1.18 (m, 9H); ^{13}C NMR δ 171.7, 154.9, 141.7, 136.2, 135.8, 127.7, 127.1, 126.5, 126.4, 120.8, 80.3, 57.4, 52.9, 28.4; *m/z* MS (TOF ES^{+}) $C_{18}H_{21}NNaO_4S$ $[M+Na]^{+}$ calcd 370.1; found 370.2; LC-MS t_R: 3.94 min.

*4.2.27. Methyl 2-((tert-butoxycarbonyl)amino)-2-(4-(1-methyl-1H-pyrazol-4-yl)phenyl)acetate (**7l**)*

1-Methyl-4-(4,4,5,5-tetramethyl-1,3,2-dioxaborolan-2-yl)-*1H*-pyrazole (181 mg) underwent Suzuki coupling according to General Procedure C, to give 127 mg (64%) of off-white solid. ^{1}H NMR δ 7.74 (s, 1H), 7.60 (s, 1H), 7.43 (d, *J* = 8.3 Hz, 2H), 7.34 (d, *J* = 8.2 Hz, 2H), 5.83–5.49 (m, 1H), 5.47–5.22 (m, 1H), 3.94 (s, 3H), 3.71 (s, 3H), 1.61–1.16 (m, 9H); ^{13}C NMR δ 171.7, 154.9, 136.5, 135.1, 132.7, 127.8, 127.4, 126.1, 122.7, 80.3, 57.4, 52.8, 39.2, 28.4; *m/z* MS (TOF ES^{+}) $C_{18}H_{24}N_3O_4$ $[MH]^{+}$ calcd 346.2; found 346.2; LC-MS t_R: 3.62 min.

*4.2.28. Methyl 2-((tert-butoxycarbonyl)amino)-2-(3'-cyano-[1,1'-biphenyl]-4-yl)acetate (**7m**)*

3-Cyanophenylboronic acid (128 mg) underwent Suzuki coupling according to General Procedure C, to give 137 mg (64%) of clear, colourless oil. ^{1}H NMR δ 7.82 (s, 1H), 7.77 (d, *J* = 7.9 Hz, 1H), 7.62 (ddd, *J* = 7.7/1.3/1.3 Hz, 1H), 7.57–7.50 (m, 3H), 7.47 (d, *J* = 8.3 Hz, 2H), 5.71 (d, *J* = 6.8 Hz, 1H),

5.38 (d, *J* = 7.1 Hz, 1H), 3.73 (s, 3H), 1.70–0.94 (m, 9H); ^{13}C NMR δ 171.4, 154.9, 141.8, 139.0, 137.4, 131.5, 131.0, 130.7, 129.8, 128.0, 127.7, 118.8, 113.1, 80.4, 57.3, 53.0, 28.4; *m/z* MS (TOF ES$^+$) $C_{21}H_{22}N_2NaO_4$ $[M+Na]^+$ calcd 389.1 found 389.2; LC-MS t_R: 3.87 min.

*4.2.29. Methyl 2-((tert-butoxycarbonyl)amino)-2-(4'-cyano-[1,1'-biphenyl]-4-yl)acetate (**7n**)*

4-Cyanophenylboronic acid (128 mg) underwent Suzuki coupling according to General Procedure C, to give 158 mg (74%) of white solid. ^{1}H NMR δ 7.71 (d, *J* = 8.4 Hz, 2H), 7.65 (d, *J* = 8.3 Hz, 2H), 7.57 (d, *J* = 8.3 Hz, 2H), 7.48 (d, *J* = 8.3 Hz, 2H), 5.70 (d, *J* = 6.7 Hz, 1H), 5.38 (d, *J* = 7.1 Hz, 1H), 3.73 (s, 3H), 1.57–1.20 (m, 9H); ^{13}C NMR δ 171.4, 154.8, 145.0, 139.3, 137.7, 132.7, 127.9, 127.82, 127.77, 118.9, 111.2, 80.4, 57.3, 53.0, 28.4; *m/z* MS (TOF ES$^+$) $C_{21}H_{23}N_2O_4$ $[MH]^+$ calcd 367.2; found 367.2; LC-MS t_R: 3.85 min.

*4.2.30. Methyl 3-([1,1'-biphenyl]-4-yl)-2-((tert-butoxycarbonyl)amino)propanoate (**7o**)*

Phenylboronic acid (102 mg) underwent Suzuki coupling according to General Procedure C, to give 135 mg (68%) of white solid. ^{1}H NMR δ 7.60–7.50 (m, 4H), 7.47–7.40 (m, 2H), 7.37–7.31 (m, 1H), 7.23–7.17 (m, 2H), 5.02 (br. d, *J* = 8.0 Hz, 1H), 4.63 (dd, *J* = 13.9/6.1 Hz, 1H), 3.74 (s, 3H), 3.17 (dd, *J* = 13.8/5.7 Hz, 1H), 3.09 (dd, *J* = 13.8/6.1 Hz, 1H), 1.43 (s, 9H); ^{13}C NMR δ 172.5, 155.3, 140.9, 140.1, 135.2, 129.9, 128.9, 127.4 (3 × CH), 127.2, 80.1, 54.5, 52.4, 38.1, 28.4; *m/z* MS (TOF ES$^+$) $C_{21}H_{26}NNaO_4$ $[M+Na]^+$ calcd 378.2; found 378.2; LC-MS t_R: 4.04 min.

*4.2.31. Methyl 2-((tert-butoxycarbonyl)amino)-3-(4-(1-methyl-1H-pyrazol-4-yl)phenyl)propanoate (**7p**)*

1-Methyl-4-(4,4,5,5-tetramethyl-1,3,2-dioxaborolan-2-yl)-*1H*-pyrazole (174 mg) underwent Suzuki coupling according to General Procedure C, to give 148 mg (74%) of white solid. ^{1}H NMR δ 7.73 (d, *J* = 0.7 Hz, 1H), 7.58 (s, 1H), 7.41–7.36 (m, 2H), 7.11 (app. d, *J* = 8.1 Hz, 2H), 5.00 (br. d, *J* = 8.0 Hz, 1H), 4.58 (dd, *J* = 13.8/6.0 Hz, 1H), 3.93 (s, 3H), 3.72 (s, 3H), 3.11 (dd, *J* = 13.8/5.7 Hz, 1H), 3.04 (dd, *J* = 13.8/6.1 Hz, 1H), 1.41 (s, 9H); ^{13}C NMR δ 172.5, 155.2, 136.8, 134.1, 131.5, 129.9, 126.9, 125.7,

123.0, 80.1, 54.5, 52.4, 39.2, 38.1, 28.4; *m/z* MS (TOF ES$^+$) $C_{19}H_{26}N_3O_4$ $[MH]^+$ calcd 360.2; found 360.2; LC-MS t_R: 3.57 min.

*4.2.32. Methyl 2-([1,1'-biphenyl]-4-yl)-2-pivalamidoacetate (**8a**)*

Phenylboronic acid (112 mg) underwent Suzuki coupling according to General Procedure C, to give 144 mg (73%) of white solid. ^{1}H NMR δ 7.60–7.54 (m, 4H), 7.47–7.40 (m, 4H), 7.38–7.32 (m, 1H), 6.68 (br. d, *J* = 6.5 Hz, 1H), 5.58 (d, *J* = 6.8 Hz, 1H), 3.76 (s, 3H), 1.24 (s, 9H); ^{13}C NMR δ 178.1, 171.8, 141.6, 140.6, 135.8, 129.0, 127.9, 127.69, 127.66, 127.3, 56.3, 53.0, 38.8, 27.6; *m/z* MS (TOF ES$^+$) $C_{20}H_{24}NO_3$ $[MH]^+$ calcd 326.2; found 326.2; LC-MS t_R: 3.84 min.

*4.2.33. Methyl 2-(2'-fluoro-[1,1'-biphenyl]-4-yl)-2-pivalamidoacetate (**8b**)*

2-Fluorophenylboronic acid (90 mg) underwent Suzuki coupling according to General Procedure C, to give 117 mg (80%) of beige solid. ^{1}H NMR δ 7.57–7.51 (m, 2H), 7.46–7.41 (m, 2H), 7.39 (dd, *J* = 7.7/1.8 Hz, 1H), 7.30 (dddd, *J* = 8.1/6.9/5.0/1.8 Hz, 1H), 7.19 (ddd, *J* = 7.5/7.5/1.2 Hz, 1H), 7.13 (ddd, *J* = 10.8/8.2/1.1 Hz, 1H), 6.73 (d, *J* = 6.7 Hz, 1H), 5.59 (d, *J* = 6.8 Hz, 1H), 3.74 (s, 3H), 1.25 (s, 9H); ^{19}F NMR δ -119.0; ^{13}C NMR δ 178.0, 171.6, 159.7 (d, J_{CF} = 248.0 Hz), 136.1 (2C), 130.7 (d, J_{CF} = 3.4 Hz), 129.6 (d, J_{CF} = 3.0 Hz), 129.3 (d, J_{CF} = 8.3 Hz), 128.3 (d, J_{CF} = 13.3 Hz), 127.3, 124.5 (d, J_{CF} = 3.7 Hz), 116.2 (d, J_{CF} = 22.7 Hz), 56.2, 52.9, 38.7, 27.4; *m/z* MS (TOF ES$^+$) $C_{20}H_{23}FNO_3$ $[MH]^+$ calcd 344.4; found 344.2; LC-MS t_R: 3.83 min.

*4.2.34. Methyl 2-(3'-fluoro-[1,1'-biphenyl]-4-yl)-2-pivalamidoacetate (**8c**)*

3-Fluorophenylboronic acid (90 mg) underwent Suzuki coupling according to General Procedure C, to give 78 mg (53%) of white solid. ^{1}H NMR δ 7.58–7.53 (m, 2H), 7.46–7.30 (m, 4H), 7.28–7.22 (m, 1H), 7.07–7.00 (m, 1H), 6.76 (d, *J* = 6.5 Hz, 1H), 5.58 (d, *J* = 6.7 Hz, 1H), 3.75 (s, 3H), 1.25 (s, 9H); ^{19}F NMR δ -112.9; ^{13}C NMR δ 178.0, 171.6, 163.2 (d, J_{CF} = 245.7 Hz), 142.8 (d, J_{CF} = 7.7 Hz), 140.2 (d, J_{CF} = 2.2 Hz), 136.4, 130.4 (d, J_{CF} = 8.4 Hz), 127.8, 127.7, 122.8 (d, J_{CF} = 2.8 Hz), 114.4 (d, J_{CF} =

21.2 Hz), 114.0 (d, J_{CF} = 22.0 Hz), 56.2, 53.0, 38.8, 27.5; *m/z* MS (TOF ES$^+$) $C_{20}H_{23}FNO_3$ $[MH]^+$ calcd 344.4; found 344.2.

*4.2.35. Methyl 2-(4'-fluoro-[1,1'-biphenyl]-4-yl)-2-pivalamidoacetate (**8d**)*

4-Fluorophenylboronic acid (128 mg) underwent Suzuki coupling according to General Procedure C, to give 159 mg (76%) of yellow solid. ^{1}H NMR δ 7.55–7.48 (m, 4H), 7.44–7.39 (m, 2H), 7.16–7.08 (m, 2H), 6.69 (br. d, *J* = 6.5 Hz, 1H), 5.57 (d, *J* = 6.7 Hz, 1H), 3.76 (s, 3H), 1.24 (s, 9H); ^{19}F NMR δ -115.30; ^{13}C NMR δ 178.1, 171.7, 162.7 (d, J_{CF} = 246.8 Hz), 140.6, 136.7 (d, J_{CF} = 3.2 Hz), 135.9, 128.8 (d, J_{CF} = 8.1 Hz), 127.7 (4 × CH), 115.9 (d, J_{CF} = 21.5 Hz), 56.3, 53.0, 38.8, 27.6; *m/z* MS (TOF ES$^+$) $C_{20}H_{23}FNO_3$ $[MH]^+$ calcd 344.2; found 344.2; LC-MS t_R: 3.87 min.

*4.2.36. Methyl 2-(2',4'-difluoro-[1,1'-biphenyl]-4-yl)-2-pivalamidoacetate (**8e**)*

2,4-Difluorophenylboronic acid (101 mg) underwent Suzuki coupling according to General Procedure C, to give 90 mg (58%) of beige solid. ^{1}H NMR δ 7.51–7.32 (m, 5H), 6.97–6.85 (m, 2H), 6.72 (d, *J* = 6.6 Hz, 1H), 5.57 (d, *J* = 6.8 Hz, 1H), 3.75 (s, 3H), 1.23 (s, 9H); ^{19}F NMR δ -111.0 (d, *J* = 7.6 Hz), -113.5 (d, *J* = 7.6 Hz); ^{13}C NMR δ 178.0, 171.6, 162.5 (dd, J_{CF} = 249.4/11.9 Hz), 159.8 (dd, J_{CF} = 250.7/11.9 Hz), 136.3, 135.3, 131.5 (dd, J_{CF} = 9.5/4.9 Hz), 129.6 (d, J_{CF} = 2.8 Hz), 127.4, 124.7 (dd, J_{CF} = 13.6/3.9 Hz), 111.8 (dd, J_{CF} = 21.1/3.8 Hz), 104.5 (dd, J_{CF} = 26.6/25.3 Hz), 56.3, 53.0, 38.8, 27.5; *m/z* MS (TOF ES$^+$) $C_{20}H_{22}F_2NO_3$ $[MH]^+$ calcd 362.4; found 362.2; LC-MS t_R: 3.85 min.

*4.2.37. Methyl 2-(2',6'-difluoro-[1,1'-biphenyl]-4-yl)-2-pivalamidoacetate (**8f**)*

2,6-Difluorophenylboronic acid (101 mg) underwent Suzuki coupling according to General Procedure C, to give 64 mg (42%) of white solid. ^{1}H NMR δ 7.50–7.41 (m, 4H), 7.32–7.19 (m, 1H), 7.00–6.93 (m, 2H), 6.67 (d, *J* = 6.8 Hz, 1H), 5.59 (d, *J* = 6.9 Hz, 1H), 3.74 (s, 3H), 1.24 (s, 9H); ^{19}F NMR δ -114.5; ^{13}C NMR δ 178.0, 171.5, 160.1 (dd, J_{CF} = 248.9/7.0 Hz), 136.6, 131.0 (dd, J_{CF} = 1.9/1.9 Hz), 129.5, 129.2 (dd, J_{CF} = 10.4/10.4 Hz), 127.2, 117.8 (dd, J_{CF} = 18.5/18.5 Hz), 112.0–111.6

(m), 56.3, 52.9, 38.8, 27.5; *m/z* MS (TOF ES$^+$) $C_{20}H_{22}F_2NO_3$ $[MH]^+$ calcd 362.4; found 362.2; LC-MS t_R: 3.82 min.

*4.2.38. Methyl 2-(3',4'-difluoro-[1,1'-biphenyl]-4-yl)-2-pivalamidoacetate (**8g**)*

3,4-Difluorophenylboronic acid (101 mg) underwent Suzuki coupling according to General Procedure C, to give 154 mg (quantitative yield) of colourless oil. ^{1}H NMR δ 7.52–7.46 (m, 2H), 7.45–7.39 (m, 2H), 7.33 (ddd, *J* = 11.5/7.5/2.1 Hz, 1H), 7.28–7.14 (m, 2H), 6.78 (d, *J* = 6.6 Hz, 1H), 5.56 (d, *J* = 6.6 Hz, 1H), 3.74 (s, 3H), 1.24 (s, 9H); ^{19}F NMR δ -137.4 (d, *J* = 21.3 Hz), -139.8 (d, *J* = 21.3 Hz); ^{13}C NMR δ 178.1, 171.5, 150.5 (dd, J_{CF} = 248.1/12.8 Hz), 150.1 (dd, J_{CF} = 248.8/12.7 Hz), 139.4, 137.6 (dd, J_{CF} = 5.9/3.9 Hz), 136.4, 127.8, 127.6, 123.1 (dd, J_{CF} = 6.2/3.5 Hz), 117.7 (d, J_{CF} = 17.4 Hz), 116.0 (d, J_{CF} = 17.8 Hz), 56.2, 53.0, 38.7, 27.4; *m/z* MS (TOF ES$^+$) $C_{20}H_{22}F_2NO_3$ $[MH]^+$ calcd 362.4; found 362.2; LC-MS t_R: 3.86 min.

*3.2.39. Methyl 2-(3',5'-difluoro-[1,1'-biphenyl]-4-yl)-2-pivalamidoacetate (**8h**)*

3,5-Difluorophenylboronic acid (101 mg) underwent Suzuki coupling according to General Procedure C, to give 84 mg (54%) of yellow oil. ^{1}H NMR δ 7.55–7.49 (m, 2H), 7.47–7.40 (m, 2H), 7.11–7.02 (m, 2H), 6.78 (dddd, *J* = 8.8/8.8/2.3/2.3 Hz, 2H), 5.57 (d, *J* = 6.6 Hz, 1H), 3.76 (s, 3H), 1.24 (s, 9H); ^{19}F NMR δ -109.5; ^{13}C NMR δ 178.2, 171.5, 163.4 (dd, J_{CF} = 248.2/13.1 Hz), 143.9 (dd, J_{CF} = 9.5/9.5 Hz), 139.2 (dd, J_{CF} = 2.5/2.5 Hz), 137.1, 127.9, 127.7, 112.1–108.1 (m), 102.9 (t, J_{CF} = 25.4/25.4 Hz), 56.3, 53.1, 38.8, 27.5; *m/z* MS (TOF ES$^+$) $C_{20}H_{22}F_2NO_3$ $[MH]^+$ calcd 362.4; found 362.2; LC-MS t_R: 3.86 min.

*3.2.40. Methyl 2-pivalamido-2-(2',4',6'-trifluoro-[1,1'-biphenyl]-4-yl)acetate (**8i**)*

2,4,6-trifluorophenylboronic acid (113 mg) underwent Suzuki coupling according to General Procedure C, to give 88 mg (54%) of colourless foam. ^{1}H NMR δ 7.43–7.31 (m, 4H), 6.95–6.84 (m, 2H), 5.51 (d, *J* = 6.9 Hz, 1H), 3.67 (s, 3H), 1.16 (s, 9H); ^{19}F NMR δ -108.5 (dd, *J* = 6.1/6.1 Hz), -111.2

(d, J = 6.1 Hz); ^{13}C NMR δ 178.0, 171.6, 160.2 (d, J_{CF} = 248.9 Hz), 160.1 (d, J_{CF} = 248.9 Hz), 136.6, 131.0 (dd, J_{CF} = 1.9/1.9 Hz), 129.5, 127.2, 117.8, (dd, J_{CF} = 18.4/18.4 Hz), 111.9–111.6 (m), 56.3, 53.0, 38.8, 27.5; *m/z* MS (TOF ES$^+$) $C_{20}H_{21}F_3NO_3$ $[MH]^+$ calcd 380.4; found 380.2; LC-MS t_R: 3.84 min.

*4.2.41. Methyl 2-pivalamido-2-(3',4',5'-trifluoro-[1,1'-biphenyl]-4-yl)acetate (**8j**)*

3,4,5-Trifluorophenylboronic acid (161 mg) underwent Suzuki coupling according to General Procedure C, to give 174 mg (75%) of white solid. ^{1}H NMR δ 7.51–7.40 (m, 2H), 7.21–7.10 (m, 2H), 6.78 (br. d, J = 6.4 Hz, 1H), 5.56 (d, J = 6.6 Hz, 1H), 3.76 (s, 3H), 1.24 (s, 9H); ^{19}F NMR δ -133.9 (d, J = 20.5 Hz), -162.2 (dd, J = 20.5/20.5 Hz); ^{13}C NMR δ 178.0, 171.5, 151.6 (ddd, J_{CF} = 249.9/10.1/4.5 Hz), 140.9–138.1 (m), 138.5–138.4 (m), 137.3, 136.9–136.6 (m), 128.0, 127.6, 111.2 (dd, J_{CF} = 15.9/6.0 Hz), 56.2, 53.1, 38.8, 27.5; *m/z* MS (TOF ES$^+$) $C_{20}H_{21}F_3NO_3$ $[MH]^+$ calcd 380.2; found 380.2; LC-MS t_R: 3.94 min.

*4.2.42. Methyl 2-(2',3',4',5',6'-pentafluoro-[1,1'-biphenyl]-4-yl)-2-pivalamidoacetate (**8k**)*

2,3,4,5,6-Pentafluorophenylboronic acid (136 mg) underwent Suzuki coupling according to General Procedure C, to give 99 mg (56%) of colourless oil. ^{1}H NMR δ 7.51–7.38 (m, 4H), 6.73 (d, J = 6.6 Hz, 1H), 5.61 (d, J = 6.8 Hz, 1H), 3.77 (s, J = 3.2 Hz, 3H), 1.24 (s, 9H); ^{19}F NMR δ -143.08 (dd, J = 22.8/8.1 Hz), -155.09 (dd, J = 21.0/21.0 Hz), -161.88–-162.07 (m); ^{13}C NMR δ 178.0, 171.4, 145.6–142.9 (m), 142.1–139.1 (m), 138.2, 139.4–136.5(m), 130.9, 127.6, 126.7, 56.2, 53.1, 38.8, 27.6; *m/z* MS (TOF ES$^+$) $C_{20}H_{19}F_5NO_3$ $[MH]^+$ calcd 416.4; found 416.2; LC-MS t_R: 3.94 min.

*4.2.43. Methyl 2-pivalamido-2-(4-(thiophen-3-yl)phenyl)acetate (**8l**)*

Thiophen-3-ylboronic acid (117 mg) underwent Suzuki coupling according to General Procedure C, to give 155 mg (77%) of yellow solid. ^{1}H NMR δ 7.61–7.55 (m, 2H), 7.44 (dd, J = 2.9/1.4 Hz, 1H), 7.40–7.34 (m, 4H), 6.65 (br. d, J = 6.5 Hz, 1H), 5.55 (d, J = 6.8 Hz, 1H), 3.75 (s, 3H), 1.23 (s, 9H); ^{13}C

NMR δ 178.0, 171.8, 141.8, 136.3, 135.6, 127.8, 127.2, 126.5, 126.4, 120.8, 56.3, 53.0, 38.8, 27.6; *m/z* MS (TOF ES$^+$) $C_{18}H_{22}NO_3S$ $[MH]^+$ calcd 332.1; found 332.2; LC-MS t_R: 3.77 min.

*4.2.44. Methyl 2-(4-(1-methyl-1H-pyrazol-4-yl)phenyl)-2-pivalamidoacetate (**8m**)*

1-Methyl-4-(4,4,5,5-tetramethyl-1,3,2-dioxaborolan-2-yl)-1*H*-pyrazole (114 mg) underwent Suzuki coupling according to General Procedure C, to give 81 mg (68%) of yellow solid. ^{1}H NMR δ 7.73 (d, *J* = 0.7 Hz, 1H), 7.59 (s, 1H), 7.46–7.42 (m, 2H), 7.36–7.31 (m, 2H), 6.63 (br. d, *J* = 6.5 Hz, 1H), 5.51 (d, *J* = 6.8 Hz, 1H), 3.94 (s, 3H), 3.73 (s, 3H), 1.22 (s, 9H); ^{13}C NMR δ 178.0, 171.8, 136.9, 134.8, 133.1, 127.8, 127.1, 126.2, 122.7, 56.3, 53.0, 39.3, 38.8, 27.5; *m/z* MS (TOF ES$^+$) $C_{18}H_{24}N_3O_3$ $[MH]^+$ calcd 330.2; found 330.2; LC-MS t_R: 3.51 min.

*4.2.45. Methyl 2-(3'-cyano-[1,1'-biphenyl]-4-yl)-2-pivalamidoacetate (**8n**)*

3-Cyanophenylboronic acid (134 mg) underwent Suzuki coupling according to General Procedure C, to give 159 mg (74%) of colourless oil. ^{1}H NMR δ 7.84–7.81 (m, 1H), 7.78 (ddd, *J* = 7.8/1.9/1.3 Hz, 1H), 7.65–7.62 (m, 1H), 7.58–7.50 (m, 3H), 7.50–7.43 (m, 2H), 6.77 (br. d, *J* = 6.5 Hz, 1H), 5.58 (d, *J* = 6.6 Hz, 1H), 3.76 (s, 3H), 1.24 (s, 9H); ^{13}C NMR δ 178.1, 171.5, 141.9, 139.2, 137.3, 131.6, 131.1, 130.8, 129.8, 128.0, 127.8, 118.9, 113.2, 56.3, 53.2, 38.8, 27.5; *m/z* MS (TOF ES$^+$) $C_{20}H_{23}FNO_3$ $[MH]^+$ calcd 351.2; found 351.2; LC-MS t_R: 3.74 min.

*4.2.46. Methyl 2-(4'-cyano-[1,1'-biphenyl]-4-yl)-2-pivalamidoacetate (**8o**)*

4-Cyanophenylboronic acid (134 mg) underwent Suzuki coupling according to General Procedure C, to give 152 mg (71%) of white solid. ^{1}H NMR δ 7.75–7.70 (m, 2H), 7.68–7.63 (m, 2H), 7.59–7.55 (m, 2H), 7.49–7.45 (m, 2H), 6.76 (br. d, *J* = 6.5 Hz, 1H), 5.58 (d, *J* = 6.6 Hz, 1H), 3.76 (s, 3H), 1.24 (s, 9H); ^{13}C NMR δ 178.0, 171.5, 145.1, 139.4, 137.6, 132.8, 127.97, 127.96, 127.9, 119.0, 111.3, 56.2, 53.2, 38.8, 27.6; *m/z* MS (TOF ES$^+$) $C_{20}H_{23}FNO_3$ $[MH]^+$ calcd 351.2; found 351.2; LC-MS t_R: 3.74 min.

*4.2.47. Methyl 3-([1,1'-biphenyl]-4-yl)-2-pivalamidopropanoate (**8p**)*

Phenylboronic acid (107 mg) underwent Suzuki coupling according to General Procedure C, to give 181 mg (91%) of white solid. ^{1}H NMR δ 7.62–7.49 (m, 4H), 7.48–7.40 (m, 2H), 7.37–7.32 (m, 1H), 7.19–7.12 (m, 2H), 6.12 (br. d, *J* = 7.5 Hz, 1H), 4.91 (ddd, *J* = 7.6/5.7/5.7 Hz, 1H), 3.77 (s, 3H), 3.23 (dd, *J* = 13.8/5.8 Hz, 1H), 3.15 (dd, *J* = 13.8/5.6 Hz, 1H), 1.17 (s, 9H); ^{13}C NMR δ 178.1, 172.4, 140.7, 140.1, 135.1, 129.9, 128.9, 127.4, 127.3, 127.1, 53.0, 52.5, 38.8, 37.5, 27.5; *m/z* MS (TOF ES^{+}) $C_{21}H_{26}NO_3$ $[MH]^{+}$ calcd 340.2; found 340.2; LC-MS t_R: 3.98 min.

*4.2.48. Methyl 3-(4-(1-methyl-1H-pyrazol-4-yl)phenyl)-2-pivalamidopropanoate (**8q**)*

1-Methyl-4-(4,4,5,5-tetramethyl-1,3,2-dioxaborolan-2-yl)-1*H*-pyrazole (182 mg) underwent Suzuki coupling according to General Procedure C, to give 114 mg (57%) of yellow solid. ^{1}H NMR δ 7.74 (d, *J* = 0.7 Hz, 1H), 7.59 (s, 1H), 7.41–7.36 (m, 2H), 7.09–7.04 (m, 2H), 6.07 (br. d, *J* = 7.5 Hz, 1H), 4.86 (dt, *J* = 7.6, 5.7 Hz, 1H), 3.94 (s, 3H), 3.75 (s, 3H), 3.17 (dd, *J* = 13.9/5.8 Hz, 1H), 3.09 (dd, *J* = 13.8/5.6 Hz, 1H), 1.16 (s, 9H); ^{13}C NMR δ 178.0, 172.4, 136.8, 134.1, 131.6, 130.0, 127.0, 125.7, 123.0, 53.0, 52.5, 39.3, 38.8, 37.6, 27.5; *m/z* MS (TOF ES^{+}) $C_{15}H_{21}BrNO_3$ $[MH]^{+}$ calcd 344.2; found 344.3; LC-MS t_R: 3.47 min.

*4.2.49. tert-Butyl (1-(4-fluorophenyl)-2-(hydroxyamino)-2-oxoethyl)carbamate (**9a**)*

Methyl 2-((*tert*-butoxycarbonyl)amino)-2-(4-fluorophenyl)acetate (**5a**) (200 mg, 0.71 mmol) was converted to the corresponding hydroxamic acid according to General Procedure D, to give 140 mg (70%) of a white solid. ^{1}H NMR (DMSO-d_6) δ 10.88 (s, 1H), 8.97 (s, 1H), 7.49–7.40 (m, 3H), 7.20–7.12 (m, 2H), 5.05 (d, *J* = 8.7 Hz, 1H), 1.37 (s, 9H); ^{13}C NMR (DMSO-d_6) δ 166.9, 161.6 (d, J_{CF} = 243.5 Hz), 154.9, 134.9, 129.1 (d, J_{CF} = 8.2 Hz), 115.0 (d, J_{CF} = 21.4 Hz), 78.4, 54.7, 28.2; *m/z* HRMS (TOF ES^{+}) $C_{13}H_{17}FN_2NaO_4$ $[M+Na]^{+}$ calcd 307.1065; found 307.1077; LC-MS t_R: 3.37 min; HPLC t_R: 5.28 min, 95%.

*4.2.50. tert-Butyl (1-(4-bromophenyl)-2-(hydroxyamino)-2-oxoethyl)carbamate (**9b**)*

2-Amino-2-(4-bromophenyl)acetic acid (**4b**) (2.00 g, 8.67 mmol) was dissolved in THF (20 mL) and water (10 mL) with stirring at RT. Boc_2O (2.09 g, 9.56 mmol, 1 eq) was added, followed by 2M NaOH $_{(aq)}$ (5.5 mL, 11 mmol, 1.27 eq). The mixture was stirred at RT overnight. TLC analysis (AcOH/MeOH/DCM 1:10:89) indicated starting material was still present, so Boc_2O (0.190 g, 0.1 eq) was added and stirring continued for 2 h at RT. The mixture was concentrated under reduced pressure to remove THF, and the resulting aqueous slurry diluted with water (20 mL). The pH was reduced with care to approximately 4, using dilute HCl $_{(aq)}$ (water acidified with 2M HCl $_{(aq)}$ to ~pH 4), before extracting with DCM (3 x 20 mL) and concentrating under reduced pressure to give 3.14 g of pale yellow viscous oil. ^{1}H NMR indicated impurities were still present, so the crude produce was dispersed in 2M NaOH $_{(aq)}$ (30 mL) and washed with Et_2O (2 x 30 mL). The aqueous layer was then carefully acidified, as before, then extracted with DCM (3 x 30 mL). The combined organic extracts were concentrated to give 2.361 g (82%) of white foamy solid, which was used without further purification. 2-(4-Bromophenyl)-2-((*tert*-butoxycarbonyl)amino)acetic acid (1.00 g, 3.03 mmol) was converted to the corresponding hydroxamic acid according to General Procedure E, using CDI (737 mg, 1.5 eq), $NH_2OH.HCl$ (421 mg, 2 eq) and anhydrous THF (15 mL). Workup was carried out using 50 mL volumes for extraction/washing. On concentration of the organic layers, 1.169 g of off-white solid was obtained. This was recrystallized from EtOH/water to give 500 mg (48%) of white crystalline solid, and 305 mg (29%) of off-white solid containing minor impurities. Total yield = 77%. ^{1}H NMR (DMSO-d_6) δ 10.90 (s, 1H), 8.99 (s, 1H), 7.54 (d, J = 8.4 Hz, 2H), 7.46 (d, J = 8.6 Hz, 1H), 7.35 (d, J = 8.4 Hz, 2H), 5.03 (d, J = 8.6 Hz, 1H), 1.37 (s, 9H); ^{13}C NMR (DMSO-d_6) δ 166.5, 157.1, 138.1, 131.1, 129.3, 120.8, 78.5, 54.9, 28.1; *m/z* HRMS (TOF ES$^+$) $C_{13}H_{17}BrN_2NaO_4$ $[M+Na]^+$ calcd 367.0264; found 367.0255; LC-MS t_R: 3.16 min; HPLC t_R: 5.85 min, 95%.

*4.2.51. tert-Butyl (3-(4-fluorophenyl)-1-(hydroxyamino)-1-oxopropan-2-yl)carbamate (**9c**)*

Methyl 3-(4-fluorophenyl)-2-((*tert*-butoxycarbonyl)amino)propanoate (**5c**) (200 mg, 0.67 mmol) was converted to the corresponding hydroxamic acid according to General Procedure D, to give 91 mg (45%) of a white solid. ^{1}H NMR (DMSO-d_6) δ 10.61 (s, 1H), 8.85 (s, 1H), 7.30–7.23 (m, 2H), 7.13–7.05 (m, 2H), 7.01 (d, *J* = 8.7 Hz, 1H), 3.98 (td, *J* = 9.5/9.5/5.1 Hz, 1H), 2.83 (dd, *J* = 13.6/5.0 Hz, 1H), 2.74 (dd, *J* = 13.6/9.9 Hz, 1H), 1.29 (s, 9H); ^{13}C NMR (DMSO-d_6) δ 168.3, 161.0 (d, J_{CF} = 241.3 Hz), 155.1, 134.2 (d, J_{CF} = 2.8 Hz), 131.0 (d, J_{CF} = 8.0 Hz), 114.7 (d, J_{CF} = 21.0 Hz), 77.9, 53.6, 36.9, 28.2; *m/z* HRMS (TOF ES$^-$) $C_{14}H_{18}FN_2O_4$ $[M-H]^-$ calcd 297.1256; found 297.1271; LC-MS t_R: 3.39 min; HPLC t_R: 5.52 min, 95%.

*4.2.52. tert-Butyl (3-(4-bromophenyl)-1-(hydroxyamino)-1-oxopropan-2-yl)carbamate (**9d**)*

Methyl 3-(4-bromophenyl)-2-((*tert*-butoxycarbonyl)amino)propanoate (**5d**) (120 mg, 0.33 mmol) was converted to the corresponding hydroxamic acid according to General Procedure D, to give 70 mg (58%) of a white solid. ^{1}H NMR (DMSO-d_6) δ 10.62 (s, 1H), 8.86 (s, 1H), 7.46 (app. d, *J* = 8.3 Hz, 2H), 7.20 (app. d, *J* = 8.3 Hz, 2H), 7.03 (d, *J* = 8.7 Hz, 1H), 3.99 (ddd, *J* = 9.4/5.2/5.2 Hz, 1H), 2.81 (dd, *J* = 13.6/5.1 Hz, 1H), 2.73 (dd, *J* = 13.5/9.9 Hz, 1H), 1.30 (s, 9H); ^{13}C NMR (DMSO-d_6) δ 168.2, 155.1, 137.5, 131.5, 130.9, 119.5, 78.0, 53.4, 37.0, 28.1; *m/z* HRMS (TOF ES$^+$) $C_{14}H_{19}BrN_2NaO_4$ $[M+Na]^+$ calcd 381.0420; found 381.0413; LC-MS t_R: 3.49 min; HPLC t_R: 6.08 min, 95%.

*4.2.53. tert-Butyl (1-(hydroxyamino)-3-(4-iodophenyl)-1-oxopropan-2-yl)carbamate (**9e**)*

Methyl 3-(4-iodophenyl)-2-((*tert*-butoxycarbonyl)amino)propanoate (**5e**) (300 mg, 0.74 mmol) was converted to the corresponding hydroxamic acid according to General Procedure D, to give 220 mg (73%) of a white solid. ^{1}H NMR (DMSO-d_6) δ 10.61 (s, 1H), 8.85 (s, 1H), 7.62 (app. d, *J* = 8.2 Hz, 2H), 7.06 (app. d, *J* = 8.2 Hz, 2H), 7.01 (d, *J* = 8.7 Hz, 1H), 3.98 (ddd, *J* = 9.3/9.3/5.2 Hz, 1H), 2.79 (dd, *J* = 13.5/5.2 Hz, 1H), 2.70 (dd, *J* = 13.6/9.9 Hz, 1H), 1.30 (s, 9H); ^{13}C NMR (DMSO-d_6) δ 168.2,

155.1, 137.9, 136.8, 131.7, 92.2, 78.0, 53.4, 37.2, 28.2; *m/z* HRMS (TOF ES$^+$) $C_{14}H_{19}IN_2NaO_4$ $[M+Na]^+$ calcd 429.0282; found 429.0282; LC-MS t_R: 3.52 min; HPLC t_R: 6.26 min, 95%.

*4.2.54. tert-Butyl (1-([1,1'-biphenyl]-4-yl)-2-(hydroxyamino)-2-oxoethyl)carbamate (**9f**)*

Methyl 2-([1,1'-biphenyl]-4-yl)-2-((*tert*-butoxycarbonyl)amino)acetate (**7a**) (142 mg, 0.42 mmol) was dissolved in MeOH (1 mL) at RT. To this was added a solution of $NH_2OH.HCl$ (43 mg, 0.62 mmol, 1.5 eq) and NaOH (50 mg, 1.25 mmol, 3 eq) in water (0.5 mL). The mixture was stirred at RT overnight. LC-MS analysis indicated the formation of both the desired hydroxamic acid, and the corresponding carboxylic acid (hydrolysis product). The mixture was concentrated under reduced pressure, and the residue taken up in acidified water (20 mL, water acidified to ~pH 4 with 2M $HCl_{(aq)}$) and extracted with EtOAc (3 x 10 mL). The combined organic layers were washed with brine (10 mL) before concentration under reduced pressure. The resulting residue was further purified by FCC (eluent MeOH/DCM 0:100 to 10:90) to give 2-([1,1'-biphenyl]-4-yl)-2-((*tert*-butoxycarbonyl)amino)acetic acid as 101 mg of glassy solid, as the major product. This was directly converted to the desired hydroxamic acid according the General Procedure E, using CDI (75 mg, 0.47 mmol, 1.5 eq), $NH_2OH.HCl$ (43 mg, 0.62 mmol, 2 eq). After stirring for 60 h, LC-MS analysis indicated conversion was not complete, so $NH_2OH.HCl$ (22 mg, 1 eq) was added and stirring continued for a further overnight period. The mixture was then worked up and purified as described, to give 34 mg (24% based on ester, 32% based on acid) of white solid. ^{1}H NMR (DMSO-d_6) δ 10.92 (s, 1H), 8.98 (d, J = 1.1 Hz, 1H), 7.70–7.57 (m, 4H), 7.57–7.40 (m, 5H), 7.39–7.32 (m, 1H), 5.10 (d, J = 8.7 Hz, 1H), 1.60–1.11 (m, 9H); ^{13}C NMR (DMSO-d_6) δ 166.9, 154.9, 139.8, 139.5, 137.9, 128.9, 127.7, 127.5, 126.7, 126.6, 78.4, 55.1, 28.2; *m/z* HRMS (TOF ES$^+$) $C_{19}H_{22}N_2NaO_4$ $[M+Na]^+$ calcd 365.1472; found 365.1469; LC-MS t_R: 3.63 min; HPLC t_R: 6.52 min, 98%.

*4.2.55. tert-Butyl (1-(2'-fluoro-[1,1'-biphenyl]-4-yl)-2-(hydroxyamino)-2-oxoethyl)carbamate (**9g**)*

Methyl 2-((*tert*-butoxycarbonyl)amino)-2-(2'-fluoro-[1,1'-biphenyl]-4-yl)acetate (**7b**) (150 mg, 0.42 mmol) was converted to the corresponding hydroxamic acid according to General Procedure D, to give 118 mg (79%) of off-white solid. ^{1}H NMR (DMSO-d_6) δ 10.93 (s, 1H), 8.99 (s, 1H), 7.57–7.37 (m, 7H), 7.36–7.25 (m, 2H), 5.12 (d, J = 8.7 Hz, 1H), 1.80–0.89 (m, 9H); ^{19}F NMR (DMSO-d_6) δ -118.46; ^{13}C NMR (DMSO-d_6) δ 166.8, 159.1 (d, J_{CF} = 245.7 Hz), 154.9, 138.4, 134.4, 130.8 (d, J_{CF} = 3.2 Hz), 129.6 (d, J_{CF} = 8.2 Hz), 128.7 (d, J_{CF} = 2.7 Hz), 127.9 (d, J_{CF} = 13.1 Hz), 127.3, 125.0 (d, J_{CF} = 3.4 Hz), 116.1 (d, J_{CF} = 22.5 Hz), 78.4, 55.2, 28.2; *m/z* HRMS (TOF ES$^+$) $C_{19}H_{20}FN_2O_4$ $[M-H]^-$ calcd 359.1413; found 359.1429; LC-MS t_R: 3.63 min; HPLC t_R: 6.55 min, > 99%.

*4.2.56. tert-Butyl (1-(3'-fluoro-[1,1'-biphenyl]-4-yl)-2-(hydroxyamino)-2-oxoethyl)carbamate (**9h**)*

Methyl 2-((*tert*-butoxycarbonyl)amino)-2-(3'-fluoro-[1,1'-biphenyl]-4-yl)acetate (**7c**) (133 mg, 0.37 mmol) was converted to the corresponding hydroxamic acid according to General Procedure D. Initially only 31 mg of product was obtained from clean fractions after FCC. Impure fractions were combined and diluted with PE. Collection of the resulting precipitate by filtration (vacuum) gave a further 32 mg of off-white solid. Overall, 63 mg (47%) of off-white solid were isolated. ^{1}H NMR (DMSO-d_6) δ 10.92 (s, 1H), 8.99 (d, J = 1.2 Hz, 1H), 7.67 (d, J = 8.3 Hz, 2H), 7.59–7.33 (m, 6H), 7.31–7.02 (m, 1H), 5.11 (d, J = 8.7 Hz, 1H), 1.65–1.00 (m, 9H); ^{19}F NMR (DMSO-d_6) δ -112.85; ^{13}C NMR (DMSO-d_6) δ 166.8, 162.7 (d, J_{CF} = 243.2 Hz), 155.8, 142.3 (d, J_{CF} = 8.0 Hz), 138.6, 138.0 (d, J_{CF} = 2.2 Hz), 130.9 (d, J_{CF} = 8.5 Hz), 127.7, 126.7, 122.7 (d, J_{CF} = 2.3 Hz), 114.2 (d, J_{CF} = 20.8 Hz), 113.4 (d, J = 22.0 Hz), 78.4, 55.1, 28.2; *m/z* HRMS (TOF ES$^+$) $C_{19}H_{21}FN_2NaO_4$ $[M+Na]^+$ calcd 383.1378; found 383.1365; LC-MS t_R: 3.65 min; HPLC t_R: 6.62 min, 98%.

4.2.57. tert-Butyl (1-(4'-fluoro-[1,1'-biphenyl]-4-yl)-2-(hydroxyamino)-2-oxoethyl)carbamate (9i)

Methyl 2-((*tert*-butoxycarbonyl)amino)-2-(4'-fluoro-[1,1'-biphenyl]-4-yl)acetate (**7d**) (149 mg, 0.41 mmol) was converted to the corresponding hydroxamic acid according to General Procedure D, to give

100 mg (67%) of off-white solid. ^{1}H NMR (DMSO-d_6) δ 10.91 (s, 1H), 8.98 (s, 1H), 7.74–7.65 (m, 2H), 7.61 (d, J = 8.3 Hz, 2H), 7.48 (d, J = 8.3 Hz, 2H), 7.43 (d, J = 8.7 Hz, 1H), 7.34–7.22 (m, 2H), 5.10 (d, J = 8.8 Hz, 1H), 1.61–1.00 (m, 9H); ^{19}F NMR (DMSO-d_6) δ -115.51; ^{13}C NMR (DMSO-d_6) δ 166.9, 161.9 (d, J_{CF} = 242.6 Hz), 154.9, 138.4, 136.3 (d, J_{CF} = 2.9 Hz), 135.5, 128.7 (d, J_{CF} = 8.2 Hz), 127.7, 126.5, 115.7 (d, J_{CF} = 21.4 Hz), 78.4, 55.1, 28.2; *m/z* HRMS (TOF ES$^+$) $C_{19}H_{21}FN_2NaO_4$ $[M+Na]^+$ calcd 383.1378; found 383.1382; LC-MS t_R: 3.59 min; HPLC t_R: 6.60 min, 99%.

*4.2.58. tert-Butyl (2-(hydroxyamino)-2-oxo-1-(2'-(trifluoromethyl)-[1,1'-biphenyl]-4-yl)ethyl)carbamate (**9j**)*

Methyl 2-((*tert*-butoxycarbonyl)amino)-2-(2'-(trifluoromethyl)-[1,1'-biphenyl]-4-yl)acetate (**7e**) (180 mg, 0.44 mmol) was converted to the corresponding hydroxamic acid according to General Procedure D, to give 127 mg (71%) off-white glassy solid. ^{1}H NMR (DMSO-d_6) δ 10.96 (s, 1H), 9.03 (s, 1H), 7.83 (d, J = 7.7 Hz, 1H), 7.71 (dd, J = 7.5/7.5 Hz, 1H), 7.61 (dd, J = 7.7/7.7 Hz, 1H), 7.55–7.43 (m, 3H), 7.38 (d, J = 7.6 Hz, 1H), 7.28 (d, J = 8.0 Hz, 2H), 5.15 (d, J = 8.9 Hz, 1H), 1.66–1.13 (m, 9H); ^{19}F NMR (DMSO-d_6) δ -55.23; ^{13}C NMR (DMSO-d_6) δ 166.9, 155.0, 140.4, 138.5, 132.3, 132.2, 131.3, 128.6, 128.1, 127.0, 126.6, 126.1 (q, J_{CF} = 5.7 Hz), 124.2 (q, J_{CF} = 273.9 Hz), 78.5, 55.1, 28.2; *m/z* HRMS (TOF ES$^+$) $C_{20}H_{21}F_3N_2NaO_4$ $[M+Na]^+$ calcd 433.1346; found 433.1328; LC-MS t_R: 3.70 min; HPLC t_R: 6.99 min, 95%.

*4.2.59. tert-Butyl (2-(hydroxyamino)-2-oxo-1-(3'-(trifluoromethyl)-[1,1'-biphenyl]-4-yl)ethyl)carbamate (**9k**)*

Methyl 2-((*tert*-butoxycarbonyl)amino)-2-(3'-(trifluoromethyl)-[1,1'-biphenyl]-4-yl)acetate (**7f**) (178 mg, 0.43 mmol) was converted to the corresponding hydroxamic acid according to General Procedure D, to give 110 mg (62%) of off-white glassy solid. ^{1}H NMR (DMSO-d_6) δ 10.93 (s, 1H), 9.00 (s, 1H), 8.05–7.91 (m, 2H), 7.80–7.66 (m, 4H), 7.53 (d, J = 8.3 Hz, 2H), 7.47 (d, J = 8.6 Hz, 1H), 5.12 (d, J = 8.7 Hz, 1H), 1.39 (s, 9H); ^{19}F NMR (DMSO-d_6) δ -60.98; ^{13}C NMR (DMSO-d_6) δ 166.8, 155.0, 140.9,

138.8, 137.8, 130.8, 130.1, 129.8 (q, J_{CF} = 31.6 Hz), 127.8, 126.9, 124.2 (q, J_{CF} = 272.5 Hz), 124.1 (q, J_{CF} = 3.7 Hz), 123.1 (q, J_{CF} = 3.9 Hz), 78.5, 55.1, 28.2; *m/z* HRMS (TOF ES$^+$) $C_{20}H_{21}F_3N_2NaO_4$ $[M+Na]^+$ calcd 433.1346; found 433.1341; LC-MS t_R: 3.72 min; HPLC t_R: 7.15 min, 98%.

*4.2.60. tert-Butyl (2-(hydroxyamino)-2-oxo-1-(4'-(trifluoromethyl)-[1,1'-biphenyl]-4-yl)ethyl)carbamate (**9l**)*

Methyl 2-((*tert*-butoxycarbonyl)amino)-2-(4'-(trifluoromethyl)-[1,1'-biphenyl]-4-yl)acetate (**7g**) (169 mg, 0.41 mmol) was converted to the corresponding hydroxamic acid according to General Procedure D. Fractions obtained after FCC were found to contain minor impurities. These were combined and diluted with PE. Collection of the resulting precipitate by filtration (vacuum) gave 68 mg (40%) of white solid. ^{1}H NMR (DMSO-d_6) δ 10.94 (s, 1H), 9.00 (s, 1H), 7.89 (d, *J* = 8.2 Hz, 2H), 7.81 (d, *J* = 8.4 Hz, 2H), 7.71 (d, *J* = 8.2 Hz, 2H), 7.54 (d, *J* = 8.3 Hz, 2H), 7.48 (d, *J* = 8.7 Hz, 1H), 5.13 (d, *J* = 8.7 Hz, 1H), 1.39 (s, 9H); ^{19}F NMR (DMSO-d_6) δ -60.88; ^{13}C NMR (DMSO-d_6) δ 166.8, 155.0, 143.8, 139.1, 137.9, 127.9 (q, J_{CF} = 31.8 Hz), 127.8, 127.5, 127.0, 125.8 (q, J_{CF} = 3.8 Hz), 124.3 (q, J_{CF} = 255.0 Hz), 78.5, 55.1, 28.2; *m/z* HRMS (TOF ES$^+$) $C_{20}H_{21}F_3N_2NaO_4$ $[M+Na]^+$ calcd 433.1346; found 433.1356; LC-MS t_R: 3.74 min; HPLC t_R: 7.21 min, 97%.

*4.2.61. tert-Butyl (2-(hydroxyamino)-2-oxo-1-(3',4',5'-trifluoro-[1,1'-biphenyl]-4-yl)ethyl)carbamate (**9m**)*

Methyl 2-((*tert*-butoxycarbonyl)amino)-2-(3',4',5'-trifluoro-[1,1'-biphenyl]-4-yl)acetate (**7h**) (152 mg, 0.38 mmol) was converted to the corresponding hydroxamic acid according to General Procedure D, to give 105 mg (69%) of off-white solid. ^{1}H NMR (DMSO-d_6) δ 10.93 (s, 1H), 9.00 (d, *J* = 1.2 Hz, 1H), 7.78–7.63 (m, 4H), 7.58–7.40 (m, 3H), 5.11 (d, *J* = 8.7 Hz, 1H), 1.38 (s, 9H); ^{19}F NMR (DMSO-d_6) δ -134.93 (d, *J* = 21.7 Hz), -163.52 (dd, *J* = 21.7/21.7 Hz); ^{13}C NMR (DMSO-d_6) δ 166.7, 155.0, 150.6 (ddd, J_{CF} = 246.2/9.5/4.1 Hz), 139.2, 138.2 (dd, J_{CF} = 248.9/15.7 Hz), 136.5 (dd, J_{CF} = 8.2/3.6 Hz), 136.1, 127.7, 126.7, 111.2 (d, J_{CF} = 21.4 Hz), 78.5, 55.1, 28.2; *m/z* HRMS (TOF ES$^+$)

$C_{19}H_{19}F_3N_2NaO_4$ $[M+Na]^+$ calcd 419.1189; found 419.1186; LC-MS t_R: 3.70 min; HPLC t_R: 6.99 min, 96%.

*4.2.62. tert-Butyl (2-(hydroxyamino)-2-oxo-1-(4-(pyridin-3-yl)phenyl)ethyl)carbamate (**9n**)*

Methyl 2-((*tert*-butoxycarbonyl)amino)-2-(4-(pyridin-3-yl)phenyl)acetate (**7i**) (121 mg, 0.35 mmol) was converted to the corresponding hydroxamic acid according to General Procedure D, to give 23 mg (19%) of white solid. ^{1}H NMR (DMSO-d_6) δ 10.93 (s, 1H), 8.99 (s, 1H), 8.88 (s, 1H), 8.57 (d, *J* = 3.6 Hz, 1H), 8.06 (d, *J* = 7.8 Hz, 1H), 7.70 (d, *J* = 8.0 Hz, 2H), 7.63–7.26 (m, 4H), 5.12 (d, *J* = 8.6 Hz, 1H), 1.39 (s, 9H); ^{13}C NMR (DMSO-d_6) δ 166.8, 155.0, 148.5, 147.7, 138.7, 136.4, 134.1, 127.8, 126.8, 123.9, 78.4, 55.1, 28.2; *m/z* HRMS (TOF ES$^+$) $C_{18}H_{21}N_3O_4$ $[MH]^+$ calcd 344.1605; found 344.1611; LC-MS t_R: 3.13 min; HPLC t_R: 4.10 min, 99%.

*4.2.63. tert-Butyl (2-(hydroxyamino)-2-oxo-1-(4-(pyridin-4-yl)phenyl)ethyl)carbamate (**9o**)*

Methyl 2-((*tert*-butoxycarbonyl)amino)-2-(4-(pyridin-4-yl)phenyl)acetate (**7j**) (177 mg, 0.52 mmol) was converted to the corresponding hydroxamic acid according to General Procedure D, to give 77 mg (44%) of off-white solid. ^{1}H NMR (DMSO-d_6) δ 10.94 (s, 1H), 9.00 (d, *J* = 1.1 Hz, 1H), 8.63 (d, *J* = 6.0 Hz, 2H), 7.78 (d, *J* = 8.3 Hz, 2H), 7.70 (dd, *J* = 4.6/1.6 Hz, 2H), 7.55 (d, *J* = 8.3 Hz, 2H), 7.50 (d, *J* = 8.7 Hz, 1H), 5.13 (d, *J* = 8.7 Hz, 1H), 1.39 (s, 9H); ^{13}C NMR (DMSO-d_6) δ 166.7, 155.0, 150.2, 146.6, 139.9, 136.4, 127.9, 126.7, 121.2, 78.5, 55.2, 28.2; *m/z* HRMS (TOF ES$^+$) $C_{18}H_{21}N_3O_4$ $[MH]^+$ calcd 344.1605; found 344.1606; LC-MS t_R: 3.11 min; HPLC t_R: 4.13 min, 97%.

*4.2.64. tert-Butyl (2-(hydroxyamino)-2-oxo-1-(4-(thiophen-3-yl)phenyl)ethyl)carbamate (**9p**)*

Methyl 2-((*tert*-butoxycarbonyl)amino)-2-(4-(thiophen-3-yl)phenyl)acetate (**7k**) (129 mg, 0.37 mmol) was converted to the corresponding hydroxamic acid according to General Procedure D, to give 94 mg (73%) of off-white solid. ^{1}H NMR (DMSO-d_6) δ 10.89 (s, 1H), 8.97 (s, 1H), 7.86 (dd, *J* = 2.9/1.3 Hz, 1H), 7.67 (d, *J* = 8.3 Hz, 2H), 7.63 (dd, *J* = 5.0/2.9 Hz, 1H), 7.55 (dd, *J* = 5.0/1.3 Hz, 1H),

7.48–7.33 (m, 3H), 5.06 (d, *J* = 8.7 Hz, 1H), 1.77–0.68 (m, 9H); ^{13}C NMR (DMSO-d_6) δ 166.9, 154.9, 141.1, 137.5, 134.5, 127.6, 127.1, 126.2, 125.9, 121.0, 78.4, 55.2, 28.2; *m/z* HRMS (TOF ES$^+$) $C_{17}H_{20}N_2NaO_4S$ $[M+Na]^+$ calcd 371.1036; found 371.1019; LC-MS t_R: 3.56 min; HPLC t_R: 6.30 min, 95%.

*4.2.65. tert-Butyl (2-(hydroxyamino)-1-(4-(1-methyl-1H-pyrazol-4-yl)phenyl)-2-oxoethyl)carbamate (**9q**).*

Methyl 2-((*tert*-butoxycarbonyl)amino)-2-(4-(1-methyl-*1H*-pyrazol-4-yl)phenyl)acetate (**7l**) (120 mg, 0.35 mmol) was converted to the corresponding hydroxamic acid according to General Procedure D, to give 73 mg (61%) of white solid. ^{1}H NMR (DMSO-d_6) δ 10.85 (s, 1H), 8.95 (s, 1H), 8.11 (s, 1H), 7.84 (d, *J* = 0.5 Hz, 1H), 7.51 (d, *J* = 8.2 Hz, 2H), 7.44–7.19 (m, 3H), 5.02 (d, *J* = 8.7 Hz, 1H), 3.85 (s, 3H), 1.69–1.03 (m, 9H); ^{13}C NMR (DMSO-d_6) δ 167.0, 154.9, 136.2, 136.0, 132.0, 127.8, 127.6, 124.7, 121.5, 78.4, 55.2, 38.7, 28.2; *m/z* HRMS (TOF ES$^+$) $C_{17}H_{22}N_4O_4$ $[MH]^+$ calcd 347.1714; found 347.1708; LC-MS t_R: 3.30 min; HPLC t_R: 5.04 min, > 99%.

*4.2.66. tert-Butyl (2-(hydroxyamino)-1-(3'-(N'-hydroxycarbamimidoyl)-[1,1'-biphenyl]-4-yl)-2-oxoethyl)carbamate (**9r**)*

Methyl 2-((*tert*-butoxycarbonyl)amino)-2-(3'-cyano-[1,1'-biphenyl]-4-yl)acetate (**7m**) (153 mg, 0.42 mmol) was converted to the corresponding hydroxamic acid according to General Procedure D, to give 91 mg (54%) of white solid. ^{1}H NMR (DMSO-d_6) δ 10.92 (s, 1H), 9.67 (s, 1H), 8.99 (s, 1H), 7.92 (s, 1H), 7.76–7.61 (m, 4H), 7.58–7.37 (m, 4H), 5.92 (s, 2H), 5.10 (d, *J* = 8.7 Hz, 1H), 1.64–1.10 (m, 9H); ^{13}C NMR (DMSO-d_6) δ 166.9, 155.0, 150.7, 139.7, 139.3, 138.1, 134.0, 128.7, 127.7, 127.1, 126.6, 124.5, 123.7, 78.4, 55.2, 28.2; *m/z* HRMS (TOF ES$^+$) $C_{20}H_{24}N_4O_5$ $[MH]^+$ calcd 401.1819; found 401.1816; LC-MS t_R: 3.17 min; HPLC t_R: 4.57 min, 95%.

*4.2.67. tert-Butyl (2-(hydroxyamino)-1-(4'-(N'-hydroxycarbamimidoyl)-[1,1'-biphenyl]-4-yl)-2-oxoethyl)carbamate (**9s**)*

Methyl 2-((*tert*-butoxycarbonyl)amino)-2-(4'-cyano-[1,1'-biphenyl]-4-yl)acetate (**7n**) (152 mg, 0.41 mmol) was converted to the corresponding hydroxamic acid according to General Procedure D, to give 67 mg (40%) of white solid. ^{1}H NMR (DMSO-d_6) δ 10.92 (s, 1H), 9.68 (s, 1H), 8.99 (d, J = 1.2 Hz, 1H), 7.85–7.59 (m, 6H), 7.60–7.28 (m, 3H), 5.85 (s, 2H), 5.10 (d, J = 8.7 Hz, 1H), 1.36 (d, J = 21.7 Hz, 9H); ^{13}C NMR (DMSO-d_6) δ 166.9, 155.0, 150.5, 140.1, 138.8, 138.1, 132.4, 127.7, 126.5, 126.3, 125.9, 78.4, 55.2, 28.2; *m/z* HRMS (TOF ES$^+$) $C_{20}H_{24}N_4O_5$ $[MH]^+$ calcd 401.1819; found 401.1815; LC-MS t_R: 3.16 min; HPLC t_R: 4.47 min, 95%.

*4.2.68. tert-Butyl (3-([1,1'-biphenyl]-4-yl)-1-(hydroxyamino)-1-oxopropan-2-yl)carbamate (**9t**)*

Methyl 3-([1,1'-biphenyl]-4-yl)-2-((tert-butoxycarbonyl)amino)propanoate (**7o**) (119 mg, 0.33 mmol) was converted to the corresponding hydroxamic acid according to General Procedure D, to give 75 mg (63%) of white solid. ^{1}H NMR (DMSO-d_6) δ 10.65 (s, 1H), 8.87 (s, 1H), 7.68–7.61 (m, 2H), 7.57 (app. d, J = 8.2 Hz, 2H), 7.48–7.42 (m, 2H), 7.37–7.31 (m, 3H), 7.05 (d, J = 8.6 Hz, 1H), 4.06 (ddd, J = 9.3/9.3/5.1 Hz, 1H), 2.89 (dd, J = 13.7/5.0 Hz, 1H), 2.80 (dd, J = 13.6/9.9 Hz, 1H), 1.30 (s, 9H); ^{13}C NMR (DMSO-d_6) δ 168.5, 155.2, 140.0, 138.1, 137.4, 129.8, 128.9, 127.2, 126.5, 126.4, 78.0, 53.6, 37.3, 28.2; *m/z* HRMS (TOF ES$^+$) $C_{20}H_{24}N_2NaO_4$ $[M+Na]^+$ calcd 379.1628; found 379.1619; LC-MS t_R: 3.60 min; HPLC t_R: 6.65 min, > 99%.

*4.2.69. tert-Butyl (1-(hydroxyamino)-3-(4-(1-methyl-1H-pyrazol-4-yl)phenyl)-1-oxopropan-2-yl)carbamate (**9u**)*

Methyl 2-((tert-butoxycarbonyl)amino)-3-(4-(1-methyl-1*H*-pyrazol-4-yl)phenyl)propanoate (**7p**) (119 mg, 0.33 mmol) was converted to the corresponding hydroxamic acid according to General Procedure D, to give 57 mg (48%) of white solid. ^{1}H NMR (DMSO-d_6) δ 10.61 (s, 1H), 8.85 (d, J = 1.4 Hz, 1H), 8.08 (s, 1H), 7.81 (d, J = 0.7 Hz, 1H), 7.45 (app. d, J = 8.1 Hz, 2H), 7.21 (app. d, J = 8.2

Hz, 2H), 6.99 (d, *J* = 8.6 Hz, 1H), 4.01 (ddd, *J* = 9.1/9.1/5.4 Hz, 1H), 3.85 (s, 3H), 2.82 (dd, *J* = 13.7/5.1 Hz, 1H), 2.74 (dd, *J* = 13.6/9.7 Hz, 1H), 1.30 (s, 9H); ^{13}C NMR (DMSO-d_6) δ 168.5, 155.1, 135.9, 135.7, 130.6, 129.6, 127.5, 124.7, 121.8, 77.9, 53.6, 38.6, 37.4, 28.2; *m/z* HRMS (TOF ES$^+$) $C_{18}H_{24}N_4O_4$ $[MH]^+$ calcd 360.1792; found 360.1781; LC-MS t_R: 3.30 min; HPLC t_R: 5.07 min, 97%.

*4.2.70. N-(1-(4-Fluorophenyl)-2-(hydroxyamino)-2-oxoethyl)pivalamide (**10a**)*

Methyl 2-(4-fluorophenyl)-2-pivalamidoacetate (**6a**) (200 mg, 0.71 mmol) was converted to the corresponding hydroxamic acid according to General Procedure D, to give 141 mg (70%) of white solid. ^{1}H NMR (DMSO-d_6) δ 10.98 (s, 1H), 9.05 (s, 1H), 7.74 (d, *J* = 8.1 Hz, 1H), 7.47–7.40 (m, 2H), 7.21–7.14 (m, 2H), 5.37 (d, *J* = 8.1 Hz, 1H), 1.13 (s, 9H); ^{13}C NMR (DMSO-d_6) δ 176.9, 166.6, 161.6 (d, J_{CF} = 243.2 Hz), 135.2 (d, J_{CF} = 3.0 Hz), 128.8 (d, J_{CF} = 8.3 Hz), 115.0 (d, J_{CF} = 21.4 Hz), 53.0, 38.1, 27.2; *m/z* HRMS (TOF ES$^+$) $C_{13}H_{17}FN_2O_3$ $[MH]^+$ calcd 269.1296; found 269.1294; LC-MS t_R: 3.32 min; HPLC t_R: 4.87 min, 95%.

*4.2.71. N-(1-(4-Bromophenyl)-2-(hydroxyamino)-2-oxoethyl)pivalamide (**10b**)*

Methyl 2-(4-bromophenyl)-2-pivalamidoacetate (**6b**) (50 mg, 0.15 mmol) was converted to the corresponding hydroxamic acid according to General Procedure D, to give 31 mg (62%) of white solid. ^{1}H NMR (DMSO-d_6) δ 11.00 (s, 1H), 9.07 (s, 1H), 7.77 (d, *J* = 8.0 Hz, 1H), 7.57–7.52 (m, 2H), 7.38–7.32 (m, 2H), 5.34 (d, *J* = 8.0 Hz, 1H), 1.13 (s, 9H); ^{13}C NMR (DMSO-d_6) δ 176.9, 166.3, 138.5, 131.2, 129.1, 120.7, 53.2, 38.1, 27.1; *m/z* HRMS (TOF ES$^+$) $C_{13}H_{17}BrN_2O_3$ $[MH]^+$ calcd 329.0495; found 329.0499; LC-MS t_R: 3.43 min; HPLC t_R: 5.48 min, 95%.

*4.2.72. 3-(4-Fluorophenyl)-N-hydroxy-2-pivalamidopropanamide (**10c**)*

Methyl 3-(4-fluorophenyl)-2-pivalamidopropanoate (**6c**) (100 mg, 0.36 mmol) was converted to the corresponding hydroxamic acid according to General Procedure D, to give 67 mg (67%) of white solid. ^{1}H NMR (DMSO-d_6) δ 10.64 (s, 1H), 8.88 (s, 1H), 7.43 (d, *J* = 8.7 Hz, 1H), 7.31–7.21 (m, 2H), 7.11–

7.02 (m, 2H), 4.39 (ddd, *J* = 8.5/8.5/6.7 Hz, 1H), 2.95–2.82 (m, 2H), 0.98 (s, 9H); ^{13}C NMR (DMSO-d_6) δ 177.0, 168.2, 160.9 (d, J_{CF} = 241.4 Hz), 134.2 (d, J_{CF} = 3.0 Hz), 131.1 (d, J_{CF} = 8.0 Hz), 114.6 (d, J_{CF} = 21.0 Hz), 51.7, 38.0, 36.7, 27.2; *m/z* HRMS (TOF ES$^+$) $C_{14}H_{19}FN_2O_3$ $[MH]^+$ calcd 283.1452; found 283.1461; LC-MS t_R: 3.36 min; HPLC t_R: 5.52 min, 95%.

*4.2.73. 3-(4-Bromophenyl)-N-hydroxy-2-pivalamidopropanamide (**10d**)*

Methyl 3-(4-bromophenyl)-2-pivalamidopropanoate (**6d**) (120 mg, 0.35 mmol) was converted to the corresponding hydroxamic acid according to General Procedure D, to give 76 mg (63%) of white solid. ^{1}H NMR (DMSO-d_6) δ 10.64 (br. s, 1H), 8.89 (br. s, 1H), 7.49–7.41 (m, 3H), 7.22–7.16 (m, 2H), 4.40 (ddd, *J* = 8.8/8.8/6.1 Hz, 1H), 2.91–2.83 (m, 2H), 0.98 (s, 9H); ^{13}C NMR (DMSO-d_6) δ 177.0, 168.1, 137.5, 131.6, 130.8, 119.4, 51.5, 38.0, 36.9, 27.2; *m/z* HRMS (TOF ES$^+$) $C_{14}H_{19}BrN_2O_3$ $[MH]^+$ calcd 343.0652; found 343.0645; LC-MS t_R: 3.43 min; HPLC t_R: 5.76 min, 95%.

*4.2.74. N-Hydroxy-3-(4-iodophenyl)-2-pivalamidopropanamide (**10e**)*

Methyl 3-(4-iodophenyl)-2-pivalamidopropanoate (**6e**) (300 mg, 0.77 mmol) was converted to the corresponding hydroxamic acid according to General Procedure D, to give 180 mg (60%) of white solid. ^{1}H NMR (DMSO-d_6) δ 10.64 (s, 1H), 8.88 (s, 1H), 7.60 (d, *J* = 8.1 Hz, 2H), 7.44 (d, *J* = 8.6 Hz, 1H), 7.05 (d, *J* = 8.1 Hz, 2H), 4.42–4.32 (m, 1H), 2.90–2.78 (m, 2H), 0.99 (s, *J* = 3.8 Hz, 9H); ^{13}C NMR (DMSO-d_6) δ 177.0, 168.0, 137.9, 136.7, 131.8, 92.1, 51.5, 38.0, 37.1, 27.2; *m/z* HRMS (TOF ES$^+$) $C_{14}H_{19}IN_2O_3$ $[MH]^+$ calcd 391.0513; found 391.0498; LC-MS t_R: 3.48 min; HPLC t_R: 5.95 min, 95%.

*4.2.75. N-(1-([1,1'-Biphenyl]-4-yl)-2-(hydroxyamino)-2-oxoethyl)pivalamide (**10f**)*

Methyl 2-([1,1'-biphenyl]-4-yl)-2-pivalamidoacetate (**8a**) (100 mg, 0.30 mmol) was converted to the corresponding hydroxamic acid according to General Procedure D, to give 64 mg (64%) of white solid. ^{1}H NMR (DMSO-d_6) δ 11.01 (s, 1H), 9.06 (s, 1H), 7.74 (d, *J* = 8.1 Hz, 1H), 7.68–7.60 (m, 4H),

7.53–7.42 (m, 4H), 7.39–7.33 (m, 1H), 5.41 (d, J = 8.1 Hz, 1H), 1.15 (s, 9H); ^{13}C NMR (DMSO-d_6) δ 176.9, 166.7, 139.8, 139.4, 138.2, 128.9, 127.5, 127.4, 126.7, 126.6, 53.5, 38.2, 27.2; *m/z* HRMS (TOF ES$^+$) $C_{19}H_{22}N_2O_3$ $[MH]^+$ calcd 327.1703; found 327.1702; LC-MS t_R: 3.51 min; HPLC t_R: 6.19 min, 98%.

*4.2.76. N-(1-(2'-Fluoro-[1,1'-biphenyl]-4-yl)-2-(hydroxyamino)-2-oxoethyl)pivalamide (**10g**)*

Methyl 2-(2'-fluoro-[1,1'-biphenyl]-4-yl)-2-pivalamidoacetate (**8b**) (112 mg, 0.33 mmol) was converted to the corresponding hydroxamic acid according to General Procedure D, to give 85 mg (76%) of white solid. ^{1}H NMR (DMSO-d_6) δ 11.03 (s, 1H), 9.07 (s, 1H), 7.76 (d, J = 8.0 Hz, 1H), 7.56–7.48 (m, 5H), 7.46–7.38 (m, 1H), 7.34–7.26 (m, 2H), 5.42 (d, J = 8.0 Hz, 1H), 1.16 (s, 9H); ^{19}F NMR (d_6-DMSO) δ -118.5; ^{13}C NMR (DMSO-d_6) δ 176.9, 166.7, 159.1 (d, J_{CF} = 245.7 Hz), 138.7, 134.3, 130.8 (d, J_{CF} = 3.3 Hz), 129.6 (d, J_{CF} = 8.3 Hz), 128.7 (d, J_{CF} = 2.7 Hz), 127.9 (d, J_{CF} = 13.2 Hz), 127.1, 125.0 (d, J_{CF} = 3.5 Hz), 116.1 (d, J_{CF} = 22.5 Hz), 53.6, 38.2, 27.2; *m/z* HRMS (TOF ES$^+$) $C_{19}H_{21}FN_2O_3$ $[MH]^+$ calcd 345.1609; found 345.1609; LC-MS t_R: 3.52 min; HPLC t_R: 6.25 min, 96%.

*4.2.77. N-(1-(3'-Fluoro-[1,1'-biphenyl]-4-yl)-2-(hydroxyamino)-2-oxoethyl)pivalamide (**10h**)*

Methyl 2-(3'-fluoro-[1,1'-biphenyl]-4-yl)-2-pivalamidoacetate (**8c**) (71 mg, 0.21 mmol) was converted to the corresponding hydroxamic acid compound according to General Procedure D, to give 45 mg (62%) of white solid. ^{1}H NMR (DMSO-d_6) δ 11.03 (s, 1H), 9.07 (s, 1H), 7.76 (d, J = 8.1 Hz, 1H), 7.71–7.65 (m, 2H), 7.55–7.46 (m, 5H), 7.23–7.15 (m, 1H), 5.42 (d, J = 8.1 Hz, 1H), 1.15 (s, 9H); ^{19}F NMR (d_6-DMSO) δ -112.8; ^{13}C NMR (DMSO-d_6) δ 176.9, 166.6, 162.7 (d, J_{CF} = 243.3 Hz), 142.3 (d, J_{CF} = 7.8 Hz), 138.9, 138.0 (d, J_{CF} = 2.2 Hz), 130.9 (d, J_{CF} = 8.6 Hz), 127.4, 126.8, 122.7 (d, J_{CF} = 2.6 Hz), 114.2 (d, J_{CF} = 21.0 Hz), 113.4 (d, J_{CF} = 22.0 Hz), 53.5, 38.2, 27.2; *m/z* HRMS (TOF ES$^+$) $C_{19}H_{21}FN_2O_3$ $[MH]^+$ calcd 345.1609; found 345.1613; LC-MS t_R: 3.53 min; HPLC t_R: 6.32 min, 96%.

*4.2.78. N-(1-(4'-Fluoro-[1,1'-biphenyl]-4-yl)-2-(hydroxyamino)-2-oxoethyl)pivalamide (**10i**)*

Methyl 2-(4'-fluoro-[1,1'-biphenyl]-4-yl)-2-pivalamidoacetate (**8d**) (99 mg, 0.29 mmol) was converted to the corresponding hydroxamic acid according to General Procedure D, to give 83 mg (83%) of white solid. ^{1}H NMR (DMSO-d_6) δ 10.99 (s, 1H), 9.06 (s, 1H), 7.74 (d, J = 8.1 Hz, 1H), 7.72–7.65 (m, 2H), 7.62 (app. d, J = 8.4 Hz, 2H), 7.48 (app. d, J = 8.3 Hz, 2H), 7.32–7.25 (m, 2H), 5.41 (d, J = 8.1 Hz, 1H), 1.15 (s, 9H); ^{19}F NMR (DMSO-d_6) δ -115.47; ^{13}C NMR (DMSO-d_6) δ 176.9, 166.7, 161.9 (d, J_{CF} = 244.3 Hz), 138.4, 138.2, 136.3 (d, J_{CF} = 3.1 Hz), 128.7 (d, J_{CF} = 8.1 Hz), 127.4, 126.6, 115.7 (d, J_{CF} = 21.3 Hz), 53.5, 38.2, 27.2; *m/z* HRMS (TOF ES$^+$) $C_{19}H_{21}FN_2O_3$ $[MH]^+$ calcd 345.1609; found 345.1613; LC-MS t_R: 3.52 min; HPLC t_R: 6.30 min, 95%.

*4.2.79. N-(1-(2',4'-Difluoro-[1,1'-biphenyl]-4-yl)-2-(hydroxyamino)-2-oxoethyl)pivalamide (**10j**)*

Methyl 2-(2',4'-difluoro-[1,1'-biphenyl]-4-yl)-2-pivalamidoacetate (**8e**) (86 mg, 0.24 mmol) was converted to the corresponding hydroxamic acid according to General Procedure D, to give 48 mg (55%) of white solid. ^{1}H NMR (DMSO-d_6) δ 11.04 (s, 1H), 9.08 (s, 1H), 7.76 (d, J = 8.0 Hz, 1H), 7.61–7.46 (m, 6H), 7.36 (ddd, J = 11.7/9.4/2.6 Hz, 1H), 7.23–7.15 (m, 1H), 5.42 (d, J = 8.0 Hz, 1H), 1.15 (s, 9H); ^{19}F NMR (DMSO-d_6) δ -111.1 (d, J = 7.5 Hz), -113.8 (d, J = 7.5 Hz); ^{13}C NMR (DMSO-d_6) δ 176.9, 166.6, 161.7 (dd, J_{CF} = 246.8, 12.2 Hz), 159.1 (dd, J_{CF} = 248.6/12.4 Hz), 138.8, 133.5, 131.9 (dd, J_{CF} = 9.7/4.8 Hz), 128.7 (d, J_{CF} = 2.4 Hz), 127.1, 124.6 (dd, J_{CF} = 13.5/3.7 Hz), 112.1 (dd, J_{CF} = 21.1/3.6 Hz), 104.5 (dd, J_{CF} = 26.7/26.1 Hz), 53.6, 38.2, 27.2; *m/z* HRMS (TOF ES$^+$) $C_{19}H_{20}F_2N_2O_3$ $[MH]^+$ calcd 363.1515; found 363.1518; LC-MS t_R: 3.55 min; HPLC t_R: 6.41 min, > 99%.

*4.2.80. N-(1-(2',6'-Difluoro-[1,1'-biphenyl]-4-yl)-2-(hydroxyamino)-2-oxoethyl)pivalamide (**10k**)*

Methyl 2-(2',6'-difluoro-[1,1'-biphenyl]-4-yl)-2-pivalamidoacetate (**8f**) (72 mg, 0.20 mmol) was converted to the corresponding hydroxamic acid according to General Procedure D, to give 49 mg (69%) of white solid. ^{1}H NMR (DMSO-d_6) δ 11.05 (s, 1H), 9.09 (s, 1H), 7.79 (d, J = 8.0 Hz, 1H),

7.57–7.39 (m, 5H), 7.26–7.17 (m, 2H), 5.43 (d, J = 8.0 Hz, 1H), 1.16 (s, 9H); ^{19}F NMR (DMSO-d_6) δ -114.8; ^{13}C NMR ($CDCl_3$) δ 177.0, 166.6, 159.4 (dd, J_{CF} = 246.5/7.1 Hz), 139.3, 131.4–128.9 (m), 127.7, 126.9, 117.4 (dd, J_{CF} = 19.2/19.2 Hz), 113.4–110.4 (m), 53.6, 38.2, 27.2; *m/z* HRMS (TOF ES$^+$) $C_{19}H_{20}F_2N_2O_3$ $[MH]^+$ calcd 363.1515; found 363.1509; LC-MS t_R: 3.50 min; HPLC t_R: 6.26 min, 96%.

*4.2.81. N-(1-(3',4'-Difluoro-[1,1'-biphenyl]-4-yl)-2-(hydroxyamino)-2-oxoethyl)pivalamide (**10l**)*

Methyl 2-(3',4'-difluoro-[1,1'-biphenyl]-4-yl)-2-pivalamidoacetate (**8g**) (150 mg, 0.40 mmol) was converted to the corresponding hydroxamic acid according to General Procedure D, to give 91 mg (64%) of white solid. ^{1}H NMR (DMSO-d_6) δ 11.03 (s, 1H), 9.08 (s, 1H), 7.81–7.72 (m, 2H), 7.66 (d, J = 8.3 Hz, 2H), 7.55–7.46 (m, 4H), 5.42 (d, J = 8.1 Hz, 1H), 1.15 (s, 9H); ^{19}F NMR (DMSO-d_6) δ -138.2 (d, J = 22.5 Hz), -140.8 (d, J = 22.5 Hz); ^{13}C NMR (DMSO-d_6) δ 176.9, 166.6, 149.8 (dd, J_{CF} = 245.1/12.7 Hz), 149.1 (dd, J_{CF} = 246.1/12.6 Hz), 138.8, 137.5 (dd, J_{CF} = 6.2/3.6 Hz), 137.2, 127.5, 126.7, 123.4 (dd, J_{CF} = 6.4/3.2 Hz), 117.9 (d, J_{CF} = 17.0 Hz), 115.7 (d, J_{CF} = 17.7 Hz), 53.5, 38.2, 27.2; *m/z* HRMS (TOF ES$^+$) $C_{19}H_{20}F_2N_2O_3$ $[MH]^+$ calcd 363.1515; found 363.1515; LC-MS t_R: 3.54 min; HPLC t_R: 6.47 min, > 99%.

*4.2.82. N-(1-(3',5'-Difluoro-[1,1'-biphenyl]-4-yl)-2-(hydroxyamino)-2-oxoethyl)pivalamide (**10m**)*

Methyl 2-(3',5'-difluoro-[1,1'-biphenyl]-4-yl)-2-pivalamidoacetate (**8h**) (83 mg, 0.23 mmol) was converted to the corresponding hydroxamic acid according to General Procedure D, to give 57 mg (68%) of white solid. ^{1}H NMR (DMSO-d_6) δ 11.03 (s, 1H), 9.08 (s, 1H), 7.78 (d, J = 8.1 Hz, 1H), 7.73 (d, J = 8.4 Hz, 2H), 7.51 (d, J = 8.3 Hz, 2H), 7.48–7.39 (m, 2H), 7.22 (dddd, J = 11.6/4.5/2.3/2.3 Hz, 1H), 5.43 (d, J = 8.1 Hz, 1H), 1.15 (s, 9H); ^{19}F NMR (DMSO-d_6) δ -109.5; ^{13}C NMR (DMSO-d_6) δ 176.9, 166.6, 162.9 (dd, J_{CF} = 245.5/13.7 Hz), 143.4, 139.6, 136.8, 127.5, 126.8, 110.1–109.5 (m), 102.7 (dd, J_{CF} = 26.0/26.0 Hz), 53.5, 38.2, 27.2; *m/z* HRMS (TOF ES$^+$) $C_{19}H_{20}F_2N_2O_3$ $[MH]^+$ calcd 363.1515; found 363.1528; LC-MS t_R: 3.57 min; HPLC t_R: 6.51 min, 97%.

*4.2.83. N-(1-(2',4',6'-Trifluoro-[1,1'-biphenyl]-4-yl)-2-(hydroxyamino)-2-oxoethyl)pivalamide (**10n**)*

Methyl 2-pivalamido-2-(2',4',6'-trifluoro-[1,1'-biphenyl]-4-yl)acetate (**8i**) (105 mg, 0.28 mmol) was converted to the corresponding hydroxamic acid according to General Procedure D, to give 58 mg (55%) of white solid. ^{1}H NMR (DMSO-d_6) δ 11.03 (s, 1H), 9.07 (s, 1H), 7.77 (d, J = 8.0 Hz, 1H), 7.52 (d, J = 8.2 Hz, 2H), 7.41 (d, J = 8.2 Hz, 2H), 7.38–7.27 (m, 2H), 5.43 (d, J = 8.0 Hz, 1H), 1.16 (s, J = 7.5 Hz, 9H); ^{19}F NMR (DMSO-d_6) δ -108.6 (dd, J = 6.1/6.1 Hz), -111.7 (d, J = 6.2 Hz); ^{13}C NMR (DMSO-d_6) δ 177.0, 166.6, 162.6 (d, J_{CF} = 16.4 Hz), 160.2, 159.6 (ddd, J_{CF} = 25.7/15.3/9.9 Hz), 139.4, 130.1, 127.0, 114.3 (d, J_{CF} = 4.8 Hz), 102.3 – 99.9 (m), 53.6, 38.2, 27.2; *m/z* HRMS (TOF ES$^+$) $C_{19}H_{19}F_3N_2O_3$ $[MH]^+$ calcd 381.1421; found 381.1419; LC-MS t_R: 3.53 min; HPLC t_R: 6.25 min, 99%.

*4.2.83. N-(2-(Hydroxyamino)-2-oxo-1-(3',4',5'-trifluoro-[1,1'-biphenyl]-4-yl)ethyl)pivalamide (**10o**)*

Methyl 2-pivalamido-2-(3',4',5'-trifluoro-[1,1'-biphenyl]-4-yl)acetate (**8j**) (50 mg, 0.13 mmol) was converted to the corresponding hydroxamic acid according to General Procedure D, to give 44 mg (88%) of white solid. ^{1}H NMR (DMSO-d_6) δ 11.02 (s, 1H), 9.07 (s, 1H), 7.78 (d, J = 8.1 Hz, 1H), 7.74–7.65 (m, 4H), 7.50 (d, J = 8.3 Hz, 2H), 5.42 (d, J = 8.1 Hz, 1H), 1.15 (s, 9H); ^{19}F NMR (DMSO-d_6) δ -134.74 (d, J = 21.7 Hz), -163.41 (dd, J = 21.7/21.7 Hz); ^{13}C NMR (DMSO-d_6) δ 176.9, 166.5, 150.6 (ddd, J_{CF} = 14.0/9.5/4.0 Hz), 139.5, 136.7–136.4 (m), 136.2–136.0 (m), 127.5, 126.8, 111.5–110.7 (m), 53.5, 38.2, 27.2; *m/z* HRMS (TOF ES$^+$) $C_{19}H_{19}F_3N_2O_3$ $[MH]^+$ calcd 381.1421; found 381.1425; LC-MS t_R: 3.60 min; HPLC t_R: 6.71 min, 98%.

*4.2.84. N-(1-(2',3',4',5',6'-Pentafluoro-[1,1'-biphenyl]-4-yl)-2-(hydroxyamino)-2-oxoethyl) pivalamide (**10p**)*

Methyl 2-(2',3',4',5',6'-pentafluoro-[1,1'-biphenyl]-4-yl)-2-pivalamidoacetate (**8k**) (92 mg, 0.22 mmol) was converted to the corresponding hydroxamic acid according to General Procedure D, to give 50 mg (55%) of white solid. ^{1}H NMR (DMSO-d_6) δ 11.12 (s, 1H), 7.74 (d, J = 7.9 Hz, 1H), 7.55 (d, J = 8.3 Hz, 2H), 7.48 (d, J = 8.2 Hz, 2H), 5.42 (d, J = 7.9 Hz, 1H), 1.14 (s, 9H); ^{19}F NMR (DMSO-d_6) δ -

143.5 (dd, *J* = 24.8/7.7 Hz), -156.0 (dd, *J* = 22.3/22.3 Hz), -162.5–-162.7 (m); ^{13}C NMR (DMSO-d_6) δ 177.5, 166.7, 145.3–142.5 (m), 141.5–138.6 (m), 138.9–136.1 (m), 130.4, 127.5, 125.3, 115.6–115.0 (m), 53.9, 38.4, 27.4; *m/z* HRMS (TOF ES$^+$) $C_{19}H_{17}F_5N_2O_3$ $[MH]^+$ calcd 417.1232; found 417.1244; LC-MS t_R: 3.61 min; HPLC t_R: 5.95 min, 95%.

*4.2.85. N-(2-(Hydroxyamino)-2-oxo-1-(4-(thiophen-3-yl)phenyl)ethyl)pivalamide (**10q**)*

Methyl 2-pivalamido-2-(4-(thiophen-3-yl)phenyl)acetate (**8l**) (89 mg, 0.27 mmol) was converted to the corresponding hydroxamic acid according to General Procedure D, to give 82 mg (91%) of white solid. ^{1}H NMR (DMSO-d_6) δ 11.00 (s, 1H), 9.05 (s, 1H), 7.86 (dd, *J* = 2.9/1.3 Hz, 1H), 7.72 (d, *J* = 8.1 Hz, 1H), 7.70–7.66 (m, 2H), 7.63 (dd, *J* = 5.0/2.9 Hz, 1H), 7.55 (dd, *J* = 5.0/1.3 Hz, 1H), 7.43 (app. d, *J* = 8.2 Hz, 2H), 5.38 (d, *J* = 8.1 Hz, 1H), 1.15 (s, 9H); ^{13}C NMR (DMSO-d_6) δ 176.8, 166.7, 141.1, 137.8, 134.4, 127.3, 127.1, 126.2, 126.0, 121.0, 53.5, 38.2, 27.2; *m/z* HRMS (TOF ES$^+$) $C_{17}H_{20}N_2O_3S$ $[MH]^+$ calcd 333.1267; found 333.1266; LC-MS t_R: 3.48 min; HPLC t_R: 6.02 min, > 99%.

*4.2.86. N-(2-(Hydroxyamino)-1-(4-(1-methyl-1H-pyrazol-4-yl)phenyl)-2-oxoethyl)pivalamide (**10r**)*

Methyl 2-(4-(1-methyl-1*H*-pyrazol-4-yl)phenyl)-2-pivalamidoacetate (**8m**) (81 mg, 0.24 mmol) was converted to the corresponding hydroxamic acid according to General Procedure D, to give 52 mg (66%) of white solid. ^{1}H NMR (DMSO-d_6) δ 10.89 (s, 1H), 9.03 (s, 1H), 8.11 (s, 1H), 7.84 (s, 1H), 7.67 (d, *J* = 8.0 Hz, 1H), 7.52 (app. d, *J* = 8.1 Hz, 2H), 7.36 (app. d, *J* = 8.1 Hz, 2H), 5.34 (d, *J* = 8.0 Hz, 1H), 3.85 (s, 3H), 1.14 (s, 9H); ^{13}C NMR (DMSO-d_6) δ 176.8, 166.8, 136.5, 136.0, 131.9, 127.8, 127.3, 124.8, 121.5, 53.5, 38.7, 38.1, 27.2; *m/z* HRMS (TOF ES$^+$) $C_{17}H_{22}N_4O_3$ $[MH]^+$ calcd 331.1765; found 331.1765; LC-MS t_R: 3.26 min; HPLC t_R: 4.71 min, > 99%.

*4.2.87. N-(2-(Hydroxyamino)-1-(3'-(N'-hydroxycarbamimidoyl)-[1,1'-biphenyl]-4-yl)-2-oxoethyl)pivalamide (**10s**)*

Methyl 2-(3'-cyano-[1,1'-biphenyl]-4-yl)-2-pivalamidoacetate (**8n**) (121 mg, 0.35 mmol) was converted to the corresponding hydroxamic acid according to General Procedure D, to give 78 mg (58%) of white solid. ^{1}H NMR (DMSO-d_6) δ 11.02 (s, 1H), 9.66 (s, 1H), 9.07 (s, 1H), 7.94–7.91 (m, 1H), 7.75 (d, *J* = 8.1 Hz, 1H), 7.71–7.63 (m, 4H), 7.51 (app. d, *J* = 8.3 Hz, 2H), 7.45 (t, *J* = 7.8 Hz, 1H), 5.92 (s, 2H), 5.42 (d, *J* = 8.0 Hz, 1H), 1.16 (s, 9H); ^{13}C NMR (DMSO-d_6) δ 176.9, 166.7, 150.7, 139.7, 139.2, 138.4, 134.0, 128.8, 127.4, 127.1, 126.7, 124.5, 123.7, 53.5, 38.2, 27.2; *m/z* HRMS (TOF ES$^+$) $C_{20}H_{24}N_4O_4$ $[MH]^+$ calcd 385.1870; found 385.1870; LC-MS t_R: 3.19 min; HPLC t_R: 4.28 min, 95%.

*4.2.88. N-(2-(Hydroxyamino)-1-(4'-(N'-hydroxycarbamimidoyl)-[1,1'-biphenyl]-4-yl)-2-oxoethyl)pivalamide (**10t**)*

Methyl 2-(4'-cyano-[1,1'-biphenyl]-4-yl)-2-pivalamidoacetate (**8o**) (62 mg, 0.18 mmol) was converted to the corresponding hydroxamic acid according to General Procedure D, to give 15 mg (22%) of white solid. ^{1}H NMR (DMSO-d_6) δ 11.01 (s, 1H), 9.68 (s, 1H), 9.06 (s, 1H), 7.79–7.72 (m, 3H), 7.70–7.64 (m, 4H), 7.49 (app. d, *J* = 8.3 Hz, 2H), 5.84 (br. s, 2H), 5.41 (d, *J* = 8.0 Hz, 1H), 1.15 (s, 9H); ^{13}C NMR (DMSO-d_6) δ 176.9, 166.7, 150.5, 140.1, 138.8, 138.4, 132.4, 127.4, 126.5, 126.3, 125.9, 53.5, 38.2, 27.2; *m/z* HRMS (TOF ES$^+$) $C_{20}H_{24}N_4O_4$ $[MH]^+$ calcd 385.1870; found 385.1883; LC-MS t_R: 3.16 min; HPLC t_R: 4.18 min, 95%.

*4.2.89. 3-([1,1'-Biphenyl]-4-yl)-N-hydroxy-2-pivalamidopropanamide (**10u**)*

Methyl 3-([1,1'-biphenyl]-4-yl)-2-pivalamidopropanoate (**8p**) (92 mg, 0.27 mmol) was converted to the corresponding hydroxamic acid according to General Procedure D, to give 50 mg (54%) of white solid. ^{1}H NMR (DMSO-d_6) δ 10.66 (s, 1H), 8.89 (s, 1H), 7.66–7.60 (m, 2H), 7.56 (app. d, *J* = 8.3 Hz, 2H), 7.49–7.41 (m, 3H), 7.37–7.30 (m, 3H), 4.49–4.41 (m, 1H), 3.00–2.90 (m, 2H), 1.00 (s, 9H); ^{13}C

NMR (DMSO-d_6) δ 177.0, 168.2, 140.0, 138.0, 137.4, 129.9, 128.9, 127.2, 126.5, 126.2, 51.7, 38.0, 37.2, 27.2; *m/z* HRMS (TOF ES$^+$) $C_{20}H_{24}N_2O_3$ $[MH]^+$ calcd 341.1860; found 341.1862; LC-MS t_R: 3.54 min; HPLC t_R: 6.35 min, > 99%.

*4.2.90. N-Hydroxy-3-(4-(1-methyl-1H-pyrazol-4-yl)phenyl)-2-pivalamidopropanamide (**10v**)*

Methyl 3-(4-(1-methyl-1*H*-pyrazol-4-yl)phenyl)-2-pivalamidopropanoate (**8q**) (85 mg, 0.25 mmol) was converted to the corresponding hydroxamic acid according to General Procedure D, to give 59 mg (69%) of white solid. ^{1}H NMR (DMSO-d_6) δ 10.64 (s, 1H), 8.88 (d, *J* = 0.9 Hz, 1H), 8.07 (s, 1H), 7.81 (d, *J* = 0.7 Hz, 1H), 7.46–7.38 (m, 3H), 7.20 (app. d, *J* = 8.2 Hz, 2H), 4.45–4.37 (m, 1H), 3.84 (s, 3H), 2.88 (d, *J* = 7.4 Hz, 2H), 0.99 (s, 9H); ^{13}C NMR (DMSO-d_6) δ 177.0, 168.3, 135.9, 135.6, 130.6, 129.7, 127.6, 124.5, 121.8, 51.8, 38.6, 38.0, 37.3, 27.2; *m/z* HRMS (TOF ES$^+$) $C_{18}H_{24}N_4O_3$ $[MH]^+$ calcd 345.1921; found 345.1909; LC-MS t_R: 3.27 min; HPLC t_R: 4.72 min, > 99%.

4.3. Biochemistry

4.3.1. Preparation of recombinant PfA-M1 and PfA-M17

The production of recombinant malaria neutral aminopeptidases *Pf*A-M1 and *Pf*A-M17 was undertaken in *Escherichia coli* and proteins purified using a two-step purification process of Ni-NTA-agarose column followed by size exclusion chromatography on a Superdex 200 16/60 using an AKTAxpress high throughput chromatography system (http://proteinexpress.med.monash.edu.au/index.htm) as described previously [9, 12]. Biochemical analysis indicated that kinetic parameters (k_{cat}, K_m, k_{cat}/K_m) of material purified and used in subsequent crystallization trials were the same as published.

4.3.2. Enzymatic analysis

Aminopeptidase assays were based on previously published protocols [8]. Briefly, the activity of both enzymes was determined by measuring the release of the fluorogenic leaving group, NHMec,

from the fluorogenic peptide *L*-Leucine-7-amido-4-methylcoumarin hydrochloride (H-Leu-NHMec) (Sigma L2145). The reactions were carried out in 384-well microtitre plates, 50 μL total volume at 37°C using a spectrofluorimeter (BMG FLUOstar) with excitation at 355 nm and emission at 460 nm. *Pf*A-M1 was pre-incubated in 100 mM Tris pH 8.0 at 37°C and *Pf*A-M17 in 50 mM Tris pH 8.0, 2 mM $CoCl_2$, with the inhibitors for 10 min prior to the addition of substrate. Inhibitor concentrations were assayed between 500pM – 500 μM. The fluorescence signal was monitored until a final steady state velocity, V, was obtained. The K_i values were then evaluated using Dixon plots of 1/V versus inhibitor concentration in which the substrate concentration was maintained below the K_m of the enzyme. Statistical analysis including point of intersection (-K_i) and graphical output was performed in GraphPad Prism® 6. Representative Dixon plots of selected inhibitors can be found in Supp Fig 8.

4.3.3. Crystallisation and X-ray Data Collection

Nine *Pf*A-M1 co-crystal structures (with compounds **9b**, **9f**, **9m**, **9q**, **9r**, **10b**, **10o**, **10q**, **10s**), and six *Pf*A-M17 co-crystal structures (with compounds **9b**, **10b**, **10o**, **10q**, **10r**, **10s**) were determined in this study. A summary of statistics is provided in Supplementary Table 1, 2 and 3. Crystals of the *Pf*A-M1 bound complexes were obtained by co-crystallization of each compound with *Pf*A-M1 in mother liquor containing 1 mM ligand. For *Pf*A-M17 bound complexes, prior to data collection, crystals were soaked in mother liquor containing 1 mM ligand and 1 mM $ZnSO_4$. Data were collected at 100 K using synchrotron radiation at the Australian Synchrotron using the macro crystallography MX1 beamline 3BM1 [32] for *Pf*A-M1 and the micro crystallography MX2 beamline 3ID1 for *Pf*A-M17. Diffraction images were processed and integrated using iMosflm [33] (*Pf*A-M1) or XDS [34] (*Pf*A-M17), scaled using Aimless [35] and solved by molecular replacement using Phaser [36] as part of the CCP4 suite [37]. The structures were refined using iterative cycles of PHENIX [38], with 5% of reflections set aside from refinement for calculation of R_{Free}. Between refinement cycles, the protein structure, solvent and inhibitors were was manually built into $2F_o–F_c$ and $F_o–F_c$ electron density maps using

COOT [39], with restraint files generated by the PRODRG2 Server [40] where necessary. The coordinates and structure factors are available from the Protein Data Bank with PDB Accession codes, *Pf*A-M1: **9b** (4ZW3), **9f** (4ZW5), **9q** (4ZW6), **9m** (4ZW7), **9r** (4ZW8), **10b** (4ZX3), **10o** (4ZX4), **10q** (4ZX5), **10s** (4ZX6), and *Pf*A-M17: **9b** (4ZX8), **10b** (4ZX9), **10o** (4ZY2), **10q** (4ZY0), **10r** (4ZY1), **10s** (4ZYQ).

4.4. Biology

4.4.1. P. falciparum culture

In vitro parasite culture of the *P. falciparum* strains 3D7, Dd2 and NITD609-R Dd2 clone#2 [28] were maintained in RPMI with 10 mM Hepes (Life Technologies), 50 μg/mL hypoxanthine (Sigma) and 5% Human serum from male AB plasma and 2.5 mg/mL AlbuMAX II® (Life Technologies). Human 0+ erythrocytes were obtained from the Australian Red Cross Blood Service (Agreement No: 13-04QLD-09). The parasites were maintained at 2-8 % parasitaemia (% P) at 5 % haematocrit (% H), incubated at 37 °C, 5 % CO_2, 5 % O_2, 90 % N_2 and 95 % humidity.

4.4.2. P. falciparum growth inhibition assay

A well-established *P. falciparum* imaging assay was used to assess parasite growth inhibition [41]. In brief, sorbitol (5% w/v) synchronisation was performed twice, approximately 8 h apart, on each synchronisation day for two consecutive ring cycles i.e. on day 1 and 3 of assay preparation. On day 2 the culture was split to approximately 2 % trophozoite parasitaemia. On day 4 the culture was split to 1-1.5% trophozoite parasitaemia, which yielded approximately 8% ring parasitaemia after 48 h on day 5, the day of the assay setup.

Compound stocks (10 mM in 100 % DMSO) were diluted 1 in 25 in H_2O just prior to use. An additional 1 in 10 dilution was performed, resulting in a 1:250 overall compound dilution and a final DMSO concentration of 0.4%. For dose response curves a three step logarithmic serial dilution was

prepared at 20 μM top concentration for test compounds for the asexual assay and 2 μM for the positive control, artemisinin. 5 μL of the diluted test compound or control solutions (2 μM artemisinin as positive and 0.4% DMSO as negative control) were added to 384 well CellCarrier imaging plates (PerkinElmer). Two biological replicates (each performed in duplicate) were performed for each compound (n=2).

Parasite cultures were added to a final concentration of 2 % parasitemia and 0.3 % haematocrit. Plates were incubated for 72 h at 37 °C, 5 % CO_2 and 95 % humidity. On day 8 the permeabilization and nuclear staining buffer was prepared in PBS containing 10 μg/mL saponin, 0.01% triton X, 5 mM EDTA (all: Sigma) and 0.5 μg/mL 4′,6-diamidino-2-phenylindole (DAPI; Life Technologies) [41].

The plates were incubated at RT overnight, before confocal imaging on an Opera™ Confocal Imager (PerkinElmer) at 405 nm excitation with a 20x water objective. Automated primary image analysis was performed concurrent with the imaging process, utilizing an Acapella® software (PerkinElmer) script to determine the number of parasites based on object size and fluorescence intensity [41]. Determination of the % growth compared to controls (2 μM artemisinin as positive and 0.4% DMSO as negative control) was performed in Microsoft Excel® 2013. Statistical analysis including IC_{50} determination and graphical output was performed in GraphPad Prism® 6 using nonlinear regression variable slope curve fitting. Representative growth inhibition and cytotoxicity curves of selected inhibitors can be found in Supp Fig 8.

4.4.3. HEK293 viability assay

To assess cytotoxicity of compounds in dose response, a resazurin-based assay was utilized to test for cell viability. In brief, HEK293 cells were grown in DMEM medium (Life Technologies) containing 10% fetal calf serum (FCS; Gibco). Cells were trypsinised, counted and seeded at 2000 cells per well in 45 μL media into TC-treated 384-well plates (Greiner) and left to adhere overnight at 37 °C, 5 % CO_2 and 95% humidity.

Test compounds were prepared by diluting compounds 1 in 25 in sterile water and then another 1 in 10 dilution, to give a top final test concentration of 40 μM, 0.4% DMSO. Plates were incubated for 72 h at 37 °C, 5% CO_2 and 95 % humidity, then the media was removed and replaced by 35 μL of 44 μM resazurin in DMEM without FCS. The plates were incubated for another 4-6 h at 37 °C, 5 % CO_2 and 95 % humidity, before reading on an EnVision® Plate Reader (PerkinElmer) using fluorescence excitation/emission settings of 530 nm/595 nm. The % growth was standardized to controls (40 μM puromycin as positive and 0.4 % DMSO as negative control) using Microsoft Excel® 2013. Statistical analysis including IC_{50} determination and graphical output was performed in GraphPad Prism® 6 using nonlinear regression variable slope curve fitting.

4.5. *In Vitro* ADME Studies

4.5.1. LogD Measurement

Partition coefficient values (LogD) of the test compound were estimated using a gradient HPLC based derivation of the method developed by Lombardo [42]. Data were collected using a Waters 2795 HPLC instrument with a Waters 2487 dual channel UV detector (operated at 220 and 254 nm) with a Phenomenex Synergi Hydro-RP 4 μm (30 mm × 2 mm) column. The mobile phase comprised aqueous buffer (50 mM ammonium acetate, pH 7.4) and acetonitrile with an acetonitrile gradient of 0% to 100% over 13.5 min. Compound retention properties were compared to a set of nine standard compounds with known partition coefficients determined using shake flask methods.

4.5.2. Solubility Estimation

Kinetic solubility was determined by serial dilution of a concentrated stock solution prepared in DMSO, spiked into either pH 6.5 phosphate buffer or HCl (0.01 M, approx pH 2.0) with the final DMSO concentration being 1%. Samples were then analysed via Nephelometry to determine a solubility range [43].

4.5.3. In vitro Plasma Stability

Human plasma (pooled; n=3 donors procured from the Australian Red Cross Blood Service) or mouse plasma (pooled; multiple mice procured from Animal Resources Centre, Perth) was separated from whole blood and stored frozen at -80°C. On the day of the experiment, frozen plasma was thawed and an aliquot spiked with a DMSO/acetonitrile/water solution of test compound to a nominal compound concentration of 500 ng/mL (final DMSO and acetonitrile concentrations were 0.2 and 0.4% (v/v), respectively). Spiked plasma was incubated at 37°C for 4 h (human) or 6 h (mouse), and at various time points, duplicate plasma samples were taken and immediately snap-frozen in dry ice. All plasma samples were stored frozen (−20°C) until analysis by UPLC/MC (using a Waters/Micromass Quattro Premier triple quadrupole mass spectrometer coupled to a Waters Acquity UPLC) relative to calibration standards prepared in matched blank plasma. At each sample time, the average concentration of test compound was expressed as a percentage remaining, and these data were used to calculate the apparent degradation half-life by fitting to an exponential decay function.

4.5.4. In vitro Microsomal Stability

Human or mouse liver microsomes (Xenotech, LLC, Lenexa, KS) were suspended in 0.1 M phosphate buffer (pH 7.4) at a final protein concentration of 0.4 mg/mL and incubated with test compound (1 μM) at 37°C. An NADPH-regenerating system (1 mg/mL NADP, 1 mg/mL glucose-6-phosphate, 1 U/mL glucose-6-phosphate dehydrogenase) and $MgCl_2$ (0.67 mg/mL) was added to initiate the metabolic reactions, which were subsequently quenched with ice-cold acetonitrile at time points ranging from 0 to 60 min. Samples were then subjected to centrifugation, and the concentration of parent compound remaining in the supernatant was monitored by LC-MS (Waters Micromass Xevo G2 QTOF coupled to a Waters Acquity UPLC). The first order rate constant for substrate depletion was determined by fitting the data to an exponential decay function, and these values were used to calculate the *in vitro* intrinsic clearance that was scaled to predict the *in vivo* intrinsic clearance.

Acknowledgements

We thank the National Health and Medical Research Council (Project Grant 1063786 to SM and PJS) and the ARC (LP120200557 to VMA) for funding support. C. Ruggeri was an Endeavour Fellowship recipient (4100-2014). We thank the Australian Synchrotron (MX-1 & MX-2) and the beamline scientists for beamtime (CAP8208) and for technical assistance. We thank the Monash Platforms (Protein Production and Crystallization) for technical assistance and the Australian Red Cross Blood Service for the provision of human blood. We thank Dr Sabine Fletcher for technical assistance with the *in vitro P. falciparum* studies and Dr Jason Dang for obtaining MS data.

Appendix A. Supplementary data

Supporting Information Available: NMR spectra of synthesized compounds, binding of selected inhibitors to *Pf*A-M1 and *Pf*A-M17, representative compound electron density, data collection and refinement statistics and SMILES codes. Accession Codes. PDB Accession codes, *Pf*A-M1: **9b** (4ZW3), **9f** (4ZW5), **9q** (4ZW6), **9m** (4ZW7), **9r** (4ZW8), **10b** (4ZX3), **10o** (4ZX4), **10q** (4ZX5), **10s** (4ZX6), and *Pf*A-M17: **9b** (4ZX8), **10b** (4ZX9), **10o** (4ZY2), **10q** (4ZY0), **10r** (4ZY1), **10s** (4ZYQ).

References

[1] WHO. *World malaria report*. World Health Organization: Geneva, Switzerland, 2014; p 1-242.

[2] A. E. Ashley, M. Dhorda, R. M. Fairhurst, C. Amaratunga, P. Lim, S. Suon, S. Sreng, J. M. Anderson, S. Mao, B. Sam, C. Sopha, C. M. Chuor, C. Nguon, S. Sovannaroth, S. Pukrittayakamee, P. Jittamala, K. Chotivanich, K. Chutasmit, C. Suchatsoonthorn, R. Runcharoen, T. T. Hien, N. T. Thuy-Nhien, N. V. Thanh, N. H. Phu, Y. Htut, K. T. Han, K. H.

Aye, O. A. Mokuolu, R. R. Olaosebikan, O. O. Folaranmi, M. Mayxay, M. Khanthavong, B. Hongvanthong, P. N. Newton, M. A. Onyamboko, C. I. Fanello, A. K. Tshefu, N. Mishra, N. Valecha, A. P. Phyo, F. Nosten, P. Yi, R. Tripura, S. Borrmann, M. Bashraheil, J. Peshu, M. A. Faiz, A. Ghose, M. A. Hossain, R. Samad, M. R. Rahman, M. M. Hasan, A. Islam, O. Miotto, R. Amato, B. MacInnis, J. Stalker, D. P. Kwiatkowski, Z. Bozdech, A. Jeeyapant, P. Y. Cheah, T. Sakulthaew, J. Chalk, B. Intharabut, K. Silamut, S. J. Lee, B. Vihokhern, C. Kunasol, M. Imwong, J. Tarning, W. J. Taylor, S. Yeung, C. J. Woodrow, J. A. Flegg, D. Das, J. Smith, M. Venkatesan, C. V. Plowe, K. Stepniewska, P. J. Guerin, A. M. Dondorp, N. P. Day, N. J. White, Spread of artemisinin resistance in *Plasmodium falciparum* malaria. New Engl. J. Med. **371** (2014) 411-423.

[3] J. Liu, E. S. Istvan, I. Y. Gluzman, J. Gross, D. E. Goldberg, *Plasmodium falciparum* ensures its amino acid supply with multiple acquisition pathways and redundant proteolytic enzyme systems. P. Natl. Acad. Sci. USA **103** (2006) 8840-8845.

[4] P. J. Rosenthal, Hydrolysis of erythrocyte proteins by proteases of malaria parasites. Curr. Opin. Hematol. **9** (2002) 140-145.

[5] M. B. Harbut, G. Velmourougane, S. Dalal, G. Reiss, J. C. Whisstock, O. Onder, D. Brisson, S. McGowan, M. Klemba, D. C. Greenbaum, Bestatin-based chemical biology strategy reveals distinct roles for malaria M1-and M17-family aminopeptidases. P. Natl. Acad. Sci. USA **108** (2011) E526-E534.

[6] M. Klemba, I. Gluzman, D. E. Goldberg, A *Plasmodium falciparum* dipeptidyl aminopeptidase I participates in vacuolar hemoglobin degradation, J. Biol. Chem. **279** (2004) 43000-43007.

[7] S. McGowan, Working in concert: The metalloaminopeptidases from *Plasmodium falciparum*, Curr. Opin. Struct. Biol. **23** (2013) 828-835.

[8] C. M. Stack, J. Lowther, E. Cunningham, S. Donnelly, D. L. Gardiner, K. R. Trenholme, T. S. Skinner-Adams, F. Teuscher, J. Grembecka, A. Mucha, P. Kafarski, L. Lua, A. Bell, J. P. Dalton,

Characterization of the *Plasmodium falciparum* M17 leucyl aminopeptidase - a protease involved in amino acid regulation with potential for antimalarial drug development, J. Biol. Chem. **282** (2007) 2069-2080.

[9] S. McGowan, C. J. Porter, J. Lowther, C. M. Stack, S. J. Golding, T. S. Skinner-Adams, K. R. Trenholme, F. Teuscher, S. M. Donnelly, J. Grembecka, A. Mucha, P. Kafarski, R. DeGori, A. M. Buckle, D. L. Gardiner, J. C. Whisstock, J. P. Dalton, Structural basis for the inhibition of the essential *Plasmodium falciparum* M1 neutral aminopeptidase, P. Natl. Acad. Sci. USA **106**, (2009) 2537-2542.

[10] T. S. Skinner-Adams, J. Lowther, F. Teuscher, C. M. Stack, J. Grembecka, A. Mucha, P. Kafarski, K. R. Trenholme, J. P. Dalton, D. L. Gardiner, Identification of phosphinate dipeptide analog inhibitors directed against the *Plasmodium falciparum* M17 leucine aminopeptidase as lead antimalarial compounds, J. Med. Chem. **50** (2007) 6024-6031.

[11] T. S. Skinner-Adams, C. L. Peatey, K. Anderson, K. R. Trenholme, D. Krige, C. L. Brown, C. Stack, D. M. M. Nsangou, R. T. Mathews, K. Thivierge, J. P. Dalton, D. L. Gardinerd, The aminopeptidase inhibitor CHR-2863 is an orally bioavailable inhibitor of murine malaria, Antimicrob. Agents Ch. **56** (2012) 3244-3249.

[12] S. McGowan, C. A. Oellig, W. A. Birru, T. T. Caradoc-Davies, C. M. Stack, J. Lowther, T. Skinner-Adams, A. Mucha, P. Kafarski, J. Grembecka, K. R. Trenholme, A. M. Buckle, D. L. Gardiner, J. P. Dalton, J. C. Whisstock, Structure of the *Plasmodium falciparum* M17 aminopeptidase and significance for the design of drugs targeting the neutral exopeptidases, P. Natl. Acad. Sci. USA **107** (2010) 2449-2454.

[13] R. Deprez-Poulain, M. Flipo, C. Piveteau, F. Leroux, S. Dassonneville, I. Florent, L. Maes, P. Cos, B. Deprez, Structure-activity relationships and blood distribution of antiplasmodial aminopeptidase-1 inhibitors, J. Med. Chem. **55** (2012) 10909-10917.

[14] M. Flipo, T. Beghyn, V. Leroux, I. Florent, B. P. Deprez, R. F. Deprez-Poulain, Novel selective inhibitors of the zinc plasmodial aminopeptidase *Pf*A-M1 as potential antimalarial agents, J. Med. Chem. **50** (2007) 1322-1334.

[15] M. Flipo, I. Florent, P. Grellier, C. Sergheraert, R. Deprez-Poulain, Design, synthesis and antimalarial activity of novel, quinoline-based, zinc metallo-aminopeptidase inhibitors, Bioorg. Med. Chem. Lett. **13** (2003) 2659-2662.

[16] K. K. Sivaraman, A. Paiardini, M. Sienczyk, C. Rugger, C. A. Oellig, J. P. Dalton, P. J. Scammells, M. Drag, S. McGowan, Synthesis and structure-activity relationships of phosphonic arginine mimetics as inhibitors of the M1 and M17 aminopeptidases from *Plasmodium falciparum*, J. Med. Chem. **56** (2013) 5213-5217.

[17] S. N. Mistry, N. Drinkwater, C. Ruggeri, K. K. Sivaraman, S. Loganathan, S. Fletcher, M. Drag, A. Paiardini, V. M. Avery, P. J. Scammells, S. McGowan, Two-pronged attack: Dual inhibition of *Plasmodium falciparum* M1 and M17 metalloaminopeptidases by a novel series of hydroxamic acid-based inhibitors, J. Med. Chem. **57** (2014) 9168-83.

[18] M. Flipo, T. Beghyn, J. Charton, V. A. Leroux, B. P. Deprez, R. F. Deprez-Poulain, A library of novel hydroxamic acids targeting the metallo-protease family: Design, parallel synthesis and screening, Bioorg. Med. Chem. **15** (2007) 63-76.

[19] S. Weik, T. Luksch, A. Evers, J. Boettcher, C. A. Sotriffer, A. Hasilik, H.-G. Loeffler, G. Klebe, J. Rademann, The potential of P1 site alterations in peptidomimetic protease inhibitors as suggested by virtual screening and explored by the use of c-c-coupling reagents, ChemMedChem **1** (2006) 445-457.

[20] Z.-L. Shen, K. K. K. Goh, C. H. A. Wong, W.-Y. Loo, Y.-S. Yang, J. Lu, T.-P. Loh, Synthesis and application of a recyclable ionic liquid-supported imidazolidinone catalyst in enantioselective 1,3-dipolar cycloaddition, Chem. Commun. **48** (2012) 5856-5858.

[21] R. M. Srivastava, M. C. Pereira, W. W. M. Faustino, K. Coutinho, J. V. dos Anjos, S. J. de Melo, Synthesis, mechanism of formation, and molecular orbital calculations of arylamidoximes, Montash. Chem. **140** (2009) 1319-1324.

[22] G. Velmourougane, M. B. Harbut, S. Dalal, S. McGowan, C. A. Oellig, N. Meinhardt, J. C. Whisstock, M. Klemba, D. C. Greenbaum, Synthesis of new (-)-bestatin-based inhibitor libraries reveals a novel binding mode in the S1 pocket of the essential malaria M1 metalloaminopeptidase, J. Med. Chem. **54** (2011) 1655-1666.

[23] J. Grembecka, A. Mucha, T. Cierpicki, P. Kafarski, The most potent organophosphorus inhibitors of leucine aminopeptidase. Structure-based design, chemistry, and activity, J. Med. Chem. **46** (2003) 2641-2655.

[24] D. A. Fidock, T. Nomura, A. K. Talley, R. A. Cooper, S. M. Dzekunov, M. T. Ferdig, L. M. B. Ursos, A. B. S. Sidhu, B. Naude, K. W. Deitsch, X. Z. Su, J. C. Wootton, P. D. Roepe, T. E. Wellems, Mutations in the *Plasmodium falciparum* digestive vacuole transmembrane protein pfcrt and evidence for their role in chloroquine resistance, Mol. Cell **6** (2000) 861-871.

[25] S. Nair, J. T. Williams, A. Brockman, L. Paiphun, M. Mayxay, P. N. Newton, J. P. Guthmann, F. M. Smithuis, T. T. Hien, N. J. White, F. Nosten, T. J. C. Anderson, A selective sweep driven by pyrimethamine treatment in southeast asian malaria parasites, Molecul. Biol. Evol. **20** (2003) 1526-1536.

[26] E. L. Flannery, C. W. McNamara, S. W. Kim, T. S. Kato, F. Li, C. H. Teng, K. Gagaring, M. J. Manary, R. Barboa, S. Meister, K. Kuhen, J. M. Vinetz, A. K. Chatterjee, E. A. Winzeler, Mutations in the p-type cation-transporter atpase 4, pfatp4, mediate resistance to both aminopyrazole and spiroindolone antimalarials, ACS Chem. Biol. **10** (2015) 413-420.

[27] M. B. Jimenez-Diaz, D. Ebert, Y. Salinas, A. Pradhan, A. M. Lehane, M.-E. Myrand-Lapierre, K. G. O'Loughlin, D. M. Shackleford, M. J. de Almeida, A. K. Carrillo, J. A. Clark, A. S.M. Dennis, J. Diep, X. Deng, S. Duffy, A. N. Endsley, G. Fedewa, W. A. Guiguemde, M. G. Gomez, G.

Holbrook, J. Horst, C. C. Kim, J. Liu, M. C. S. Lee, A. Matheny, M. Santos Martinez, G. Miller, A. Rodriguez-Alejandre, L. Sanz, M. Sigal, N. J. Spillman, P. D. Stein, Z. Wang, F. Zhu, D. Waterson, S. Knapp, A. Shelat, V. M. Avery, D. A. Fidock, F.-J. Gamo, S. A. Charman, J. C. Mirsalis, H. Ma, S. Ferrer, K. Kirk, I. Angulo-Barturen, D. E. Kyle, J. L. DeRisi, D. M. Floyd, R. K. Guy, (+)-SJ733, a clinical candidate for malaria that acts through atp4 to induce rapid host-mediated clearance of plasmodium, P. Natl. Acad. Sci. USA **111** (2014) E5455-E5462.

[28] M. Rottmann, C. McNamara, B. K.S. Yeung, M. C. S. Lee, B. Zou, B. Russell, P. Seitz, D. M. Plouffe, N. V. Dharia, J. Tan, S. B. Cohen, K. R. Spencer, G. E. Gonzalez-Paez, S. B. Lakshminarayana, A. Goh, R. Suwanarusk, T. Jegla, E. K. Schmitt, H.-P. Beck, R. Brun, F. Nosten, L. Renia, V. Dartois, T. H. Keller, D. A. Fidock, E. A. Winzeler, T. T. Diagana, Spiroindolones, a potent compound class for the treatment of malaria, Science **329** (2010) 1175-1180.

[29] A. B. Vaidya, J. M. Morrisey, Z. Zhang, S. Das, T. M. Daly, T. D. Otto, N. J. Spillman, M. Wyvratt, P. Siegl, J. Marfurt, G. Wirjanata, B. F. Sebayang, R. N. Price, A. Chatterjee, A. Nagle, M. Stasiak, S. A. Charman, I. Angulo-Barturen, S. Ferrer, M. Belen Jimenez-Diaz, M. Santos Martinez, F. Javier Gamo, V. M. Avery, A. Ruecker, M. Delves, K. Kirk, M. Berriman, S. Kortagere, J. Burrows, E. Fan, L. W. Bergman, Pyrazoleamide compounds are potent antimalarials that target na+ homeostasis in intraerythrocytic *Plasmodium falciparum*, Nat. Commun. **5** (2014) article number 5521.

[30] L. Foquet, C. C. Hermsen, G.-J. van Gemert, E. Van Braeckel, K. E. Weening, R. Sauerwein, P. Meuleman, G. Leroux-Roels, Vaccine-induced monoclonal antibodies targeting circumsporozoite protein prevent *Plasmodium falciparum* infection, J. Clin. Invest. **124** (2014) 140-144.

[31] M. P. G. Jepsen, P. S. Jogdand, S. K. Singh, M. Esen, M. Christiansen, S. Issifou, A. B. Hounkpatin, U. Ateba-Ngoa, P. G. Kremsner, M. H. Dziegiel, S. Olesen-Larsen, S. Jepsen, B.

Mordmueller, M. Theisen, The malaria vaccine candidate gmz2 elicits functional antibodies in individuals from malaria endemic and non-endemic areas, J. Infect. Dis. **208** (2013) 479-488.

[32] N. P. Cowieson, D. Aragao, M. Clift, D. J. Ericsson, C. Gee, S. J. Harrop, N. Mudie, S. Panjikar, J. R. Price, A. Riboldi-Tunnicliffe, R. Williamson, T. Caradoc-Davies, Mx1: A bending-magnet crystallography beamline serving both chemical and macromolecular crystallography communities at the australian synchrotron, J. Synchrotron Radiat. **22** (2015) 187-190.

[33] T. G. G. Battye, L. Kontogiannis, O. Johnson, H. R. Powell, A. G. W. Leslie, iMOSFLM: A new graphical interface for diffraction-image processing with mosflm, Acta Crystallogr. D. **67** (2011) 271-281.

[34] W. Kabsch, XDS, Acta Crystallogr. D. **66** (2010) 125-132.

[35] P. R. Evans, G. N. Murshudov, How good are my data and what is the resolution? Acta Crystallogr. D. **69** (2013) 1204-1214.

[36] A. J. McCoy, R. W. Grosse-Kunstleve, P. D. Adams, M. D. Winn, L. C. Storoni, R. J. Read, Phaser crystallographic software, J. Appl. Crystallogr. **40** (2007) 658-674.

[37] M. D. Winn, C. C. Ballard, K. D. Cowtan, E. J. Dodson, P. Emsley, P. R. Evans, R. M. Keegan, E. B. Krissinel, A. G. W. Leslie, A. McCoy, S. J. McNicholas, G. N. Murshudov, N. S. Pannu, E. A. Potterton, H. R. Powell, R. J. Read, A. Vagin, K. S. Wilson, Overview of the CCP4 suite and current developments, Acta Crystallogr. D. **67** (2011) 235-242.

[38] P. D. Adams, P. V. Afonine, G. Bunkoczi, V. B. Chen, I. W. Davis, N. Echols, J. J. Headd, L.-W. Hung, G. J. Kapral, R. W. Grosse-Kunstleve, A. J. McCoy, N. W. Moriarty, R. Oeffner, R. J. Read, D. C. Richardson, J. S. Richardson, T. C. Terwilliger, P. H. Zwart, Phenix: A comprehensive python-based system for macromolecular structure solution, Acta Crystallogr. D. **66** (2010) 213-221.

[39] P. Emsley, B. Lohkamp, W. G. Scott, K. Cowtan, Features and development of coot, Acta Crystallogr. D. **66** (2010) 486-501.

[40] A. W. Schuttelkopf, D. M. F. van Aalten, PRODRG: A tool for high-throughput crystallography of protein-ligand complexes, Acta Crystallogr. D. **60** (2004) 1355-1363.

[41] S. Duffy, V. M. Avery, Development and optimization of a novel 384-well anti-malarial imaging assay validated for high-throughput screening, Am. J. Trop. Med. Hyg. **86** (2012) 84-92.

[42] F. Lombardo, M. Y. Shalaeva, K. A. Tupper, F. Gao, Elogd(oct): A tool for lipophilicity determination in drug discovery. 2. Basic and neutral compounds, J. Med. Chem. **44** (2001) 2490-2497.

[43] C. D. Bevan, R. S. Lloyd, A high-throughput screening method for the determination of aqueous drug solubility using laser nephelometry in microtiter plates, Anal. Chem. **72** (2000) 1781-1787.

Table 1

Inhibition of *Pf*A-M1 and *Pf*A-M17 by hydroxamic acid compounds **9a-b**, **f-s** and **10a-b, f-t**. K_i values are the mean of three independent experiments.

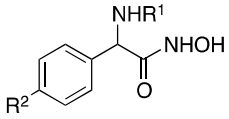

No.	R^1	R^2	K_i (μM)	
			*Pf*A-M1	*Pf*A-M17
2[17]	Boc	pyrazole	0.85	0.028
3[17]	C(O)^{t}Bu	pyrazole	0.72	0.028
9a	Boc	F	5.3	1.7
9b	Boc	Br	0.027	0.080
9f	Boc	phenyl	37	0.055
9g	Boc	2-fluorophenyl	0.95	0.041
9h	Boc	3-fluorophenyl	0.95	0.13
9i	Boc	4-fluorophenyl	100	0.074
9j	Boc	2-(trifluoromethyl)phenyl	0.75	0.12
9k	Boc	3-(trifluoromethyl)phenyl	2.9	0.14
9l	Boc	4-(trifluoromethyl)phenyl	>500	0.47
9m	Boc	3,4,5-trifluorophenyl	19	0.20
9n	Boc	3-pyridyl	1.1	0.22
9o	Boc	4-pyridyl	0.91	0.54
9p	Boc	thiophen-3-yl	20	0.064
9q	Boc	1-methylpyraz-4-yl	1.9	0.056
9r	Boc	3-(amidoximo)phenyl	1.1	0.14
9s	Boc	4-(amidoximo)phenyl	0.40	0.018
10a	C(O)^{t}Bu	F	4.0	0.029
10b	C(O)^{t}Bu	Br	0.065	0.041
10f	C(O)^{t}Bu	phenyl	1.6	0.007
10g	C(O)^{t}Bu	2-fluorophenyl	1.6	0.012
10h	C(O)^{t}Bu	3-fluorophenyl	0.55	0.0062
10i	C(O)^{t}Bu	4-fluorophenyl	6.5	0.033
10j	C(O)^{t}Bu	2,4-difluorophenyl	2.5	0.0052
10k	C(O)^{t}Bu	2,6-difluorophenyl	4.8	0.013
10l	C(O)^{t}Bu	3,4-difluorophenyl	1.4	0.0064
10m	C(O)^{t}Bu	3,5-difluorophenyl	0.58	0.092
10n	C(O)^{t}Bu	2,4,6-trifluorophenyl	5.9	0.0025
10o	C(O)^{t}Bu	3,4,5-trifluorophenyl	0.078	0.060
10p	C(O)^{t}Bu	2,3,4,5,6-pentafluorophenyl	1.8	0.0084
10q	C(O)^{t}Bu	thiophen-3-yl	0.64	0.0091
10r	C(O)^{t}Bu	1-methylpyrazol-4-yl	11	0.0072
10s	C(O)^{t}Bu	3-(amidoximo)phenyl	5.4	0.0097
10t	C(O)^{t}Bu	4-(amidoximo)phenyl	4.3	0.0086

Table 2

Inhibition of *Pf*A-M1 and *Pf*A-M17 by hydroxamic acid compounds **9c-e**, **t-u** and **10c-e, u-v**. K_i values are the mean of three independent experiments.

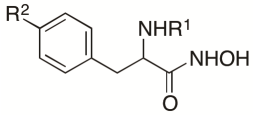

No.	R^1	R^2	K_i (μM)	
			*Pf*A-M1	*Pf*A-M17
9c	Boc	F	18	2.8
9d	Boc	Br	39	7.7
9e	Boc	I	4.3	21
9t	Boc	phenyl	> 500	5.2
9u	Boc	1-methylpyrazol-4-yl	120	14
10c	C(O)^{t}Bu	F	63	0.037
10d	C(O)^{t}Bu	Br	87	0.42
10e	C(O)^{t}Bu	I	15	0.016
10u	C(O)^{t}Bu	phenyl	27	0.65
10v	C(O)^{t}Bu	1-methylpyrazol-4-yl	39	0.74

Table 3
Growth inhibition of cultured *Pf* by selected hydroxamic acid compounds

	IC_{50} ± SEM (nM)	**IC_{50} ± SEM** (nM)	**IC_{50} ± SEM** (nM)
	Pf-3D7	Dd2 Parent	Dd2 SpiroR
Artesunate	2.1 ± 0.2	1.3 ± 0.4	0.9 ± 0.3
2[17]	783 ± 87		
3[17]	227 ± 4		
9b	293 ± 10		
9g	633 ± 24		
9q	978 ± 106		
9r	679 ± 33		
9s	334 ± 31		
10a	1530 ± 60	2010 ± 20	2090 ± 50
10b	169 ± 17	194 ± 14	163 ± 45
10f	96 ± 17	190 ± 12	219 ± 71
10g	131 ± 5	207 ± 10	210 ± 25
10h	162 ± 4	226 ± 10	316 ± 21
10i	126 ± 4	225 ± 29	193 ± 7
10j	109 ± 2	164 ± 46	216 ± 39
10k	142 ± 17	251 ± 35	246 ± 34
10l	139 ± 0.1	170 ± 52	195 ± 17
10m	144 ± 0.0	239 ± 34	232 ± 43
10n	125 ± 13	267 ± 47	450 ± 38
10o	126 ± 2	189 ± 23	107 ± 20
10p	130 ± 38	461 ± 42	408 ± 52
10q	103 ± 3	110 ± 7	100 ± 5
10s	469 ± 28	819 ± 48	627 ± 2
10t	249 ± 23	303 ± 35	384 ± 8

NC = No curve, activity not sufficient to fit curve to data.

Table 4
Solubility and stability characteristics of **10o**.

Parameter	Value
Solubility (µg/mL)[a]	
pH 2	12.5–25
pH 6.5	12.5–25
$LogD_{pH\ 7.4}$[b]	3.0
Stability in Liver Microsomes	
Mouse: $t_{1/2}$ (min) / CL_{int} (µL/min/mg protein)	69 / 25
Human: $t_{1/2}$ (min) / CL_{int} (µL/min/mg protein)	221 / 8
Plasma Stability[c]	
Mouse : t1/2 (h)	>25
Human : t1/2 (h)	>17

[a] Kinetic solubility determined by nephelometry

[b] Value measured by the chromatographic LogD technique.

[c] No measureable degradation

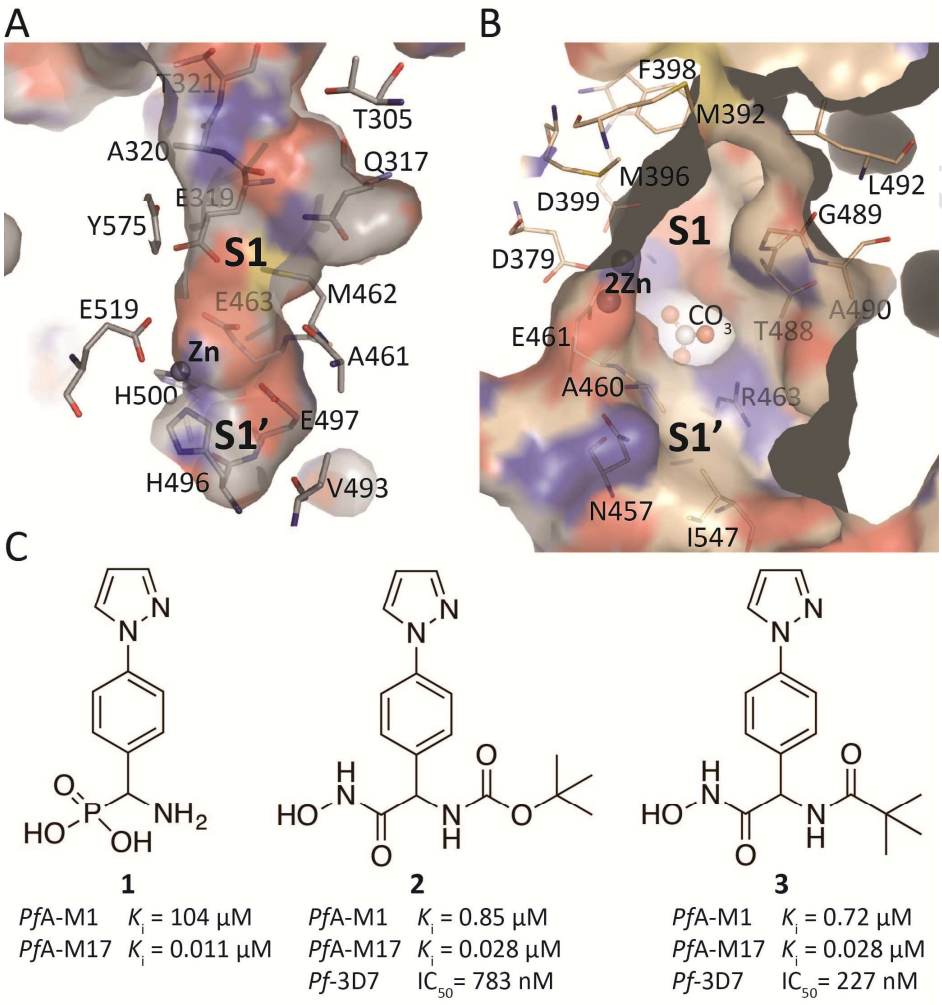

Fig. 1. Solvent accessible surface diagrams of the active sites of *Pf*A-M1 (A) and *Pf*A-M17 (B). Positions of active site residues, catalytic zinc ions, and, for *Pf*A-M17, catalytic carbonate ions, are shown. (C) ((4-(1*H*-Pyrazol-1-yl)phenyl)(amino)methyl)phosphonic acid [16] (**1**), *tert*-butyl (1-(4-(1*H*-pyrazol-1-yl)phenyl)-2-(hydroxyamino)-2-oxoethyl)carbamate [17] (**2**) and *N*-(1-(4-(1*H*-pyrazol-1-yl)phenyl)-2-(hydroxyamino)-2-oxoethyl)pivalamide [17] (**3**).

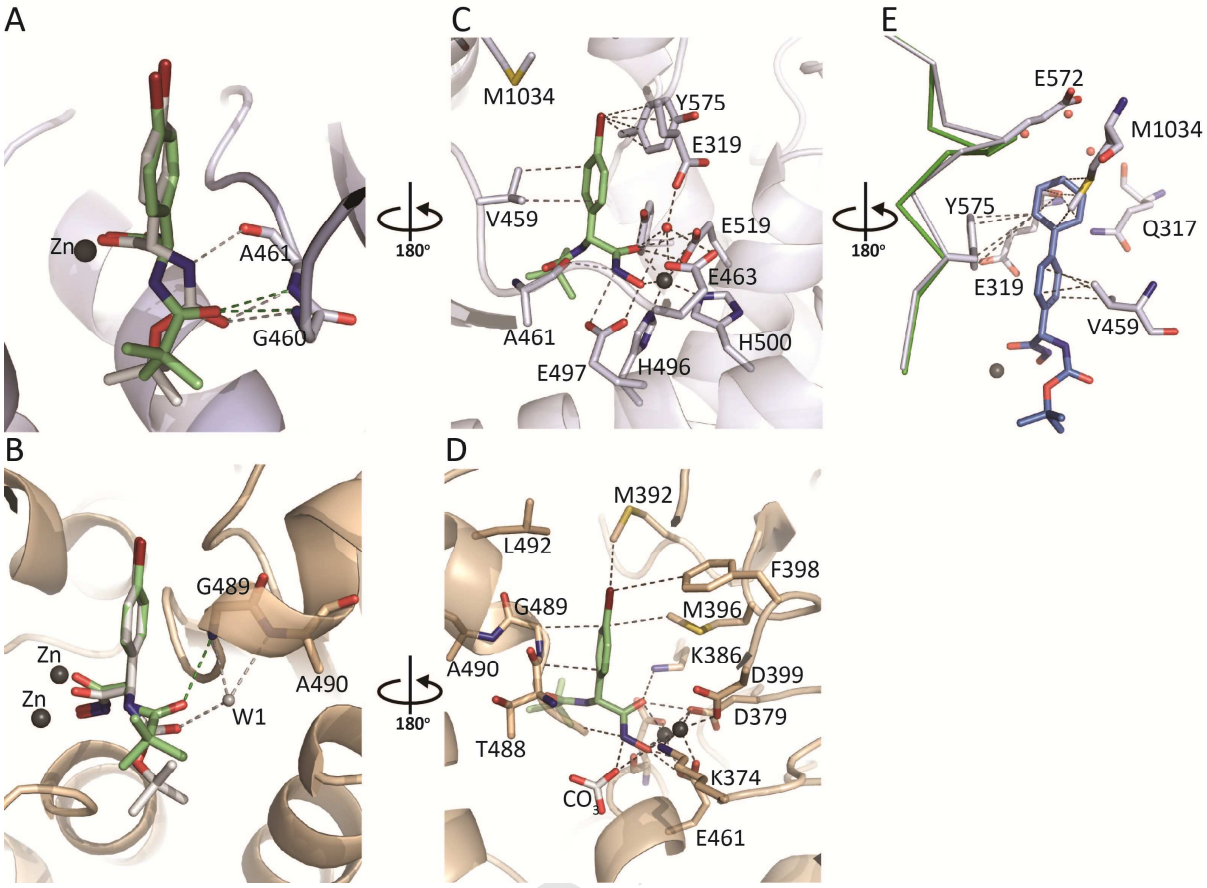

Fig. 2. Binding pose of hydroxamic-acid inhibitors to *Pf*A-M1 (grey cartoon) and *Pf*A-M17 (wheat cartoon). **A** and **B**, Overlay of **9b** (grey sticks) with **10b** (green sticks) when bound to *Pf*A-M1 (**A**) or *Pf*A-M17 (**B**). Interactions between the *tert*-butyl containing moieties (*N*-Boc in **9b** and *N*-pivaloyl in **10b**) and binding pocket residues are shown as dashed lines in grey (**9b**) or green (**10b**). **C** and **D**, Compound **10b** (green sticks) bound to *Pf*A-M1 (**C**) and *Pf*A-M17 (**D**). Interactions formed between the hydroxamic acid and S1-binding scaffold with the active sites are shown as dashed lines. Interactions between the S1' anchor and the binding sites are not shown. **E**, Interactions formed between the biphenyl substituent of **9f** (blue) and *Pf*A-M1. Cα chain shown for *Pf*A-M1 active site helix when **9b** (green chain) and **9f** (grey chain) are bound.

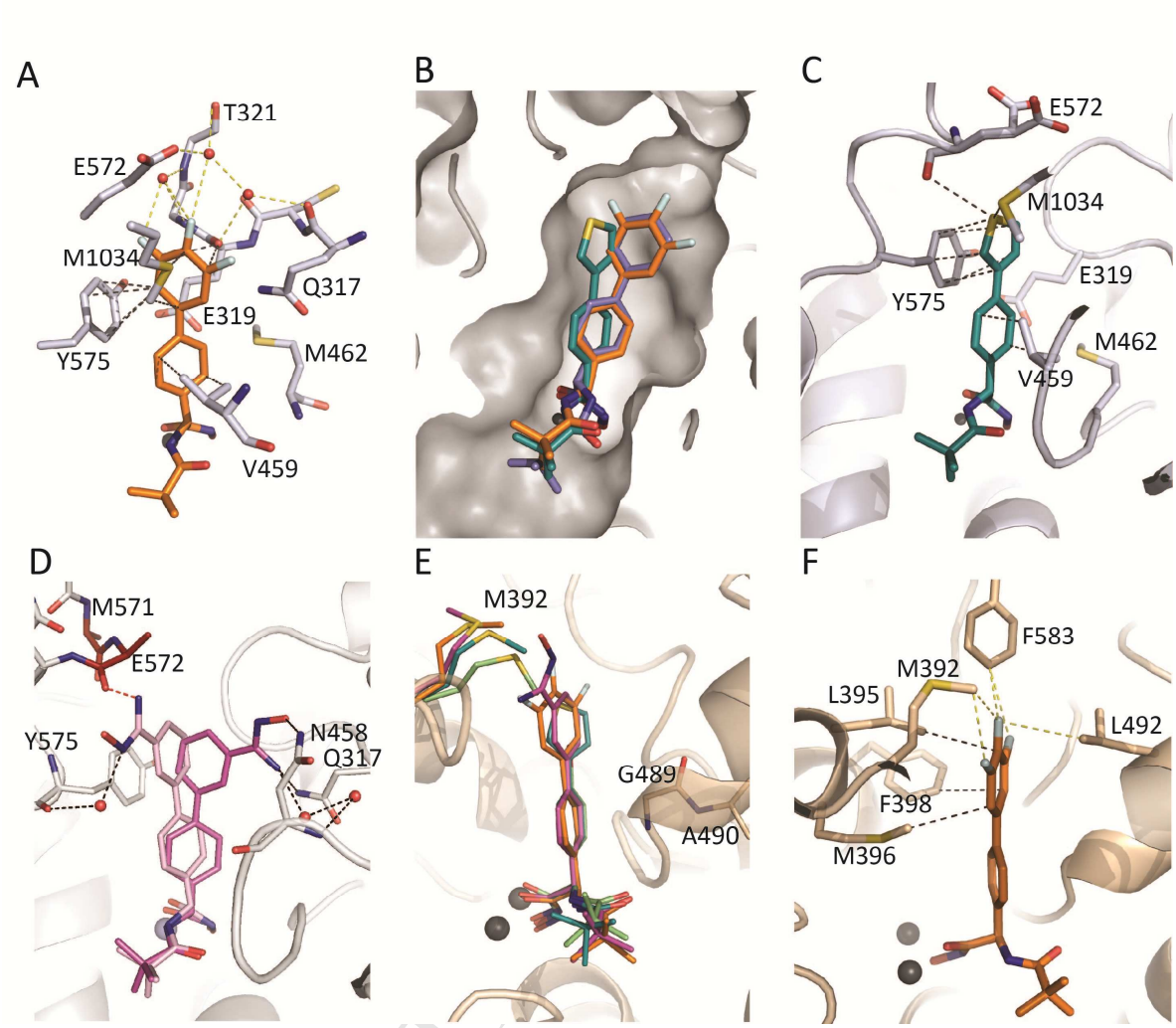

Fig. 3. Binding of pivalamide series to *Pf*A-M1 (grey) and *Pf*A-M17 (wheat). **A**, Interactions between the substituted biaryl of **10o** (orange sticks) and *Pf*A-M1 (grey). Fluorine-hydrogen-bonds shown as orange dashed lines and hydrophobic interactions shown as black dashed lines. **B**, Shifted binding pose of **10q** (teal) when bound to *Pf*A-M1 (shown as grey surface) compared to **10o** (orange) and **9f** (blue). **C**, Interactions between the biphenyl system of **10q** (teal) and *Pf*A-M1 (grey), shown as black dashed lines. **D**, dual binding pose of **10s** (pink) when bound to *Pf*A-M1. Disordered residues shown as red sticks. **E**, Compounds **10o** (orange), **10q** (teal) and **10s** (pink) bound to *Pf*A-M17 (wheat). Active site methionine residue M392 (stick representation, coloured according to inhibitor bound) is observed to shift in and out of the pocket depending on interactions with compound. **F**, Interactions between the substituted biaryl of **10o** (orange sticks) and *Pf*A-M17 (wheat). Fluorine-hydrogen-bonds are shown as orange dashed lines and hydrophobic interactions shown as black dashed lines.

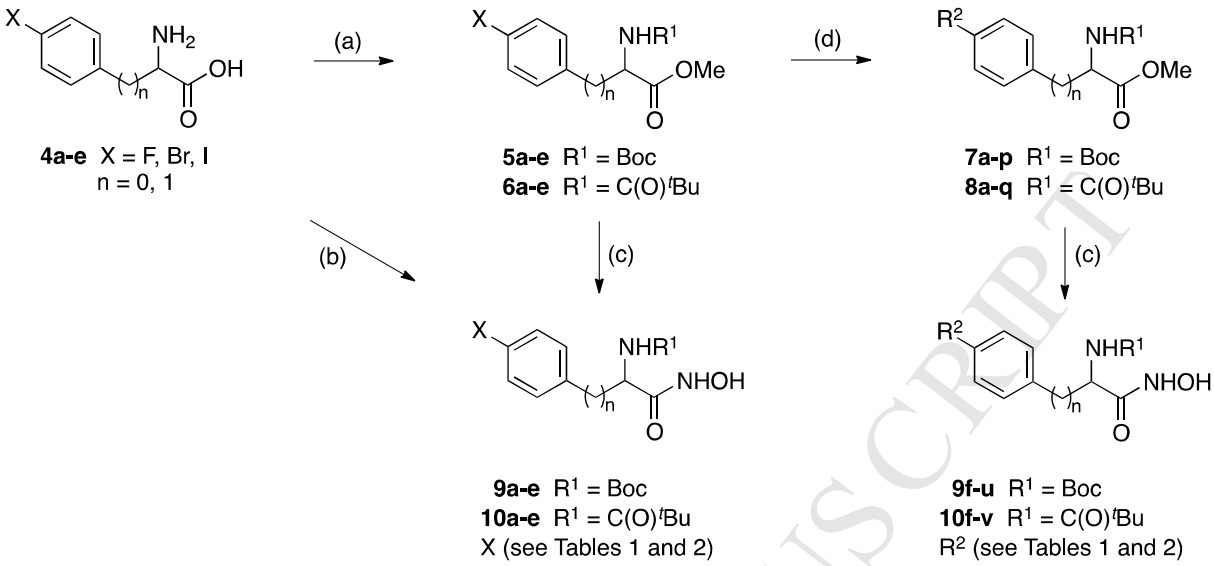

Scheme 1. [a] Reagents and conditions: (a) i. cat. concd H_2SO_4, MeOH, reflux; ii. Boc_2O, THF, water, rt, or pivaloyl chloride, Et_3N, DCM, rt; (b) i. Boc_2O, 2M NaOH $_{(aq)}$, THF, water; ii. CDI, dry THF, rt; iii. $NH_2OH.HCl$; (c) i. dry MeOH, rt; ii. $NH_2OH.HCl$, 5M KOH/MeOH, dry MeOH (premixed), rt; (d) cat. $PdCl_2(PPh_3)_2$, boronic acid or boronate ester, degassed 1M Na_2CO_3 $_{(aq)}$, degassed THF, 100 °C.

Potent dual inhibitors of *Plasmodium falciparum* M1 and M17 aminopeptidases through optimization of S1 pocket interactions

Pages ##-##

Nyssa Drinkwater, Natalie B. Vinh, Shailesh N. Mistry, Rebecca S. Bamert, Chiara Ruggeri, John P. Holleran, Sasdekumar Loganathan, Alessandro Paiardini, Susan A. Charman, Andrew K. Powell, Vicky M. Avery, Sheena McGowan, Peter J. Scammells

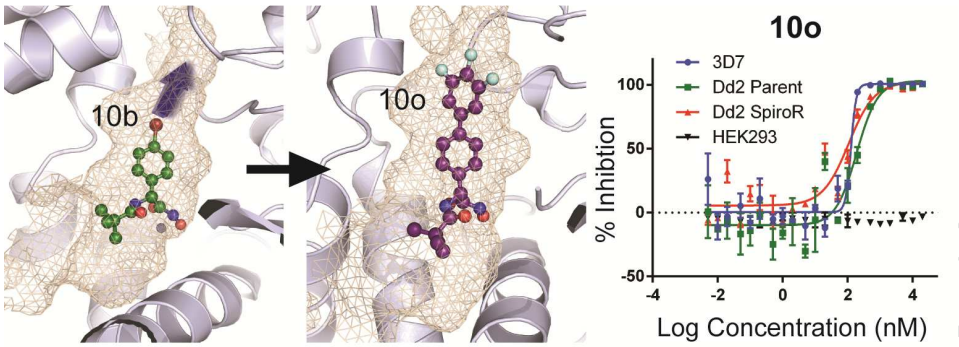

Ms. Ref. No.: **EJMECH-D-15-02218**

Title: Potent dual inhibitors of *Plasmodium falciparum* M1 and M17 aminopeptidases through optimization of S1 pocket interactions

RESEARCH HIGHLIGHTS:

- Dual inhibition of *Pf*A-M1 and *Pf*A-M17 is proposed as a novel antimalarial strategy.
- Compound series containing hydroxamic acid zinc binding group optimized by SBDD.
- Compounds elaborated into S1 pockets of *Pf*A-M1 and *Pf*A-M17.
- Optimized compounds possess superior *Pf*A-M1 and *Pf*A-M17 inhibitory activity.
- The potent, dual inhibitors inhibit multi-drug resistant *Pf* growth in culture.